A Multimodal Approach To Restoring Motor Function After Spinal Cord Injury: Exploring The Use Of Plant-Based Biomaterials & Stimulating Propriospinal Interneurons

Lauren Couvrette

Thesis submitted to the University of Ottawa in partial
fulfillment of the requirements for the Doctorate in Philosophy in Biology

Department of Biology
Faculty of Science
University of Ottawa

Table of Contents

Abstract

Spinal cord injury (SCI) presents a significant challenge in regenerative medicine due to its complex pathophysiology & extensive molecular barriers that hinder repair. Overcoming these challenges requires interdisciplinary strategies that combine molecular biology, bioengineering, neuroscience, and rehabilitative therapy. In particular, the neural tissue engineering approach aims to produce an implantable scaffold that can support regeneration of spinal cord tissue in the hopes of forming relay circuits or promoting the regrowth of native axons. These biomaterials can be engineered to create a favorable environment that facilitates axonal infiltration into the damaged regions of the central nervous system. This thesis explores the use of decellularized plant tissue as a biomaterial for 3D cell culture & neural tissue engineering. We first demonstrate the ability of plant-derived scaffolds to support proliferation of neural stem cells *in vitro* and guide their differentiation into the neuronal lineage. Subsequently, we assess the scaffold's potential to support motor recovery in a rat model of complete spinal cord injury. Our findings highlight a potential therapeutic application for plant-based biomaterials and show their ability to be functionalized with peptide coatings. Finally, we identify dI3 neurons as key contributors to the re-activation of spinal locomotor circuits in response to cutaneous sensory input below the injury. Together, these results highlight the promise of multimodal therapeutic strategies for motor recovery after spinal cord injury.

Résumé

Les lésions médullaires représentent un défi majeur en médecine régénératrice en raison de leur pathologie complexe et des barrières moléculaires importantes qui empêchent la régénération. Plusieurs stratégies interdisciplinaires on tenté de surmonter ces défis en combinant la biologie moléculaire, la bio-ingénierie, la neuroscience et la thérapie de réadaptation. L'ingénierie tissulaire neuronale vise à produire un biomatériel implantable capable d'encourager la régénération des neurones afin de former des circuits de relais ou de favoriser la régénération des axones. Ces biomatériaux peuvent être conçus pour produire un environnement favorable à l'infiltration axonale dans les régions endommagées du système nerveux central. Cette thèse explore l'utilisation de tissus végétaux décellularisés comme biomatériau pour la culture cellulaire en 3D et l'ingénierie tissulaire neuronale. Nous démontrons d'abord la capacité des tissus végétaux décellularisés à soutenir la prolifération des cellules souches neurales *in vitro* et à guider leur différenciation vers la lignée neuronale. Ensuite, nous évaluons le potentiel de ce biomatériel à soutenir la rétablissement de la capacité motrice dans un animal modèle de lésion médullaire complète. Nos résultats mettent en évidence une application thérapeutique potentielle des biomatériaux d'origine végétale et démontrent leur capacité à être fonctionnalisés par des revêtements peptidiques. Enfin, nous identifions les neurones dI3 comme des contributeurs à la réactivation des circuits locomoteurs en réponse aux stimulations sensorielles cutanées. L'ensemble de ces résultats met en évidence le potentiel de stratégies thérapeutiques multimodales pour la récupération des habiletés motrices après une lésion médullaire.

Acknowledgements

I would like to express my heartfelt thanks to both of my supervisors for their guidance, generosity, and encouragement. Dr. Andrew Pelling introduced me to the fascinating world of biomaterials, and our meetings always left me feeling inspired. His insight and support throughout the project have been invaluable. I am grateful to Dr. Tuan Bui for providing his expertise in neuroscience, which was instrumental to the success of the project. His dedication to students and down-to-earth attitude fostered a positive lab environment that deeply enriched my experience as a graduate student.

I would like to acknowledge all members of the Bui lab and Pelling lab for their contribution to this thesis. Without their support, this work would not be possible. Thank you to Krystal Walker, Rose Boudria, Arman Bayat, Dr. Nicolette Mogilever, Ruthie Monty, Dr. Maxime Leblanc-Latour, Dr. Ziba Jaberansari, and Dr. Daniel Modulevsky for their contribution to animal surgeries, data collection and analysis. Thank you to Dr. Sara Goltash, Dr. Alex Laliberté, Emam Khan for their contribution in animal surgeries, post-operative care, data analysis, and behavioral assays. Thank you to the Animal Care and Veterinary Service staff and the University of Ottawa Louise Pelletier Histology Core. I greatly appreciate the funding support from the Li Ka Shing Foundation, the Natural Sciences and Engineering Research Council, and the Canadian Institutes of Health Research.

Finally, I would like to express my deepest gratitude to my friends and family — in particular, my mom & dad for their unwavering support and for helping me move 3 times during graduate school. I also thank (soon to be Dr) Annabelle Pfeifle for indulging my obsession with rats and for her help with Prism. I thank my partner Glib for moral support & late-night drives to the animal facility.

Statement of Contributions

I, Lauren Couvrette, was the predominant contributor to the work within this thesis. Experiments were designed, performed, and analyzed by myself, with the help of Dr. Andrew Pelling and Dr. Tuan Bui. Members of the Bui Lab and Pelling Lab contributed to animal surgeries, behavioral testing and post-operative care. Manuscripts were written by myself, edited by Dr. Andrew Pelling and Dr. Tuan Bui, and reviewed by all listed authors.

Conferences

- Poster Presentation at Society for Neuroscience Conference (2024, Chicago, USA)
- Presentation at Canadian Spinal Cord Injury Meeting (2024, Banff, CA)
- Poster Presenter at Canadian Biomaterials Society Conference (2023, Halifax, CA)
- Poster Presenter at Brain & Mind Institute Stem Cell Research Spotlight (2023, Ottawa, CA)
- Poster Presenter at Ottawa-Carleton Institute of Biology Symposium (2023, Ottawa, CA)

List of Figures

List of Abbreviations

BBB – Basso Beattie Bresnahan Open-field Assessment

BMS – Basso Mouse Scale

CNS – Central Nervous System

CPG – Central Pattern Generator

CSPGs – Chondroitin Sulfate Proteoglycans

CTb – Cholera Toxin Subunit B

GFAP – Glial Fibrillary Acidic Protein

DA – Dextran Amine

DREADD – Designer Receptors Exclusively Activated by Designer Drugs

ECM – Extracellular Matrix

EES – Electrical Epidural Stimulation

NF200 – Neurofilament 200kd Protein

NSC – Neural Stem Cell

PLO – Poly-L-Ornithine

PNS – Peripheral Nervous System

5-HT – Serotonin

SCI – Spinal Cord Injury

Chapter 1: General Introduction

1.1 Spinal Cord Injury Pathophysiology

Traumatic spinal cord injury (SCI) is a debilitating neurological condition with far-reaching consequences for patients, including loss of motor function and significant limitations to quality of life. Mechanical trauma to the spinal cord is a primary injury mechanism that results in spinal shock, systemic hypotension, ischemia, compromised blood–spinal cord barrier, and damage to ascending and descending pathways in the cord (Hachem & Fehlings, 2021; Quadri et al., 2020). In human patients, the most common form of mechanical trauma is impact with persistent compression, that often occurs through injuries in which fragments of bone compress the cord (Sekhon & Fehlings, 2001). SCI can also result from forcible stretching of the cord, referred to as a distraction injury, or severing of the cord, which can vary from minor laceration with spared tissue to complete transection of the cord (Dumont et al., 2001). This primary mechanical trauma triggers a secondary injury phase that involves self-propagating biochemical events, which lead to progressive tissue degeneration. Secondary injury mechanisms include glutamate excitotoxicity, free radical production, immune-mediated neurotoxicity, and activation of apoptotic pathways (E. Park et al., 2004; Quraishe et al., 2018). These processes lead to death of perilesional neural cells and ultimately create an expanding cavity of necrotic tissue within the cord (Anjum et al., 2020).

Within the first hour post-injury, blood supply is disrupted at the injury site, instigating tissue ischemia, hypoxia, and oxidative damage (Visavadiya et al., 2016). The integrity of cell membranes is broken, which alters permeability and results in calcium dysregulation, mitochondrial dysfunction, and rapid energy loss (Hellenbrand et al., 2021). In particular, damaged cell membranes allow for abnormal calcium influx which can activate calpains, causing dysfunction of mitochondria and exacerbating cell death (Schanne et al., 1979). In turn, neuronal death leads to excessive release of neurotransmitters and impaired reuptake of glutamate. The ensuing elevation in extracellular glutamate concentrations elicits

prolonged excitatory synaptic transmission (S. Li & Stys, 2000a; Panter et al., 1990). Specifically, excess glutamate causes overactivation of N-methyl-D-aspartate and kainate receptors, thereby impairing ionic homeostasis in astrocytes and oligodendrocytes (S. Li & Stys, 2000b). This further contributes to mitochondrial dysfunction and cell death.

During the acute-to-subacute period after injury, tissue damage spreads via lipid peroxidation (HALL & BRAUGHLER, 1986), a highly destructive reaction in which reactive oxygen species react with membrane polyunsaturated fatty acids, that subsequently react with oxygen to form a lipid peroxyl radical that continues the chain reaction. Simultaneously, microglia become activated in the acute phase after SCI and a plethora of immune cells are recruited to the injury site, including neutrophils and macrophages (Hausmann, 2003). After trauma to the spinal cord, release of inflammatory cytokines is upregulated and the immune response escalates, causing additional cell death. Immune-cell mediated injury occurs via release of proteases, free radicals and cytokines that further perturb homeostasis in the spinal cord. Scar forming astrocytes generate a glial scar around the core of the lesion (Leal-Filho, 2011; T. Yang et al., 2020). As the injury progresses, this region of apoptotic cells spreads further and there is demyelination of surviving axons. Post-traumatic inflammation in the spinal cord persists long after the initial injury and plays a dual role, since some immune responses are neuroprotective while others are neurodegenerative (Rust & Kaiser, 2017). For instance, recruitment of neutrophils to the site of injury helps eliminate tissue debris and restore homeostasis. Many infiltrating immune cells secrete neuroprotective cytokines as well as growth factors that support neurons and limit toxicity (Donnelly & Popovich, 2008). To illustrate, macrophages and activated microglia contribute to the repair process after SCI by phagocytosing myelin debris and damaged cells as well as expressing growth promoting factors. Moreover, microglia and cytokines are considered to play a critical role in the regulation of neurogenesis

after SCI (Rodríguez-Barrera et al., 2021). However, later phases of the immune response have deleterious effects which exacerbate tissue damage.

The intermediate-to-chronic phase of SCI pathology is characterized by the formation of cystic cavities in the cord, vascular reorganization (Whetstone et al., 2003), extracellular matrix remodelling, plasticity within existing neural circuits (Asboth et al., 2018a; Ding et al., 2005; Jacobi & Bareyre, 2015; Lemieux et al., 2024), and a gradual decline in inflammatory cell presence at the injury site (Ahuja et al., 2017). However, resolution of inflammation after SCI is incomplete (Allison & Ditor, 2015) and persistent neuroinflammation becomes an important contributor to secondary injury (Fig. 1.1). In animal models as well as human SCI patients, both immune depression and autoimmunity have been reported (Allison & Ditor, 2015; Jones, 2014; Schwab et al., 2023; Sterner & Sterner, 2023). Spinal cord injury-induced immunodeficiency predisposes patients to infections such as pneumonia (JOHNSON & WANG, 2008) and is thought to be mediated by a sympathetic-neuroendocrine adrenal reflex (Prüss et al., 2017). Concurrently, SCI triggers synthesis of autoantibodies against neuronal and myelin antigens in humans, leading to post-traumatic antibody-mediated autoimmunity (Schwab et al., 2023). Some anti-inflammatory treatment strategies have been explored on the basis that disrupting leukocyte-mediated activity in the injured cord may be neuroprotective (Gaudet & Popovich, 2014; Gris et al., 2004; Popovich et al., 1999). Overall, the pathology of SCI is multifactorial and is an active area of research.

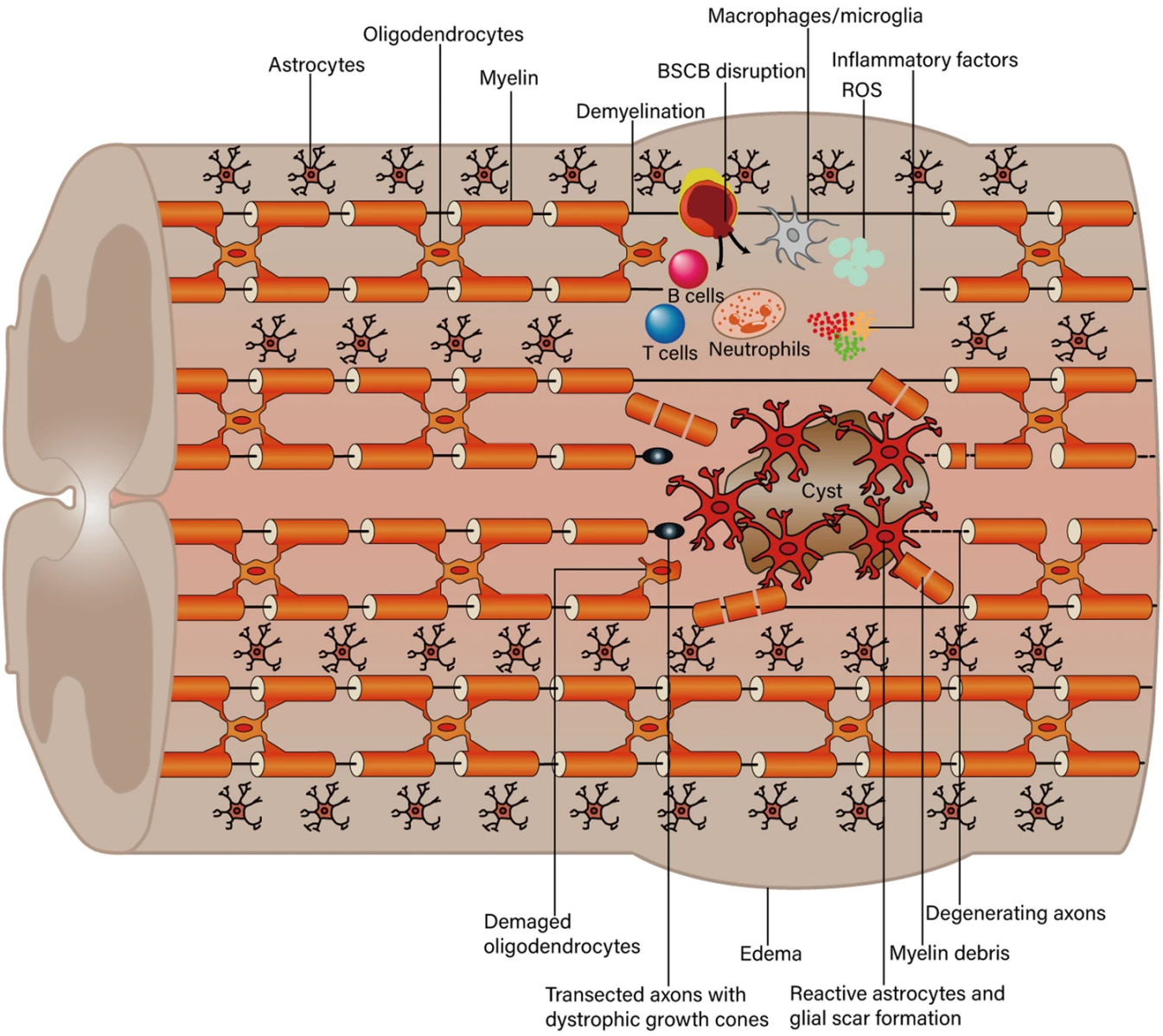

Figure 1.1. Schematic representation of the injured spinal cord. (Figure borrowed from(K. Chen et al., 2024) https://creativecommons.org/licenses/by/4.0/))

1.1.2 Astrocytes and The Glial Scar

Astroglia is a class of neural cells with many subtypes including radial astrocytes, ependymocytes, fibrous astrocytes, protoplasmic astrocytes, and other specialized subtypes. These star-shaped glial cells are morphologically diverse and perform a variety of functions within the central nervous system (CNS). Protoplasmic astrocytes have extensive arborisation and are found in the grey matter, whereas fibrous astrocytes are larger with fewer processes and reside in the white matter. In the healthy CNS, astrocytes express an intermediate filament protein called glial fibrillary acidic protein (GFAP), which is commonly used as a marker for this cell type. GFAP expression in astrocytes varies in different parts of the nervous

system (Yoon et al., 2017) and is influenced by external factors such as physical exercise and environmental enrichment (Saur et al., 2014).

Historically, astrocytes were largely considered to be a homogenous cell population with static, supportive functions such as regulating extracellular potassium concentration, providing structural support to neurons, and maintaining the blood-brain barrier. However, recent studies have demonstrated that in addition to controlling ion and neurotransmitter homeostasis, astrocytes are also active participants in neuronal development and synaptic plasticity (Clarke & Barres, 2013; Farhy-Tselnicker & Allen, 2018; Verkhratsky et al., 2021). In the past decade, astrocytes were shown to play a critical role in synapse formation and elimination, which involves astrocyte-secreted signaling molecules such as brain-derived neurotrophic factor, thrombospondins, and transforming growth factor β1. In addition, astrocytes regulate synapse function by direct contact with neurons, which induces protein kinase C signalling (Hama et al., 2004). In contrast to neurons, astrocytes are electrically non-excitable, relying instead on Ca^{2+} and Na^{+} signalling. They participate in the tripartite synapse by releasing gliotransmitters such as glutamate, ATP, and GABA, thereby influencing information processing within neuronal networks. Overall, the heterogeneity of astrocytes in terms of morphology, gene expression, function, and response to injury is an area of intense investigation (Pestana et al., 2020; Schober et al., 2022; Yoon et al., 2017).

Injury to nervous tissue triggers reactive astrogliosis, which is a continuum of progressive changes in astrocytic behavior. Following SCI, reactive astrocytes proliferate extensively at the injury site, increase GFAP expression, and undergo hypertrophy of their processes which interdigitate to form a glial scar (Sofroniew, 2009). The astrocytic/glial scar is a complex meshwork of different cell types and has both deleterious and beneficial effects after SCI (M. A. Anderson et al., 2016a; Gu et al., 2019; Rudge & Silver, 1990). Fibroblasts produce collagen, fibronectin, and other ECM components that make up the core of the glial scar. During the acute period after insult, reactive astrocytes migrate to the injury site, where they

have neuroprotective roles including absorption of excess glutamate and production of extracellular matrix components that are needed for the reconstruction of the blood-spinal cord barrier (H.-G. Lee & Quintana, 2024; Sofroniew, 2015). The glial scar acts as a physical barrier to mitigate the propagation of inflammation, thereby preventing further damage to surrounding tissue (Okada et al., 2018). As a result of hemorrhage in the spinal cord, astrocytes are exposed to plasma factors such as fibrinogen, which induces an increase in the production of chondroitin sulphate proteoglycans (CSPGs) (Schachtrup et al., 2010). In the chronic phase, the glial scar matures into a dense interwoven network containing excess CSPGs (Sharma et al., 2012) that act as potent inhibitors of axon regrowth (Buss et al., 2009; Qian & Zhou, 2020) and remyelination (Y. He et al., 2020). Hence, the scar contributes to regeneration failure, in part, by obstructing sprouting axons. Recent work also suggests that they play an immunomodulatory role in SCI pathology (Y. He et al., 2020), with some reports of CSPGs preventing the conversion of pro-inflammatory immune cells to a pro-repair phenotype (Francos-Quijorna et al., 2022). Many SCI therapeutic approaches aim to manipulate the glial scar to enhance neural regeneration. Some minimize scar formation (Dias et al., 2018; Tysseling-Mattiace et al., 2008) by inhibiting signaling pathways involved in astrocyte and fibroblast deposition into the lesion, while others attempt to resolve the mature glial scar by enzymatically degrading CSPGs (Sharifi et al., 2022). Several studies demonstrate that attempts at eliminating the glial scar by ablation of astrocytes or microglia ultimately exacerbate tissue degeneration and result in worse functional outcomes (M. A. Anderson et al., 2016b; Bellver-Landete et al., 2019; Perez-Gianmarco & Kukley, 2023).

1.1.3 Endogenous Neural Stem Cell Activation after Spinal Cord Injury in Mammals

Neural stem cells (NSCs) are self-renewing multipotent cells capable of differentiating into neurons, astrocytes, and oligodendrocytes (Gage, 2000). These stem cells exist within distinct niches in the central and peripheral nervous systems of adult mammals (Llorente et al., 2022). Stem cell niches are highly specialized microenvironments that allow for the tight regulation required to maintain cells in a

state of reversible cell cycle arrest, which preserves their undifferentiated state. In the brain, populations of NSCs were identified in the subventricular zone, located within the lateral ventricle, and the subgranular zone in the hippocampus. In these two niches, neurogenesis has been observed in several mammals, including rodents and primates (Amrein, 2015). Similarly, the adult mammalian spinal cord also harbours a pool of stem and progenitor cells that are known as multiciliated ependymal cells (Ortiz-Álvarez et al., 2019). Within the spinal cord, ependymal cells are found in the lining of the central canal along the entire rostro-caudal axis, though reports suggest that a higher concentration of these stem cells are present in the lumbar spinal cord (Weiss et al., 1996). These cells are thought to remain in a dormant state during adulthood, though they can be activated by physical exercise or spinal cord injury. Importantly, injury to the spinal cord triggers an increase in the proliferation of ependymal cells and modulates their expression of various transcription factors and receptors (C. B. Johansson et al., 1999; Rodriguez-Jimenez et al., 2023). These activated ependymal cells migrate to the injury site, where they may contribute to regeneration by differentiating into glial cells or releasing neurogenic factors (Barnabé-Heider et al., 2010a; Lacroix et al., 2014). Although ependymal cells can differentiate into neurons *in vitro*, the same has not been demonstrated following SCI *in vivo* (J. Li et al., 2023).

1.1.4 Neuroplasticity and Axon Regeneration after SCI

In response to injury, neurons in the adult mammalian peripheral nervous system (PNS) undergo changes in intracellular signaling and gene expression that activate a regenerative state (Huebner & Strittmatter, 2009; van Niekerk et al., 2016). This allows for the formation of new growth cones, which are sensory motile hand-like structures composed of actin and microtubules that emerge from the tip of severed axons (Hur et al., 2012). Assembly of new growth cones is a prerequisite for axonal regrowth, since they are the site of extension of new processes (Bradke et al., 2012). While damaged PNS neurons can regenerate axons, mature neurons in the CNS are unable to self-repair to the same extent.

CNS neurons lose some regenerative ability due in part to changes that occur during maturation, leading to differences in the expression and cellular distribution of key proteins (Huebner & Strittmatter, 2009). For instance, the expression of Rab11, a protein involved in the trafficking of axon growth-related molecules, becomes progressively excluded from axons during neuronal maturation, which contributes to regeneration decline (Koseki et al., 2017). Likewise, reduced neurotrophin signalling in the mature CNS also hinders regeneration after injury (B. Zheng & Tuszynski, 2023). More broadly, failure of regeneration in the CNS has been attributed to the inactive growth programme in these neurons. Whereas axonal injury in the PNS triggers an increase in the expression of hundreds of regeneration-associated genes (RAGs), there is a paucity of RAG expression in axotomized CNS neurons (Fawcett & Verhaagen, 2018). In addition, regeneration in the CNS is restricted by the instability and disorganization of microtubules, which contributes to the formation of retraction bulbs, the nongrowing counterparts of growth cones (Kulkarni et al., 2022). Another important limiting factor of regeneration in CNS neurons is the presence of axon growth-repulsive factors in the post-injury microenvironment, such as CSPGs and myelin-derived inhibitors (Qian & Zhou, 2020; B. Zheng & Tuszynski, 2023). Overall, axon repair in the CNS is extremely limited, leading to a loss of supraspinal input below the injury.

The loss of excitatory drive to spinal motor circuits is associated with persistent deficits in motor function. However, despite the lack of regeneration in the CNS, functional plasticity within neural circuits can produce partial motor recovery (Bareyre et al., 2004; Frigon & Rossignol, 2006a). As demonstrated by experimental models of SCI and human patients, spinal neural circuits surrounding an injury undergo synaptic reorganization, which enables some recovery of movement (Asboth et al., 2018b; Barbeau & Rossignol, 1987; Cadotte et al., 2012; Ding et al., 2005; Edgerton et al., 2004; Endo et al., 2008; Frigon & Rossignol, 2006b; Kazim et al., 2021; Rossignol & Frigon, 2011).

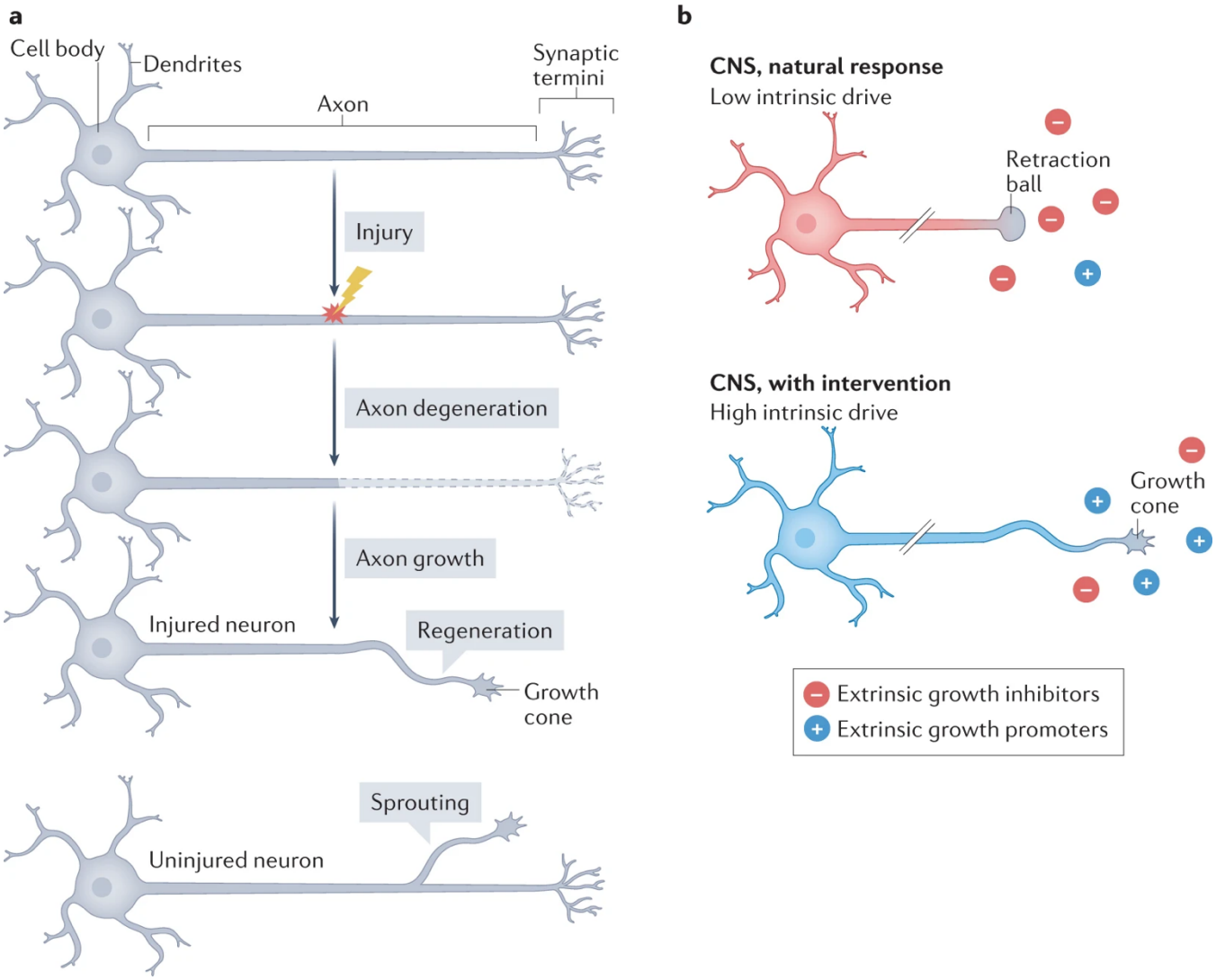

Figure 1.2. Forms of axonal repair and its regulation. A. Sprouting (axonal growth from uninjured neurons) and regeneration (axonal growth from injured neurons) after injury. **B.** Regulation of axon repair in the central nervous system. (Figure borrowed from (B. Zheng & Tuszynski, 2023), License number: 5982521480184)

Sprouting occurs in the CNS after complete injuries (Fig. 1.2), though regeneration of injured axons is extremely limited (Krenz & Weaver, 1998; B. Zheng & Tuszynski, 2023). By contrast, after incomplete injuries, substantial plasticity has been observed in both uninjured fibers and in damaged axons. In humans and animal models of incomplete SCI, compensatory sprouting occurs in the corticospinal tract, which is involved in voluntary motor control (Brown & Martinez, 2019; Fouad et al., 2001; Rosenzweig et al., 2009). In monkeys, corticospinal plasticity above and below the level of injury is associated with motor recovery (Nakagawa et al., 2015; Rosenzweig et al., 2010). In rats, incomplete SCI induces sprouting of corticospinal tracts that enable detour circuits to be formed with propriospinal

neurons (Bareyre et al., 2004). It has also been suggested that plasticity in uninjured premotor pathways such as the rubrospinal and reticulospinal tracts can support motor recovery (Ballermann & Fouad, 2006; Eilfort et al., 2024a, 2024b; Siegel et al., 2015; Weishaupt et al., 2013). There are reports of neuroplasticity in these tracts, in both humans and animal models of incomplete SCI. Finally, sprouting of propriospinal neurons can form relay circuits that transmit information past the injury and can support functional recovery (J. Cheng & Guan, 2023; Courtine et al., 2008; Filli & Schwab, 2015; Laliberte et al., 2019a).

Ascending tracts also undergo considerable remodelling, including the dorsal column-medial lemniscus pathway which carries sensory information to supraspinal centers (Kerschensteiner et al., 2005). After SCI, approximately 25% of severed dorsal column axons are capable of spontaneous outgrowth, though they fail to reach their original trajectories (Kerschensteiner et al., 2005). In mice and rats, sprouting of the ascending axons of dorsal root ganglion neurons mediates functional recovery after SCI (Granier et al., 2020; Hollis et al., 2015). In addition, post-SCI plasticity occurs in ascending propriospinal networks (Côté et al., 2012), which may contribute to the formation of detour circuits. Some of the reorganizations in spinal circuitry may be maladaptive and contribute to neuropathic pain or spasticity (Ferguson et al., 2012; Grau et al., 2017; X.-Y. Li et al., 2016; Weaver et al., 1997). To illustrate, one study reports that SCI induces sprouting in cutaneous sensory afferents which extend their projection area into regions of the spinal cord that are not typically innervated (H. J. Lee et al., 2019).

Aside from changes in the spinal cord, SCI also triggers neuroplasticity in the brain, as demonstrated by rodent and primate injury models (Serradj et al., 2017). In the sensory cortex, there is an expansion of spared sensory regions into de-afferented areas. Similarly, cortical motor maps undergo reorganization after SCI (Mohammed & Hollis, 2018).

1.2 Therapeutic Approaches to Spinal Cord Injury

An effective treatment strategy is urgently needed for SCI repair and due to the many challenges described above, a multitude of approaches are currently being explored (Fig. 1.3), including stem cells, biomaterials, growth factors, and pharmaceuticals (Kjell & Olson, 2016a). Neurotrophic factors such a NGF, BDNF, NT3, bFGF can be part of a therapeutic strategy to modulate cells' behavior, thereby improving their survival and outgrowth (Harvey et al., 2015). Cell-based approaches aim to transplant various stem cells in the hopes that they will secrete anti-inflammatory factors and differentiate into functional cells (Nandoe Tewarie et al., 2009; Q. Tang et al., 2021). This type of therapy has been shown to promote angiogenesis and modulate the immune response, leading to a regenerative effect and partial recovery from injury (Gabel et al., 2017; Yousefifard et al., 2016). However, exogenous cell transplantation is accompanied by significant drawbacks such as the risk of rejection or cancer, leading to a paucity of clinical trials. In addition, the inhospitable microenvironment in the injured cord has led to poor cell survival after transplantation, stifling its potential in SCI repair (S. Lee et al., 2015; Urdzíková et al., 2014; J. Wang et al., 2020; Z. Zhang et al., 2019).

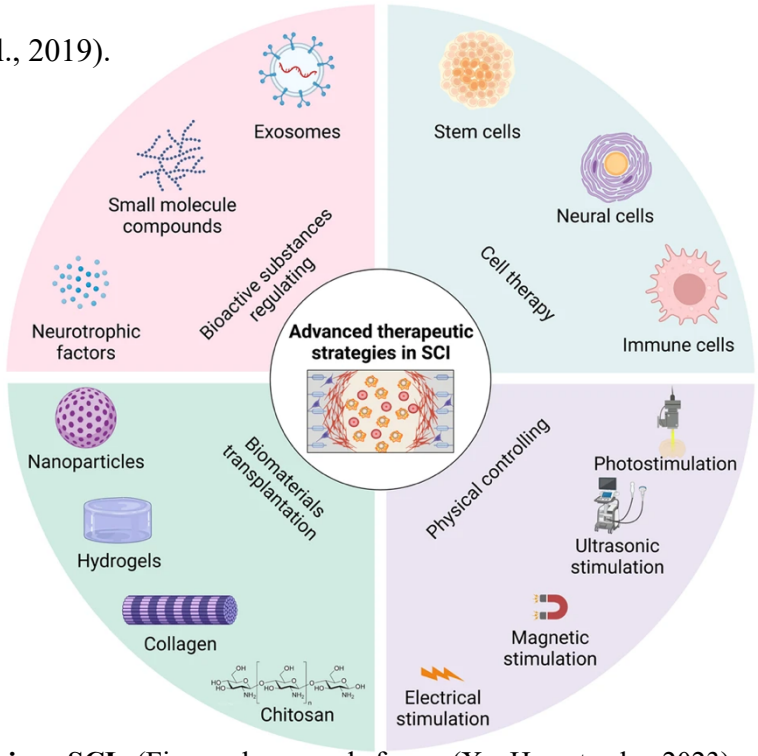

Figure 1.3. Therapeutic strategies for repairing SCI (Figure borrowed from (X. Hu et al., 2023), https://creativecommons.org/licenses/by/4.0/)

1.2.1 Scaffold-based Therapeutics for Spinal Cord Injury

To improve on purely cell-based therapies, the neural tissue engineering approach aims to produce a scaffold that can support regeneration of spinal cord tissue (Doblado et al., 2021) and address secondary injury mechanisms by providing physical or trophic support to the damaged spinal cord. In this regard, biomaterials are emerging as an important component of combinatorial therapies, which are needed to address the multifaceted nature of spinal cord injury (Ashammakhi et al., 2019; Straley et al., 2010; Tsintou et al., 2015). Scaffold-based strategies are being investigated for their regenerative potential alone or in combination with cells, growth factors, or pharmacologic agents (Führmann et al., 2017). Due to the complex pathophysiology of SCI, the field of regenerative medicine has seen a shift toward combinatorial treatments over the past few decades (Griffin & Bradke, 2020; Y. Zheng et al., 2020).

Some key elements to consider in the development of biomaterials for SCI include biocompatibility, porosity, mechanical strength, elasticity, surface chemistry, hydrophobicity and rate of degradation. The biomaterial's interaction with cells in the injury site is of particular importance, as there is potential to influence cell behavior. An ideal biomaterial for SCI repair should promote cell adhesion and ECM deposition, while allowing for the exchange of nutrients and oxygen. It must also be biocompatible and non-immunogenic. The presence of interconnected pores within a biomaterial is essential for cell infiltration and diffusion of nutrients. Pore size also has the potential to affect myelination of axons that regenerate into implanted biomaterials. This is an important consideration since myelination is essential for efficient transduction of signals and the majority of the descending corticospinal tract is myelinated. Many therapeutic strategies employ biomaterials with various three-dimensional geometries that provide structural scaffolding to guide axonal outgrowth (Nguyen et al., 2017; Sarker et al., 2018). Anisotropic structures that resemble the native ECM of the spinal cord have the potential to guide axonal projections (Xue et al., 2021). For example, *Álvarez et al.* synthesized supramolecular peptide fibril scaffolds that enhanced axonal regrowth and functional recovery (Álvarez et al., 2021). These scaffolds

create a favorable environment for neurite outgrowth and provide physical guidance cues to axonal projections, while closely mimicking the mechanical properties of the native tissue (Luo et al., 2021). Further, tissue engineering scaffolds can serve as carriers of bioactive components or cells to prevent secondary damage and enhance regeneration (Hakim et al., 2019). Various biomaterials have been studied for this purpose, including ceramics, hydrogels, collagen scaffolds, alginate scaffolds, PLGA scaffolds, hyaluronic acid scaffolds, and chitosan scaffolds.

1.2.1.1 Synthetic materials as regenerative scaffolds for SCI repair

Various synthetic polymers are used to construct scaffolds for SCI repair, since they have controllable mechanical properties and high batch-to-batch consistency. However, a major limitation of several synthetic biomaterials is hydrophobicity, which can lead to suboptimal cell adhesion. Another important concern with synthetic materials is the release of toxic by-products during degradation. Despite this, biocompatible synthetic polymers such as polyethylene glycol (PEG) have been investigated as part of therapeutic strategies for SCI. PEG is a water-soluble synthetic polymer that is stable and non-toxic (K. Chen et al., 2024). When applied to the injured spinal cord, PEG acts as a fusogen that repairs damaged neuronal membranes (X. Lu et al., 2018; A. Wang et al., 2016), thereby protecting neurons from Ca^{2+}-induced damage. This biomaterial can also be cross-linked to form porous hydrogels that provide a framework for regenerating tissue. For instance, *Estrada et al*. showed that an injectable PEG biopolymer-matrix can support regeneration of myelinated axons into the lesion and lead to a significant improvement in motor ability in a rat model of chronic SCI (Estrada et al., 2014).

Polycaprolactone (PCL)-based biomaterials have many applications in tissue engineering, including bone, tendon, skin, and nerve repair. This biomaterial has a slow degradation rate *in vivo* (B. Guo & Ma, 2014) and is often used to deliver cells to the injury site (X. Zhou et al., 2018). In one study, PCL-based scaffolds were shown to reduce glial scarring after complete SCI in a rat model, which

enhanced functional outcome (S. Zhang et al., 2018). In addition, nerve guidance scaffolds fabricated from PCL microtubes were implanted into a rat spinal cord and successfully supported axon growth (Shahriari et al., 2017). Overall, PCL is a popular material in regenerative medicine due to its safety and high processability, though it has yet to be tested in human clinical trials as a therapeutic strategy for SCI.

Biomaterials made from poly(lactic-co-glycolic acid) (PLGA) have also been studied for their ability to support spinal cord regeneration in various animal models (S. Liu et al., 2019). PLGA is a biocompatible copolymer with adjustable physical properties that can serve as a drug carrier for SCI repair. However, its hydrophobicity leads to poor cell attachment unless the surface is chemically modified. PLGA-based scaffolds have produced significant motor improvements and increased tissue remodelling in African green monkeys with an incomplete SCI (Slotkin et al., 2017). This finding led to the initiation of the 'INSPIRE' human clinical trials, which are still ongoing.

1.2.1.2 Natural materials as regenerative scaffolds for SCI repair

Collagen is one of the most promising biomaterials for SCI and has been studied extensively for this application (Breen et al., 2017a; K. Chen et al., 2024; Kourgiantaki et al., 2020; X. Li et al., 2017; Y. Yang et al., 2021; Zou et al., 2020). As a major component of the ECM, collagen exhibits excellent biocompatibility and cell adhesion properties. It can be used for delivery of cells, bioprinting scaffolds, electrospinning fibers, or producing hydrogels. For instance, injectable collagen hydrogels were shown to reduce glial scarring in a rat model of SCI (Breen et al., 2017a). However, some types of collagen, such as type-I, have been reported to stimulate astrocyte reactivity and worsen glial scarring (Hara et al., 2017). Collagen biomaterials may be chemically cross-linked (Tamura et al., 2022) or mixed with other materials such as chitosan (Sun et al., 2019) to produce scaffolds that have an optimized mechanical strength for spinal cord repair. Collagen-based scaffolds can also be functionalized to further promote SCI repair, as demonstrated by several animal studies. For example, linearly ordered collagen scaffolds were functionalized with cetuximab, which resulted in tissue repair and motor recovery after SCI in dogs (X.

Li et al., 2017). Importantly, collagen is one of the few biomaterials that have entered clinical trials (K. Chen et al., 2024). In two human SCI patients, collagen scaffolds loaded with mesenchymal stem cells promoted recovery of sensory and motor functions (Xiao et al., 2018).

Fibrin is another natural biomaterial that has been investigated as a tissue engineering scaffold due to its many advantages including biocompatibility, excellent cell attachment, and degradability. Fibrin is involved in the coagulation cascade and serves as a remodelable matrix for tissue repair (Roberts et al., 2020). Currently, fibrin is used clinically as a tissue adhesive for skin repair (Currie et al., 2001) and several groups have shown the potential of fibrin-based biomaterials for SCI. For instance, aligned fibrin hydrogels were made by electrospinning and implanted in a dorsal hemisected spinal cord injury model to promote new axon regrowth and improvements in locomotor performance (Yao et al., 2018). In a rat model of SCI, fibrin scaffolds were shown to be conducive to regeneration and cellular migration (Johnson et al., 2010). In addition, injectable fibrin scaffolds may be a delivery vehicle to transplant cells into the lesion site (X. He et al., 2022). In such gels, stiffness can be influenced by modulating the relative amounts of fibrinogen and thrombin, although poor mechanical strength remains an important limitation to fibrin-based constructs for SCI (Z. Yu et al., 2020).

Alginate is a natural material suitable for use in neural tissue engineering. This polysaccharide can be extracted from brown algae and is often used in hydrogels for SCI (Jarrah et al., 2022). Alginate gels are biocompatible, chemically modifiable and can be cross-linked to create anisotropic capillary structures. Studies demonstrate the potential of non-functionalized alginate hydrogels in reducing fibrous scarring and supporting recovery from SCI (Huang et al., 2020; Sitoci-Ficici et al., 2018). Further, alginate was shown to enhance elongation of regenerating axons in the spinal cord of young rats (Kataoka et al., 2004). These scaffolds can also be seeded with cells or growth factors to induce recovery of motor function after SCI (Grulova et al., 2015).

Hyaluronic acid (HA) is a key structural component in the native extracellular matrix of the central nervous system and can be made into hydrogel scaffolds that provide neuroprotection and promote repair from SCI (Kushchayev et al., 2016; Thompson et al., 2018). Injectable hydrogels made from HA were reported to induce angiogenesis, remyelination, axonal regeneration, and functional recovery after SCI (P. Fan et al., 2024). Such scaffolds are often used to deliver and retain cells at the injury site, as they are known to increase the stability and survival of implanted cells (Mothe et al., 2013). The glial scar is also a common target for hyaluronic acid biomaterials, as high molecular weight HA is known to affect the behavior of astrocytes after SCI (Dovedytis et al., 2020). One important drawback of HA-scaffolds is poor cell adhesion (X. Wang et al., 2012), which can be addressed by adding peptide coatings or creating composite scaffolds with other materials.

Plant tissue has emerged as a material of interest for various tissue engineering applications, including for the repair of skin (Dikici et al., 2019; Peng et al., 2022), tendon (Contessi Negrini et al., 2020), nerve (F. Chen et al., 2021), and bone (Balasundari et al., 2012; Contessi Negrini et al., 2020; J. Lee et al., 2019). Plant tissue can be decellularized using detergents, sonication, enzymatic digestion, or freeze-thawing methods to produce cellulose-based scaffolds (Bilirgen et al., 2021; F. Chen et al., 2021; Y.-W.; Fontana et al., 2017a; Harris, Lacombe, Liyanage, et al., 2021; Hickey et al., 2018a, 2023; J. Lee et al., 2019; Phan et al., 2020; Robbins et al., 2020; Salehi et al., 2020; Toker-Bayraktar et al., 2023; Varhama et al., 2019; Y. Wang et al., 2020a). Apple hypanthium-derived cellulose was first used as a scaffold for 3D mammalian cell culture (Modulevsky et al., 2014), with several other groups following suit (Bilirgen et al., 2021; Fontana et al., 2017b; Gershlak et al., 2017; Toker et al., 2020a). Importantly, plant cellulose biomaterials were shown to be biocompatible and support cell infiltration *in vivo* (Hickey et al., 2018b; Modulevsky et al., 2014, 2016). Plant scaffolds can be functionalized with chemical coatings to promote cell adhesion (Couvrette et al., 2023; Fontana et al., 2017a) or to control their mechanical

properties and attain values similar to those of specific human tissues (Harris, Lacombe, & Zenhausern, 2021).

One major advantage of plant scaffolds is their interconnected porosity. The topography and internal microstructures that occur naturally within plant tissue present a unique opportunity to influence cell behavior, signaling, alignment and migration *in vivo* (Honig et al., 2020; Y. Wang et al., 2020b). For example, topographical cues within decellularized green onion scaffolds were shown to promote alignment of skeletal muscle tissue *in vitro* (Y.-W. Cheng et al., 2020b). Similarly, celery-derived scaffolds have been used for tissue engineering of tendons (Contessi Negrini et al., 2020). The topography of these vegetal scaffolds guided the growth and alignment of L929 fibroblasts.

Some challenges exist around using plant-based biomaterials for tissue engineering applications. For certain species, decellularization dramatically reduces the mechanical strength of the plant, which is an important limitation for their use as tissue scaffolds (Toker-Bayraktar et al., 2023). As well, the degradation behavior of scaffolds *in vivo* should be considered and optimized for specific applications. These issues may be solved by using cross-linking or other methods to adjust mechanical strength and durability. Finally, reproducibility may be a challenge if the cultivating conditions of plants used in these studies are not standardized. This is often the case, since the plants are typically sourced from grocery stores, leading to batch-to-batch variations that can alter the plants' characteristics.

1.3 Rodent Model of Spinal Cord Injury

Several experimental animal models of SCI have been developed to better understand SCI pathology and to test treatments aimed at producing functional recovery. Rodent models are widely used in preliminary studies to mimic various types of SCI, including contusion, compression, distraction, transection & chemical injury. Contusion models of SCI rely on impactor devices to inflict an acute injury

using the weight-drop technique. By contrast, compression SCI models involve prolonged compression of the spinal cord, which is intended to replicate the damage caused by dislocations and burst fractures in humans (Cheriyan et al., 2014). Distraction SCI devices are used to cause damage by controlled stretching of the cord while other devices produce dislocation-type SCI by displacing vertebrae to reproduce the anterior fracture-dislocation injuries. Surgical transection of the cord is a particularly useful model for testing implantable biomaterials.

Despite the general pathophysiology of SCI being shared between most species, there are key differences between rodent models and human SCI (Kjell & Olson, 2016b). In addition to anatomical and functional differences between species, there are differences in injury complexity, immune responses to SCI, and post-injury neuroplasticity (Filipp et al., 2019; Sharif-Alhoseini et al., 2017). To illustrate, in mice there is no formation of fluid-filled cysts after injury (Hachem & Fehlings, 2021; Ma et al., 2001; METZ et al., 2000) which is common in human SCI and in rat models of SCI. In rats, there is only slight plasticity of the corticospinal tract after hemisection, whereas extensive spontaneous plasticity of corticospinal axons is seen in monkeys (Rosenzweig et al., 2010). It is therefore important to interpret results from experimental SCI models cautiously when attempting to translate them to human applications.

Various behavioral examinations have been developed to assess recovery of motor and sensory function in rat models of SCI. The limb grip strength test (K. D. Anderson et al., 2005) and the forelimb reaching task are used to evaluate motor recovery in rat models of cervical SCI, which profoundly affects motor control of the forelimb (Ahmed et al., 2019). Standardized tests are used to assess locomotor recovery and coordination, including the BBB open field assessment (BASSO et al., 1995), the swim test (Smith, Burke, et al., 2006; Xu et al., 2015), the inclined plane test (Rivlin & Tator, 1977), and horizontal ladder walking. To monitor changes in sensory ability in rat SCI models, the Von Frey filament test (Chaplan et al., 1994) and hot-cold sensory tests have been useful.

Several factors have an influence on motor recovery in animal models of SCI, including housing conditions and physical activity levels. For instance, the presence of environmental enrichment in the animals' cages can enhance neuroplasticity, thereby improving sensory and motor recovery (Berrocal et al., 2007; Clemenson et al., 2015; De Virgiliis et al., 2020; Hutson et al., 2019; Koopmans et al., 2012; McDonald et al., 2018; Neves et al., 2023; Tai et al., 2021). In rodent SCI models, enrichment potentiates the regenerative ability of neurons via Creb-binding protein-mediated histone acetylation, which increases expression of regeneration-associated genes (Hutson et al., 2019). In addition, physical activity such as treadmill training is known to partially restore animals' motor ability after SCI (Shibata et al., 2021). Similarly, an enriched cage design that encourages climbing was shown to improve locomotor recovery in SCI mice (Burke et al., 2023). Other factors such as the breeding colony from which animals originate can also produce variability in animals' motor ability (O'Bryant et al., 2011).

1.4 Neural Control of Mammalian Locomotion & the Role of Sensory Feedback

Vertebrate locomotion depends on the activity of central pattern generators (CPGs) (Grillner, 1981), which are spinal neuronal circuits that coordinate muscle activation to produce rhythmic movements (Grillner & Kozlov, 2021). Activity of the mammalian locomotor CPG is initiated by descending inputs from supraspinal command centers such as the mesencephalic locomotor region in the brainstem (Kozlov et al., 2009; MacKay-Lyons, 2002). These descending fibers innervate excitatory ˙interneurons, which in turn excite motoneurons and certain inhibitory interneurons to produce flexor–extensor and left–right alternation during walking (Manira, 2009). Motoneurons within the locomotor CPG network receive alternating glutamatergic excitation and GABAergic & glycinergic inhibition as well as neuromodulation from noradrenaline and serotonin (Grillner, 2003; Rank et al., 2011). In addition to facilitating the activation of ion currents that generate locomotor rhythms (Tazerart et al., 2007),

monoamines such as serotonin activate receptors on spinal motoneurons, which facilitates persistent inward currents (PICs) that increase motoneuron excitability and ultimately enable muscle contraction (Hultborn et al., 2003; Rekling et al., 2000). The basic locomotor pattern generated by spinal CPGs is continuously modulated by supraspinal input as well as sensory feedback, which is necessary to adjust motor patterns to the dynamically changing environment (Oliver et al., 2021; Pearson, 2004). Sensory afferents have widespread projections by which they affect the excitability of neural targets throughout the CNS, including motoneurons, spinal interneurons, and neurons that ascend to supraspinal structures. The dorsal horn of the spinal cord acts as a sensory processing center, where many populations of spinal neurons integrate sensory inputs from proprioceptive, cutaneous, and nociceptive afferents to shape sensory integration and motor control (Fig. 1.4) (Orlovsky et al., 1999; Windhorst, 2007).

Proprioceptive information relating to the position of limbs in space and their degree of weight bearing is relayed to the CNS by afferents of muscle spindles (group Ia and II) and Golgi tendon organs (group Ib) (Proske & Gandevia, 2012). These afferents have nuclei in the dorsal root ganglion at each segment of the spinal cord. Processing of proprioceptive information occurs both at the level of the spinal cord and in supraspinal structures such as the cerebellum and somatosensory cortex (Santuz et al., 2022). Proprioceptive feedback contributes to the regulation of normal locomotor patterns as it influences activation of motoneurons in many vertebrates and invertebrates alike (Head & Bush, 1991; Zill, 1985). Muscle spindle afferents provide information about changes in muscle length occurring at specific times during the step cycle, while Golgi tendon organ afferents transduce total muscle force (Frigon et al., 2021). This information is particularly important for facilitating switching between phases of the gait cycle. In the cat, sensory feedback from Golgi tendon organs was shown to mediate the activation of extensor muscles based on their degree of loading (Gossard et al., 1994; Pearson & Collins, 1993). In humans, stretching of the soleus muscle during walking generates afferent feedback from group Ia pathways which

enhances the locomotor drive (Mazzaro et al., 2005). Similarly, feedback from muscle spindles regulates stepping in mice and the absence of proprioceptive feedback causes the locomotor pattern to degrade (Akay et al., 2014). In particular, mice with attenuated proprioceptive feedback exhibit a loss of inter-joint coordination and alternation of flexor/extensor muscles.

Cutaneous afferents innervate the skin and transmit tactile sensory information to the brainstem for processing by cuneate neurons (Wei et al., 2024). Low-threshold mechanoreceptors gather information about pressure, texture, and vibration on the external surface of the body. These include Merkel discs (slowly adapting type 1) that respond to static pressure on the skin, Ruffini endings (slowly adapting type 2) that sense skin stretching, Meissner corpuscles (rapidly adapting Type 1) that sense light touch and low frequency vibrations, and Pacinian corpuscles (rapidly adapting type 2) that detect rapid vibrations. Cutaneous afferents project to the dorsal horn of the spinal cord, where some ascend to the brain while most synapse on locally projecting interneurons (Abraira & Ginty, 2013). This cutaneous feedback plays an important role in regulating body balance (Zehr & Stein, 1999), fine control of locomotion, and scaling the motor responses initiated by other sensory cues (Bolton & Misiaszek, 2009). Cutaneous input participates in correction of limb and foot placement, which is particularly important in challenging tasks such as crossing a ladder or slope walking (Bouyer & Rossignol, 2003a; H. Park et al., 2019). To illustrate, cutaneous afferent feedback can elicit the stumbling corrective reaction in mice, allowing animals to step over obstacles (Mayer & Akay, 2018). Overall, cutaneous input appears to have a modulatory influence on locomotion.

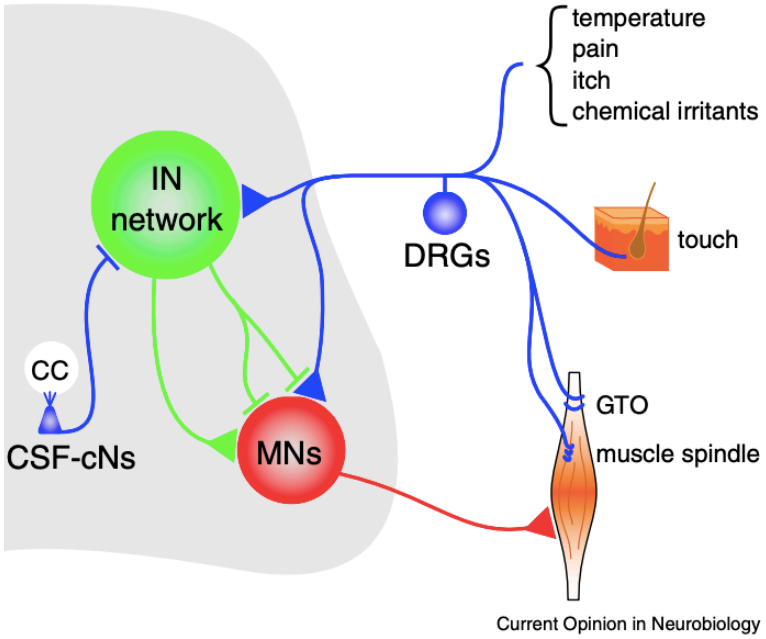

Figure 1.4 Sensory feedback circuits in the spinal cord. Peripheral sensory information (cutaneous and proprioceptive) is carried by dorsal root ganglion (DRG) neurons and provides excitatory input either directly to motor neurons (MNs) or to the spinal interneuron (IN) network. (Borrowed from (Böhm & Wyart, 2016), License number: 5982730647912)

1.4.1 Role of Sensory Feedback in Locomotion after SCI

Afferent feedback is not generally considered to act as a driving force for normal locomotor CPG function, but rather as a modulatory input that adapts locomotor patterns to the environment. In animals with intact spinal cords, locomotor CPGs can generate basic rhythmic movements in the absence of sensory feedback (Bouyer & Rossignol, 2003a; Klarner & Zehr, 2018; Rossignol et al., 2006; Rybak et al., 2006). For instance, it is possible for cats to recover basic movement patterns after surgical removal of cutaneous feedback (Bouyer & Rossignol, 2003a). Therefore, sensory input is not essential for the generation of locomotor patterns in intact animals.

However, sensory signaling is critical for the recovery of locomotion after SCI, as it may become instructive to locomotor CPGs in a feedforward manner (Courtine et al., 2009) and spinal circuits may use sensory input to generate motor output with limited commands from the brain (Takeoka, 2020). This is well illustrated by the spinal cord's ability to generate rhythmic motor activity upon epidural electrical stimulation (EES), which recruits sensory afferents to activate motoneurons in spinal circuits caudal to an

injury (Courtine et al., 2009; Lavrov et al., 2008; Musienko et al., 2007) (Capogrosso et al., 2013; Formento et al., 2018).

Furthermore, sensory inputs have been proposed to facilitate neuroplasticity in these networks that could be beneficial to recovery of locomotor function (Côté & Gossard, 2004; Frigon et al., 2021; Merlet et al., 2021; Smith, Shum-Siu, et al., 2006a; Takeoka, 2020; Takeoka et al., 2014; Takeoka & Arber, 2019; Yen et al., 2014). As fMRI studies in both rats and humans have demonstrated, spinal processing of sensory input is altered after SCI, with a significant amplification of peripheral inputs caudal to the injury (Cadotte et al., 2012; Endo et al., 2008). In particular, proprioceptive afferents contribute to locomotor recovery after SCI through activity-dependent reorganization (Takeoka & Arber, 2019). *Takeoka et al.* demonstrated that after SCI, proprioceptive afferent connectivity is altered below the injury and that group Ia afferents form new synaptic contacts with hindlimb motoneuron pools (Takeoka & Arber, 2019). It is proposed that increased proprioceptive input to spinal motoneurons may compensate for the lack of descending input after SCI (Takeoka, 2020) and that proprioceptive input to spinal circuits acts as a driving force for motor output after injury (Takeoka & Arber, 2019). This aligns with the findings of earlier studies, which demonstrated that spinalized mice without functional muscle spindle feedback are unable to recover hindlimb motor function (Takeoka et al., 2014) and that augmented proprioceptive feedback enhances the effect of locomotor training on motor recovery in humans (Yen et al., 2014).

The role of cutaneous afferents in motor recovery after SCI was investigated in 1995 by Muir and Steeves, who found that phasic stimulation of cutaneous receptors improved leg motion during swimming in spinal hemisected chicks (Muir & Steeves, 1995). Importantly, this swimming assessment was used to study cutaneous feedback in the absence of limb loading. Similarly, in rats with an incomplete SCI, increased cutaneous feedback improves hindlimb function during swimming (Smith, Shum-Siu, et al., 2006b). Moreover, cutaneous feedback was shown to enhance plantar stepping in spinal rats in the upright

posture (Sławińska et al., 2012). Likewise, studies performed on spinalized cats also suggest a role for cutaneous inputs in recovery of locomotion. *Bouyer et al* found that cutaneous denervation of the hind paws before spinal transection impairs recovery of both paw placement and weight support in cats (Bouyer & Rossignol, 2003a, 2003b). Further, in transected cats that had recovered some hindlimb locomotion, subsequent cutaneous denervation of hind paws caused the loss of proper paw placement and a reduction in weight support. Although a role has been established for cutaneous feedback in motor recovery after SCI, the relative contribution of cutaneous and proprioceptive feedback is still unclear.

Possible mechanisms have been proposed to explain sensory-mediated plasticity after SCI. The synaptic competition model, for instance, supposes that descending pathways and ascending sensory pathways compete for space in the spinal cord (Jiang et al., 2016). According to this model, the removal supraspinal input caused by the injury could stimulate sprouting in sensory afferents, which would usurp the space left by transected corticospinal fibers (Merlet et al., 2021). In other words, strengthened synaptic connections between sensory afferents and motoneurons in CPGs below the injury might compensate for the loss of supraspinal drive after SCI (Eisdorfer et al., 2020).

Another hypothesis proposes that propriospinal circuits caudal to the injury may be dynamically reorganized to activate motor pools in lumbar CPGs (Eisdorfer et al., 2020), with mounting evidence pointing to propriospinal interneurons as key players in this plasticity (J. Cheng & Guan, 2023; Laliberte et al., 2019b). For example, V2a neurons are part of the mammalian locomotor network and have been implicated in CPG activation after SCI (Kathe et al., 2022; Squair et al., 2023). In mice, lumbar V2a neurons become hypersensitive to serotonin after injury, which may contribute to plasticity of the locomotor network (Husch et al., 2012). Another population of spinal neurons known as V3s receive direct sensory input from group Ia proprioceptive afferents and interface with motoneurons within CPG circuits,

although it is unclear if they participate in generating locomotor patterns (Chopek et al., 2018; Lin et al., 2019). Spinal dI3 neurons are a population of excitatory neurons in the spinal cord that transmit sensory input to motoneurons and have an essential role in recovery of locomotor activity after SCI (Brownstone & Bui, 2010; T. V. Bui et al., 2013; T. V Bui et al., 2016; Goltash et al., 2023). In the intermediate spinal cord, dI3 neurons can be identified by the expression of the Islet-1 (Isl1) transcription factor and they are known to project ipsilaterally within the spinal cord (T. V Bui et al., 2016). Previous work from our lab found changes in sensory inputs to dI3 neurons after SCI (Goltash et al., 2023). Taken together, these findings indicate a possible role for dI3s in the re-activation of motor circuits using sensory input. In short, spontaneous neuroplasticity occurring below the level of the spinal cord injury contributes to recovery of locomotor function and the importance of sensory feedback appears to be heightened after injury.

Hypothesis & Objectives

1. I hypothesize that plant-based scaffolds can be functionalized to support the growth of rat fetal neural stem cells (NSCs) *in vitro*.
   1.1. Cellulose scaffolds will be coated with poly-L-Ornithine and I will study the effect on neuronal cell attachment and proliferation.
   1.2. I hypothesize that the scaffold's topographical cues can influence the behavior of NSCs. I predict that the plant biomaterial's naturally occurring microarchitecture will provide physical guidance for cell growth and alignment.
   1.3. I will assess the ability of NSCs adhered to the plant scaffold to undergo multi-lineage differentiation *in vitro*. Specifically, I will determine if scaffold seeded NSCs can differentiate into neurons and astrocytes.

2. I hypothesize that plant-derived scaffolds can produce motor recovery in a rat model of SCI.
   2.1. Biocompatibility of the PLO-coated scaffold will be assessed by a 12-week subcutaneous implantation study in adult Sprague Dawley rats. Immune reaction will be assessed via histological analysis (Hematoxylin & Eosin staining) and Masson's Trichrome staining to visualize collagen deposition into the biomaterial. In addition, immunostaining will be done for relevant markers such as CD45 (hematopoietic cells) and CD31 (endothelial cells) to show immune cell infiltration and biomaterial vascularization.
   2.2. The PLO-coated biomaterial will then be implanted into a T8 complete transection injury as an acute treatment. Spinal cord tissue regeneration will be examined and locomotor recovery will be tracked.
      2.2.1. For 14 weeks following the spinal cord surgery, recovery of motor function in rats will be evaluated using the Basso Beattie Bresnahan (BBB) open-field assessment. Moreover, a weekly swim test will be performed to evaluate forelimb & hindlimb movements and body position. Proprioception will be assessed by an inclined plane test.
      2.2.2. Post-injury neural architecture will be visualized using neuronal tracers to determine if axons regenerate across the injury site. The descending corticospinal tract will be labelled via tracer injection into the rats' motor cortex while ascending sensory tracts will be labelled by tracer injection in the sciatic nerve. Samples will then be imaged by confocal laser scanning microscopy and the number of axons will be quantified in the treatment and control tissue.
      2.2.3. Changes in the injury microenvironment and regeneration of spinal cord tissue will be evaluated by immunostaining with markers such as β III tubulin (nascent neurons), NF200 (myelinated neurons), 5-HT (serotonin), and GFAP (astrocytes).

3. I hypothesize that cutaneous input below the level of SCI plays a role in the re-activation of spinal motor circuits
   3.1. I will test whether additional cutaneous input affects motor output
   3.2. I predict that removal of cutaneous input may reduce motor output
   3.3. I will investigate whether dI3 neurons play a role in sensory-dependant motor recovery after SCI

Chapter 2: Plant cellulose as a substrate for 3D neural stem cell culture

This chapter was adapted from a published research paper:

Couvrette, L. J., Walker, K. L. A., Bui, T. V., & Pelling, A. E. (2023). Plant Cellulose as a Substrate for 3D Neural Stem Cell Culture. Bioengineering, 10(11), 1309.
https://doi.org/10.3390/bioengineering10111309

2.1 Abstract

Neural stem cell (NSC) based therapies are at the forefront of regenerative medicine strategies for various neural defects and injuries such as stroke, traumatic brain injury and spinal cord injury. For several clinical applications, NSC therapies require biocompatible scaffolds to support cell survival and to direct differentiation. Here, we investigate decellularized plant tissue as a novel scaffold for three-dimensional (3D) *in vitro* culture of NSCs. Plant cellulose scaffolds were shown to support attachment and proliferation of adult rat hippocampal neural stem cells (NSCs). Further, NSCs differentiated on the cellulose scaffold had significant increases in their expression of neuron-specific beta-III tubulin and glial fibrillary acidic protein compared to 2D culture on a polystyrene plate, indicating that the scaffold may enhance differentiation of NSCs towards astrocytic and neuronal lineages. Our findings suggest that plant-derived cellulose scaffolds have the potential to be used in neural tissue engineering and can be harnessed to direct differentiation of NSCs.

2.2 Introduction

Neural stem cells (NSCs) are self-renewing cells that proliferate *in vitro* and maintain the capacity to differentiate into neurons, astrocytes, and oligodendrocytes (Gage, 2000). NSC transplantation is being investigated as a therapeutic strategy for numerous disorders of the central nervous system (Cao et al., 2002; Y. Tang et al., 2017) and many preclinical studies report promising results (Zhao et al., 2019; J. Zhu et al., 2005). However, there are currently important limitations to the efficacy of NSC therapies such as low transplant survival and poor efficiency of neuronal differentiation. To overcome these issues, biocompatible scaffolds have emerged as a vehicle to engraft NSCs while supporting survival of the transplanted cells (Tejeda et al., 2022). Cell scaffolds can enhance therapeutic efficacy of NSCs by promoting strong cell adhesion, guiding cell migration, and shielding transplanted NSCs from the cytotoxic injury environment occurring in CNS injuries (Hwang et al., 2014; Tejeda et al., 2022). Moreover, since NSC differentiation is mechanosensitive (W. Chen et al., 2014; Rammensee et al., 2017), scaffolds' physical properties such as porosity and elastic modulus can be exploited to influence stem cell differentiation (Czeisler et al., 2016; Lim et al., 2010; F. Liu et al., 2021). It has been shown that stiffer matrices tend to be myogenic whereas softer matrices favor neuronal differentiation (Engler et al., 2006) and promote expression of the neuronal marker βIII-tubulin in adult neural stem-cells(Saha et al., 2008). Scaffold alignment also guides stem cell differentiation (Metavarayuth et al., 2016; Subramony et al., 2013) and studies indicate that anisotropic topographies support further axonal extension relative to isotropic topographies (W. Li et al., 2015).

In addition to physical cues, manipulating surface chemistry has been extensively investigated as a method to direct migration, proliferation, and differentiation of NSCs (Flanagan et al., 2006; Joseph et al., 2021; Ren et al., 2009; J.-H. Wang et al., 2006). For instance, *Ge et al.* studied the effects of Poly-L-ornithine (PLO) on cell behavior *in vitro* and determined that NSCs cultured on PLO had enhanced cell

migration (Ge et al., 2016). We hypothesized that this coating would enhance attachment and growth of cells to a plant scaffold and encourage migration into its channels. As well, PLO was shown to induce preferential differentiation into neuronal and oligodendrocytic cell types (Ge et al., 2015). This is of particular importance, since one of the key challenges in NSC therapies is directing the differentiation of neural stem cells towards the neuronal lineage. Finally, Ping, Jie et al. demonstrated that poly-l-ornithine enhances myelin regeneration and promotes locomotor recovery in an animal model of focal demyelination (Xiong et al., 2023), suggesting that PLO has potential to be part of a regenerative therapeutic strategy for injuries of the central nervous system. Likewise, NH_2-terminated surfaces have been shown to promote neuronal differentiation of NSCs (Ren et al., 2009) . Further, some researchers have harnessed both topography and surface chemistry to direct stem cell behavior on scaffolds (Edelbrock et al., 2021; Macgregor et al., 2017).

In recent years, various three-dimensional cell culturing methods have been developed using scaffold-based technologies. These systems more accurately represent the *in vivo* microenvironment compared to traditional two-dimensional culture on polystyrene (Fontoura et al., 2020) and the behavior of cells within 3D systems is more physiologically relevant, making it a better cell culturing method for tissue engineering and drug discovery (Belfiore et al., 2021; Breslin & O'Driscoll, 2013; Du et al., 2009; Hong et al., 2020; Marei et al., 2022; Yoshii et al., 2015). As such, various scaffold-based neural constructs have been developed for use in disease modeling, regenerative medicine, and the study of the stem cell niche (Bao et al., 2018; Edmondson et al., 2014; Y. Hu et al., 2022; Vagaska et al., 2020).

In the past decade, plant-derived scaffolds have been used successfully in numerous independent studies, by many research groups worldwide. The biocompatibility of plant scaffolds has been extensively studied both *in vitro* and *in vivo.* Many plant species and tissues such as apple (Modulevsky et al., 2016),

leek (Toker et al., 2020b), parsley (Gershlak et al., 2017), spinach (Robbins et al., 2020), green onion (Y.-W. Cheng et al., 2020b), *Flammulina velutipes* (F. Chen et al., 2021), tobacco BY-2 cells (Phan et al., 2020), *Camellia japonica* (Varhama et al., 2019) and brown seaweed (K. Y. Lee & Mooney, 2012) have been studied with many cell lines including C2C12 myoblasts, human foreskin fibroblasts, HeLa cells (Modulevsky et al., 2014), NIH 3T3 cells (Hickey et al., 2023), human mesenchymal stem cells and human pluripotent stem cell derived cardiomyocytes (Gershlak et al., 2017). For example, spinach leaves were decellularized while maintaining their vascular architecture, which was then repopulated with human dermal microvascular endothelial cells (Dikici et al., 2019). In addition to the extensive *in vitro* biocompatibility testing, several plant species have been studied *in vivo* for applications such as cardiac tissue repair (Dai et al., 2023), tissue engineering of skin (Dikici et al., 2019; Peng et al., 2022; T. Zhu et al., 2019), tendons (Contessi Negrini et al., 2020) and bone (Balasundari et al., 2012; Contessi Negrini et al., 2020; J. Lee et al., 2019; Maxime Leblanc Latour, 2020; Venkatesan & Kim, 2010). Plant-based biomaterials were shown to support cell infiltration and vascularization *in vivo* (Hickey et al., 2018b; Modulevsky et al., 2014, 2016). In one study, *Flammulina velutipes* mushroom was successfully used as a nerve guidance conduit in a rat model of sciatic nerve defect (F. Chen et al., 2021). As evidenced above, plant-derived biomaterials are becoming increasingly attractive for biomedical applications, which can be attributed in part to improved cost effectiveness, scalability, and lower immunogenicity relative to animal sources.

Here, we investigate the viability of a plant-derived biomaterial as a 3D *in vitro* culture system for adult rat neural stem cells. We hypothesized that the stalks of *Asparagus officinalis*, which are composed of linearly arranged microchannels, would produce a scaffold with an interesting surface topology for the culture of neural stem cells, as topology is known to influence NSC differentiation and axon guidance. We first examined the asparagus scaffold's physical characteristics by scanning electron microscopy and

mechanical testing. Next, the scaffold's ability to support attachment and migration of NSCs was assessed for various time periods. Further, we examined the differentiation potential of neural stem cells in this 3D culture system by immunostaining for markers including neuron-specific β-III tubulin and glial fibrillary acidic protein.

2.3 Results

2.3.1 Characterization of plant cellulose scaffold

Raw *Asparagus officinalis* stalks were cut into discs of 4mm in diameter and 1.2mm in height, which were then decellularized to remove all native cells. The resulting scaffold is composed of vascular bundles (VBs) interspersed between parenchyma (Fig. 2.1A). Naturally occurring structures within the scaffold were characterized by scanning electron microscopy (Fig. 2.1B-D). A majority of the scaffold's surface consists of parenchyma that have an average pore diameter of 39 ± 15μm. In addition, each scaffold was found to contain 14 ± 2 vascular bundles, which are aligned channels that traverse the length of the scaffold, with an average spacing of 602 ± 61μm. The distribution of channel diameters observed in these scaffolds may be conducive to cell survival, since such porous networks have previously been demonstrated to enable nutrient exchange and waste removal within scaffolds (Loh & Choong, 2013; Rasoulianboroujeni et al., 2018). The Young's Modulus of the cellulose scaffold in culture media at 37˚C is 128 ± 20 kPa (n = 5) when measured parallel to the long axis. Moreover, the scaffolds were coated overnight in poly-L-ornithine (PLO) to promote cell attachment. Surface modification with PLO was confirmed with SEM (Fig. 2.1D).

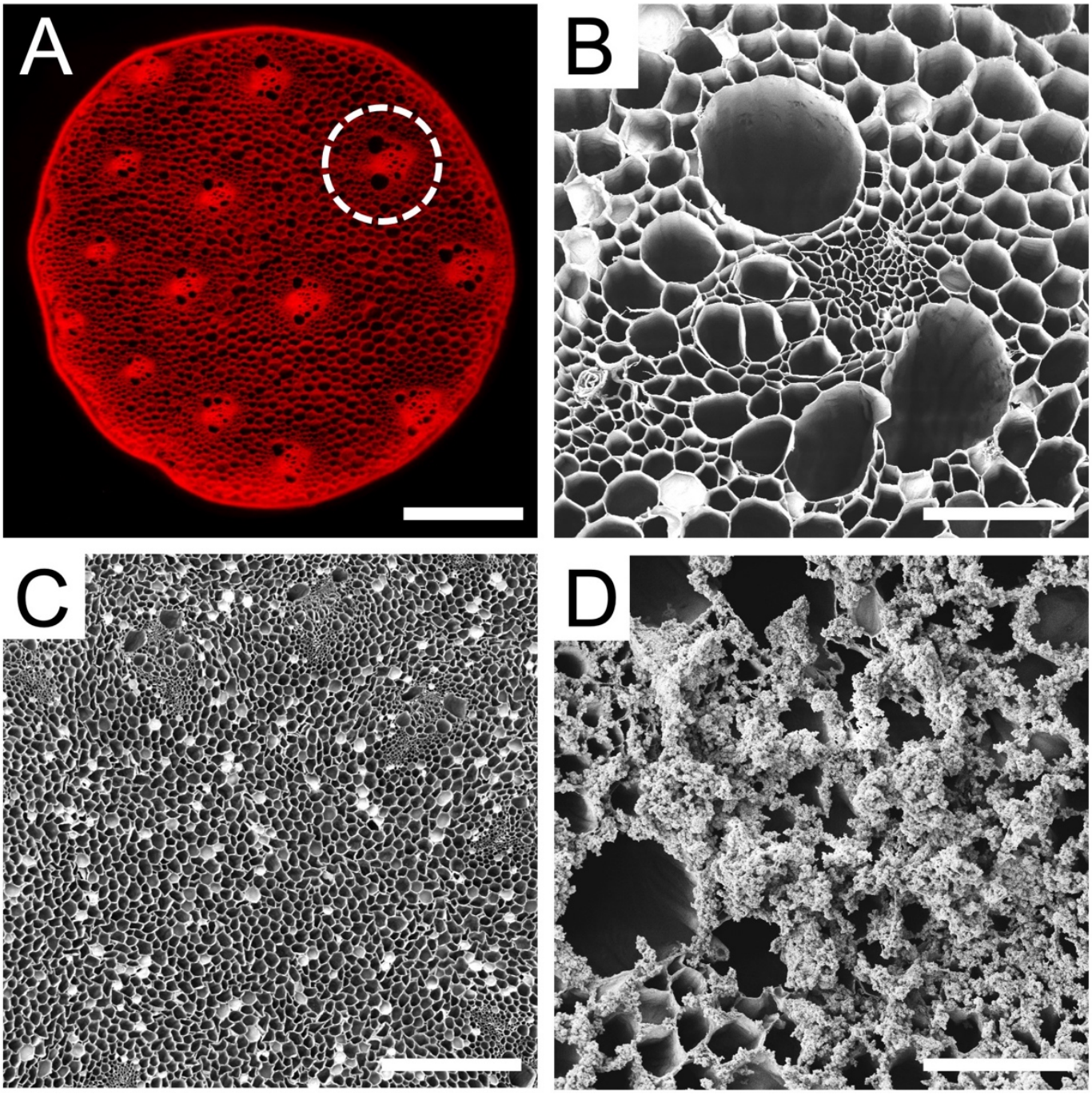

Figure 2.1. Cross sections of decellularized *Asparagus officinalis* scaffolds. A. Confocal microscope maximum intensity projection of a decellularized asparagus scaffold stained with Congo Red for cellulose. The decellularization process preserves vascular bundles (VBs, circled), which are microchannels that run along the asparagus stalk and separated by porous parenchyma tissue (scale bar = 1mm). **B.** High magnification SEM of an individual VB within scaffold which reveals the long microchannels (scale bar = 100µm). **C.** SEM of the parenchyma tissue which reveals numerous pores with a wide distribution of diameters (scale bar = 500µm) **D.** Higher magnification SEM of a scaffold coated with poly-L-ornithine, a positively charged synthetic amino acid which gives the scaffold surface a sabulous appearance (scale bar = 100µm).

2.3.2 Cellulose scaffold supports rat NSC attachment and proliferation

A single-cell suspension of NSCs was seeded onto PLO coated scaffolds and cultured for 3 to 14 days. As early as 3 days in culture, neurospheres had attached to the cellulose scaffold and were visualized through F-actin staining (Fig. 2.2A). Many neurospheres with diameters of 50μm to 300μm were found on the surface of the scaffold (Fig. 2.2B). By 14 days in culture the same high density of neurospheres on the scaffolds was observed to persist (Fig. 2.2C). In order to examine how the NSCs penetrated into the VB microchannels, the scaffold was sectioned longitudinally along it long axis. This allowed us to visualize the migration of NSCs and neurospheres down the cellulose channels (Fig. 2.2D). Importantly, NSC cells and neurospheres were observed inside of the scaffold as well as on its surface. Finally, we also observed that NSCs were able to migrate out of the attached neurospheres (Fig. 2.2E). Groups of cells were observed migrating and extending out from several neurospheres onto the scaffold. In addition to microscopic examination, cell proliferation was also assessed. This was achieved on the scaffolds with an AlamarBlue assay, which monitors the chemical reduction of culture media to detect metabolic activity of cells. Over 5 days in culture (Fig. 2.3), the percentage of reduced AlamarBlue reagent increased progressively, indicating continued growth of NSCs on the scaffold. When compared to NSCs grown as a monolayer on a polystyrene culture plate, cells on the scaffold had a slight reduction in metabolic activity during the first 5 days of growth but exhibited a similar trend.

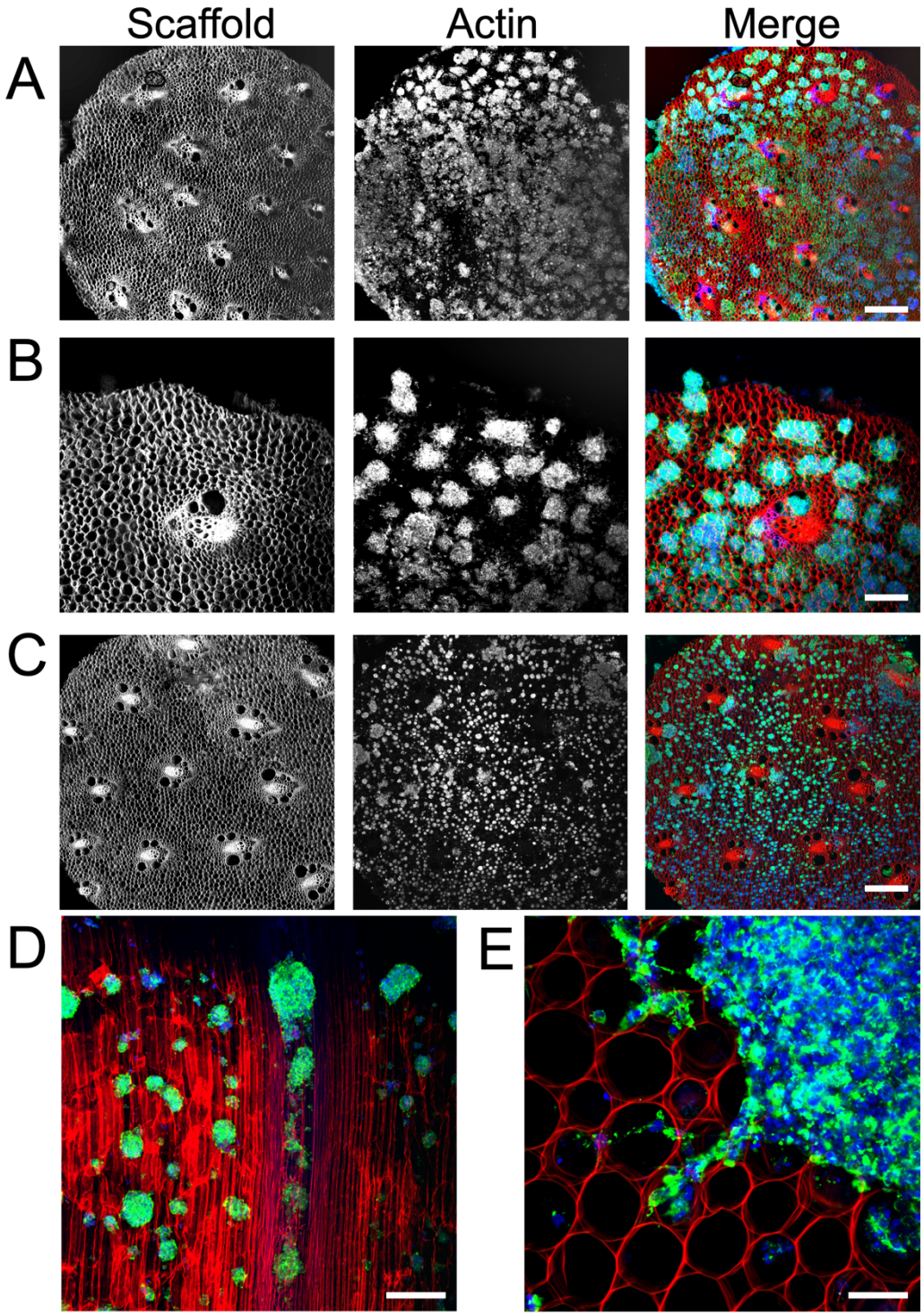

Figure 2.2. Confocal microscopy (maximum intensity projection) of adult rat NSCs cultured on decellularized, PLO coated asparagus scaffold. F-actin was stained with phalloidin (green), nuclei were stained with Hoechst 33342 (blue) and the cellulose scaffold was stained with congo red (red). **A.** 4X magnification of NSCs grown on scaffold for 3 days revealing numerous neurospheres (scale bar = 500µm). **B.** 10X magnification cross section of NSCs on scaffold at 3 days in culture shows the distribution of neurospheres at greater detail (scale bar = 100µm). **C.** 4X magnification of NSCs grown on scaffold for 14 days reveals the continued presence and distribution of neurospheres on the scaffold surface (scale bar = 500µm). **D.** After sectioning the scaffold longitudinally along its long axis (parallel to the direction of the VB microchannels) a 10X magnification image reveals the NSCs migrating into scaffold channels at 3 days in culture (scale bar = 200µm). The highly aligned structure of the cellulose scaffold is easily observed (red) and the presence of NSCs and neurospheres are observed deep within the scaffold. **E.** 40X magnification cross section of NSCs grown on scaffold for 14 days (scale bar = 50µm) reveals groups of NSCs migrating and projecting out of the edge of a single neurosphere.

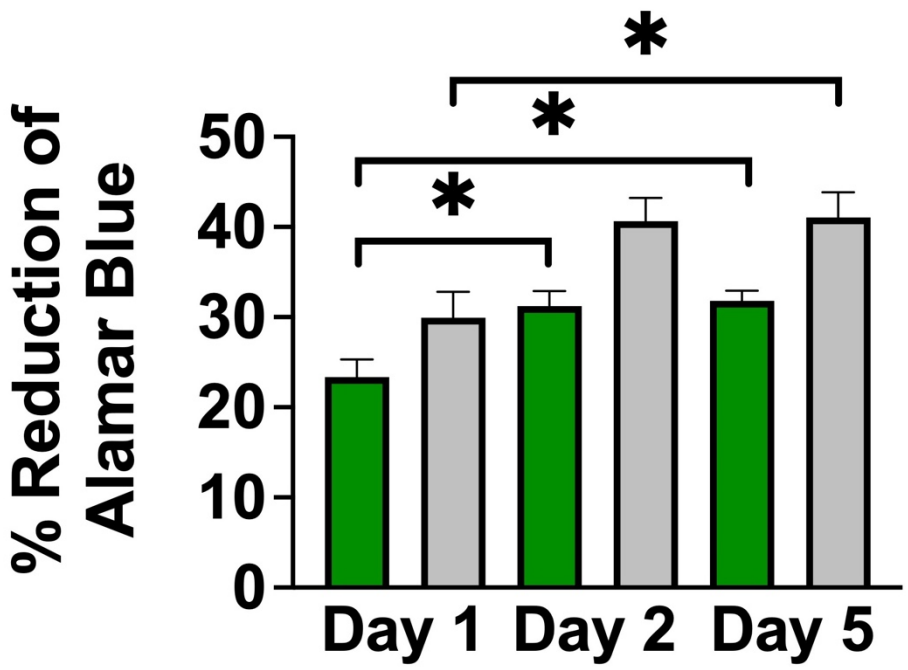

Figure 2.3. Evaluation of cell proliferation by Alamar Blue assay. The percent reduction of AlamarBlue reagent by NSCs grown on a cellulose scaffold (in green) compared to a polystyrene culture plate (in grey) over 5 days in culture. Metabolic activity of cells increased over 5 days in culture, indicating continued growth of NSCs on the scaffold. Statistical significance (* indicates $p < 0.01$) was determined using a student's t-test. (Error bars represent standard deviation, N=3 for each condition)

2.3.3 Plant cellulose scaffold enhances neuronal and astrocytic differentiation

To determine the effects of this 3D culture system on NSC differentiation potency, we monitored the expression of lineage specific markers. A single-cell suspension of NSCs was simultaneously seeded onto PLO-coated scaffolds and onto a PLO-coated culture plates at equal seeding densities. After seven days in differentiation media, cells were fixed and immunostained for glial fibrillary acidic protein (GFAP, an astrocytic marker) or neuron specific ßIII-tubulin (immature neuron marker). Immunostaining revealed a significantly higher fraction of GFAP positive cells were observed on the cellulose scaffold (18.45 ± 2.8%) compared to the 2D monolayer on a polystyrene culture plate (3.50 ± 2.7%) (Fig. 2.4A-C) ($p < 0.01$, n = 6). Similarly, immunostaining revealed enhanced expression of ßIII-tubulin on the 3D scaffold (Fig. 2.4D-F). Cells in 2D condition were 0.79 ± 0.7% ßIII-tubulin positive whereas cells grown on the 3D scaffold were 16.46 ± 4.5% ßIII-tubulin positive, which represents a significant increase in expression of this early neuronal marker ($p < 0.001$, n = 13). Both findings demonstrate that NSCs retain their ability to differentiate into various lineages when cultured in this 3D cellulose scaffold.

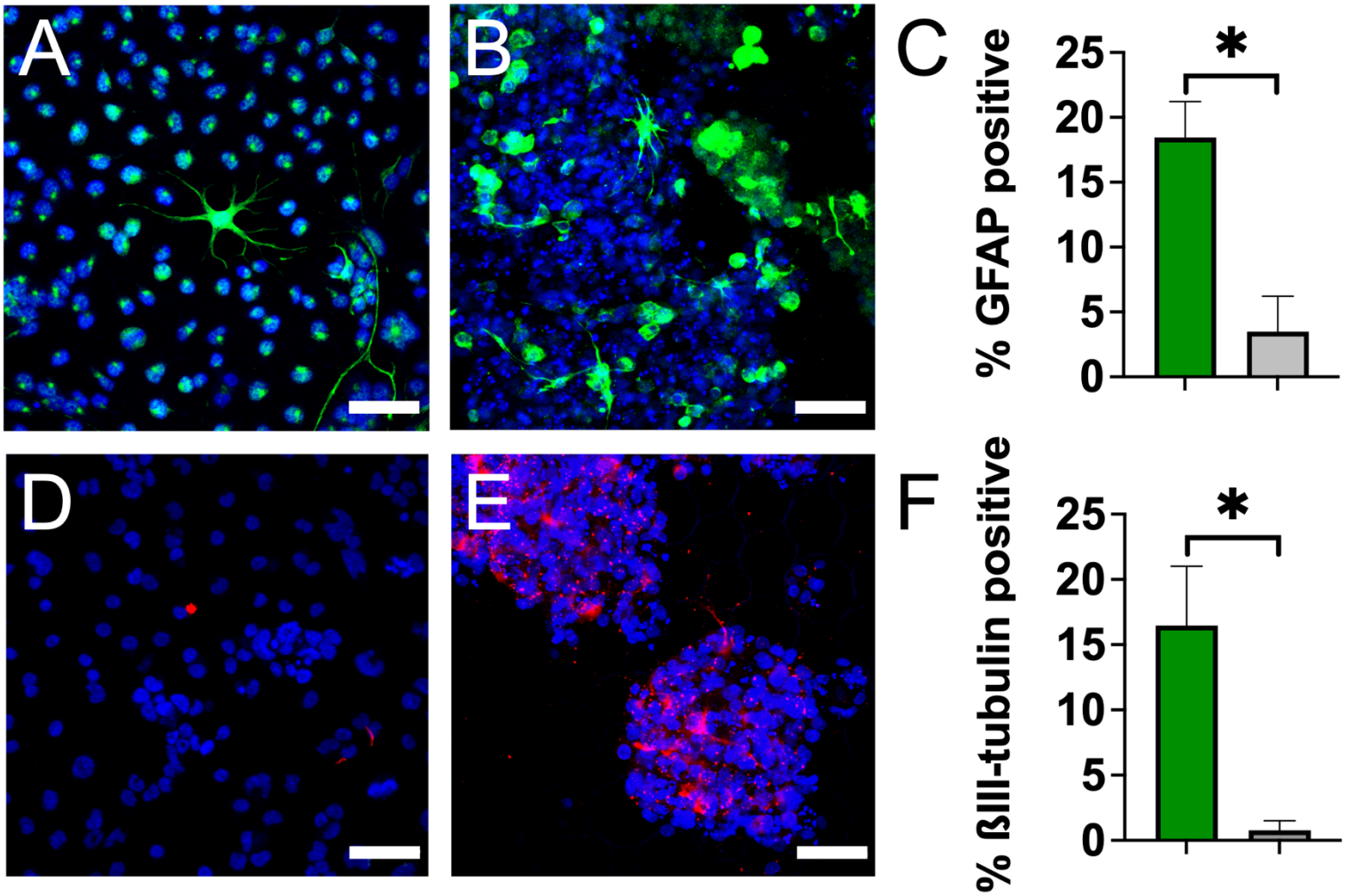

Figure 2.4. **NSC lineage analysis by immunostaining reveals enhanced neuronal and astrocytic differentiation on cellulose scaffold.** Representative confocal microscopy (maximum intensity projections) of adult rat NSCs after 7 days in culture in differentiation media. Nuclei were stained with Hoechst 33342 (blue). **A.** NSCs grown on PLO-coated culture plates (2D) stained for GFAP (green) (scale bar = 50µm). GFAP positive cells were identified as possessing green signal throughout the entire cell body and not just localized to the nucleus **B.** NSCs grown on PLO coated scaffold (3D) stained for GFAP (green) (scale bar = 50µm). **C.** Percentage of GFAP positive adult rat NSCs after 7 days in culture on 3D scaffolds (in green) compared to 2D polystyrene plates (in grey). Statistical significance (* indicates $p<0.01$) was determined using a student's t-test. **D.** NSCs grown on PLO-coated culture plates (2D) stained for ßIII-tubulin (red) (scale bar = 50µm). **E.** NSCs grown on PLO-coated scaffold (3D) stained for ßIII-tubulin (red) (scale bar = 50µm). **F.** Percentage of ßIII-tubulin positive adult rat NSCs after 7 days in culture on 3D cellulose scaffold (in green) compared to 2D polystyrene plate (in grey). Statistical significance (* indicates $p<0.01$) was determined using a student's t-test.

2.4 Discussion

There is growing interest in the use of plant-based scaffolds in tissue engineering (Bilirgen et al., 2021; Fontana et al., 2017b; Toker et al., 2020b). Importantly, since they are constituted primarily of cellulose, plant scaffolds are biocompatible and therefore ideal for applications such as mammalian cell culture or tissue engineering. In this study, we developed a 3D cell culture scaffold consisting of decellularized *Asparagus officinalis* stalks that supported attachment, proliferation, and differentiation of rat adult neural stem cells. After decellularization, the cellulose scaffold was seeded with primary neural stem cells isolated from the hippocampus of adult Fisher 344 rats. Microscopic examination of the scaffolds revealed a system of aligned channels with various diameters, which we predicted would allow for efficient transport of nutrients and provide guidance cues for cell attachment. Other groups have demonstrated that the topography of scaffolds affects cell migration and alignment. In particular, many report that cells respond to parallel linear structures by aligning along the axis of the substrate (Leclech & Villard, 2020; W. Li et al., 2015). We believe the aligned channels within our plant scaffold can potentially act as physical scaffolding to guide the alignment and migration of NSCs by providing cues for contact guidance. Within the scaffold, the parenchyma has pores with smaller diameters (~39μm) relative to the pores of the vascular bundles. However, others have reported successful 3D culture of NSCs in scaffolds with pore sizes that are in a similar size range(Kourgiantaki et al., 2020; Sheets et al., 2020). Our results demonstrate that within 3 days, NSCs attached to the scaffold, both as individual cells and neurospheres of diverse sizes (Fig. 2.2). Groups of NSCs appear to migrate out from the neurospheres attached to PLO-coated scaffolds. This behavior can be explained by the fact that PLO enhances migration by promoting filopodia formation (Ge et al., 2016). In fact, Poly-L-ornithine is widely used in neuroscience to enhance cell attachment and promote cell migration. Subsequent F-actin staining revealed the morphology of neurospheres within the biomaterial and highlighted the migration of NSCs into the channels of the scaffold. Further, NSCs were found to proliferate within the 3D culture system, as demonstrated by an

Alamar Blue assay (Fig. 2.3). Taken together, these data suggest the scaffold is biocompatible and has appropriate physical characteristics to allow for neural stem cell growth *in vitro*.

The behavior of cells cultured in 3D systems is often different from that in 2D, including the rate of proliferation (Fallica et al., 2012; Luca et al., 2013). Interestingly, the percent reduction in AlamarBlue reagent was consistently lower in the 3D scaffold compared to the 2D monolayer culture system, suggesting a slight inhibition of NSC growth on the scaffolds. This difference can be attributed in part to the increased heterogeneity in the 3D culture system, where NSCs assembled into neurospheres attached to the scaffold. While the outer surface of these neurospheres consists of cells with high rates of proliferation, the inner layers of NSCs tend to be quiescent or necrotic due to reduced access to oxygen, nutrients, and growth factors. Therefore, this difference in reduction of AlamarBlue may result from heterogeneity rather than purely from differences in the rate proliferation.

Finally, NSCs grown on the scaffolds were cultured in differentiation media and their expression of cytosolic markers GFAP & ßIII-tubulin was evaluated after 7 days. Remarkably, this plant-derived scaffold appears to enhance NSC differentiation towards astrocytes and neurons, as evidenced by significant increases in GFAP positive and ßIII-tubulin positive cells on the scaffold compared to 2D controls (Fig. 2.4). It is well established that the differentiation of stem cells can be influenced by several extrinsic and intrinsic factors including chemical cues, the physical characteristics of the environment, and the surrounding cell types (W. Li et al., 2015; Metavarayuth et al., 2016; Subramony et al., 2013). Therefore, the differences observed in our differentiation experiments are likely due to a complex interplay of cues provided by the scaffold. An important factor in guiding the fate of NSCs is scaffold architecture and anisotropy. It was previously reported that anisotropic contact promotes neuronal differentiation of NSCs (Baek et al., 2018). In accordance, we propose that the cellulose scaffold's aligned channels provide geometric cues that may modulate differentiation toward higher neurogenesis. In addition, scaffold

elasticity is another key factor which mediates stem cell fate (Bao et al., 2018). To determine the elastic modulus of the scaffold, mechanical tests were performed after 1 week in media at 37˚C. The Young's modulus of the scaffold was determined to be 128 ± 20 kPa when measured parallel to the long axis, which is softer than polystyrene cell culture plates (E = 3.73 GPa) (Oral et al., 2011). The scaffold's elasticity is within the range reported for brain and spinal cord tissue (Hung et al., 1981; Tsai et al., 2004) and is similar to other scaffolds that are currently being investigated for therapeutic use in spinal cord injury (260–300 kPa) (Koffler et al., 2019). Previous studies have shown that softer growth substrates tend to favor neuronal differentiation (Banerjee et al., 2009; Engler et al., 2006; Saha et al., 2008). Here, the difference in stiffness between the scaffold and the polystyrene cell culture plate likely contributed to the increase in neuronal differentiation. As well, the 3D growth environment may have enhanced cell-cell signaling for lineage differentiation, which could induce more differentiation of NSCs on the scaffold relative to 2D culture, as others have reported (Bozza et al., 2014; H. F. Lu et al., 2012; P. Zhou et al., 2020).

Interestingly, we observed many neurospheres forming in the confined circular pores of the parenchyma tissue (Fig 2.2A-C). In previous work, we have shown how embryonic stem cell spheroid formation can be stimulated by the physical confinement of cells in small microscale environments (Hadjiantoniou et al., 2016). This is not dissimilar to what takes place in traditional hanging drop and round bottom multi-well culture models designed for stimulating spheroid formation (Temple et al., 2022). In such environments, cells become trapped and interact more frequently which nucleates the formation of a spheroid. Here, we speculate that a similar phenomenon is taking place leading to a significant increase in the number of spheroids on and inside of the scaffold as opposed to on a flat substrate. However, at this point the precise mechanism which leads to enhanced NSC differentiation on these scaffolds is unclear and future work will be required to understand this phenomenon. In summary, we

have demonstrated that cellulose scaffolds support the growth and differentiation of neural stem cells *in vitro*. Our findings suggest that plant derived scaffolds could facilitate the production of large numbers of specifically differentiated cells needed for NSC research or regenerative medicine.

2.5 Methods

2.5.1 Biomaterial Scaffold Production: Asparagus scaffolds were prepared utilizing decellularization methods described previously. Using a 4 mm biopsy punch, Asparagus officinalis sections were cut and placed into a 50ml Falcon tube containing 0.1% sodium dodecyl sulphate (SDS) (Sigma-Aldrich). The dimensions of the final scaffold are 4mm in diameter and 1.2mm in thickness. Samples were shaken for 72 hours at 180 RPM at room temperature. The resulting asparagus cellulose scaffolds were then transferred into new sterile microcentrifuge tubes, washed and incubated for 12 hours in phosphate-buffered saline (PBS). Following the PBS washing steps, the asparagus were then incubated in 100 mM CaCl2 for 24 hours at room temperature and washed 3 times with dH2O. Samples were then sterilized in 70% ethanol overnight. Finally, they were then washed 12 times with sterile 1X PBS.

2.5.2 Scanning Electron Microscopy: Scanning electron microscopy was performed at the 2-week timepoint. NSC-seeded scaffolds were fixed with 4% PFA and dehydrated through successive gradients of ethanol (50%, 70%, 95% and 100%). Samples were dried with a critical point dryer (SAMDRI-PVT-3D) then gold-coated at a current of 15mA for 3 minutes with a Hitachi E-1010 ion sputter device. SEM imaging was conducted at voltages ranging from 2.00–10.0 kV on a JSM-7500F Field Emission SEM (JEOL).

2.5.3 Mechanical Testing: After 7 days in culture media at 37˚C, scaffolds (4mm diameter x 1.2mm height) were placed onto a CellScale UniVert (CellScale) compression platform for tensile testing. Each scaffold (n=15) was compressed mechanically to a maximum 30% strain, at a compression speed of 50 μm/s. The elastic modulus was determined from the slope of the linear region of the resulting stress-strain curves.

2.5.4 Cell culture, scaffold seeding and differentiation: The resulting cellulose scaffolds were incubated in poly-L-ornithine (Sigma, 20μg/ml in dH2O) overnight at room temperature. PLO-coated scaffolds were rinsed twice with sterile water before being transferred into a 96-well plate. Rat adult hippocampal neural stem cells (Sigma SCR022) were cultured in serum free medium (1X KnockOut D-MEM/F-12 with 2% StemPro Neural Supplement (ThermoFisher A1050801), 20 ng/mL bFGF, 20 ng/mL EGF, and 2mM GlutaMAX-I) and incubated at 37°C and 5% CO^2. Culture vessels were also coated with 20 μg/ml poly-L-ornithine overnight at room temperature and 10 μg/ml laminin then rinsed twice with sterile water. An 80 μL droplet containing 200 000 cells was deposited onto every scaffold, which was then incubated at 37°C and 5% CO^2. After 4 hours of incubation, 2 mL of StemPro NSC SFM complete medium was added to each scaffold, which was then incubated for 48 hours before transferring scaffolds to a new 96-well plate. For 2-4 weeks, media was exchanged daily. For neuronal and astrocyte differentiation, cells were cultured in 1X KnockOut DMEM/F-12 supplemented with 2% B27 (cat. 17504044 ThermoFisher), 2mM GlutaMAX-I (ThermoFisher)) for 7 days.

2.5.5 Staining and Confocal Microscopy: Cell attachment and morphology was documented by phase contrast microscopy at day 3, 7, and 14 post seeding. Staining and confocal microscopy was performed at 72h or 14 days in culture. NSC-seeded scaffolds were fixed with warm 4% paraformaldehyde for 10

minutes then incubated 3 minutes in warm permeabilization buffer (0.5% Triton-X, 20 mM HEPES, 300mM Sucrose, 50mM NaCl, 3mM MgCl2, 0.05% sodium azide). Samples were then incubated for 15 minutes in Fluorescein Phalloidin (1:100, ThermoFisher F432) to stain F-actin. Samples were rinsed with PBS and incubated in Hoechst (1:200, ThermoFisher) for 10 minutes to label nuclei. Scaffolds were incubated in 0.2% Congo Red (Sigma) for 15 minutes before a final PBS rinse. For immunostaining GFAP and b-tubulin, cells or cell-seeded scaffolds were fixed in 4% paraformaldehyde for 15 minutes at room temperature. Samples were incubated for 5 minutes in permeabilization buffer (0.5% Triton-X, 20 mM HEPES, 300mM Sucrose, 50mM NaCl, 3mM MgCl2, 0.05% sodium azide). After blocking in 6% Normal Goat Serum in 1X PBS for 10 minutes, samples were incubated in rabbit anti-GFAP antibody (cat. AB5804 Sigma, 1:1000 in 1X PBS) or mouse anti-b-III tubulin antibody (cat. MAB1195 R&D systems, 10ug/ml in 1X PBS) overnight at 4˚C. The following day, samples were washed twice in 1xPBS (5 mins, RT) followed by a 2-hour incubation in secondary antibody: goat anti-rabbit IgG Alexa Fluor 488 (cat. A11008 Invitrogen, 1:500 in 1X PBS) or goat anti-mouse IgG Alexa Fluor 594 (cat. A11005 Invitrogen, 1:200 in 1X PBS). Samples were then washed in 1X PBS and counterstained with Hoescht 33342 (1:2000 in 1X PBS) for 10 minutes. All samples were then mounted in Vectashield (Vector Labs) and imaged on with a Nikon A1R laser scanning confocal microscope with appropriate filter sets and laser lines.

2.5.6 Image analysis: For ßIII-tubulin stains, analysis was performed on 13 images at 40X magnification for each condition (Figure 2.4). Total cell number was determined by cell counting Hoescht-labeled nuclei using FIJI. Cells were considered ßIII-tubulin^{+} when signal from red and blue channels were colocalized. For GFAP stains, analysis was performed on 6 images at 40X magnification for each condition (Figure 2.4). Cells were considered GFAP^{+} when signal from green and blue channels were colocalized.

2.5.7 Alamar Blue Cell Proliferation Assay: To measure cell proliferation, an Alamar blue assay was performed according to the manufacturer's protocol. Briefly, PLO-coated asparagus scaffolds were placed into the wells of a 96-well plate and seeded with 100 000 adult rat hippocampal neural stem cells. After 1, 2 or 5 days, cell-seeded scaffolds were transferred into a new well and 200µL of fresh media containing 10% Alamar blue (cat. BUF012A Bio-Rad) was added to each scaffold. After 4 hours of incubation at 37˚C, 100µL of media was removed from each well and deposited into an empty well before reading absorbance at 570nm and 600nm on a spectrophotometer (Epoch 2, BioTek). Each timepoint included biological triplicates for cell-seeded scaffolds (n = 3), 2D controls (NSCs grown on a PLO-coated well, n = 3) and blanks (media only, n = 3). Absorbances were corrected by subtracting the average absorbance of blanks at 570nm & 600nm.

2.5.8 Statistical Analysis: p values were calculated using two-tailed Student's t test. Results were considered as statistically significant when $p < 0.01$. Numerical data are expressed as mean ± standard deviation.

Chapter 3: PLO-coated plant cellulose in a rodent model of complete spinal cord injury

This chapter was adapted from a preprint (research paper submitted):
Couvrette, L. J., Walker, K. L. A., Bayat, A., Modulevsky, D. J., Laliberté, A., Cuerrier, C. M., Leblanc-Latour, M., Hickey, R. J., Boudria, R., Monty, R., Obhi, R.-J. K., Shore, I., Galuta, A., Tsai, E. C., Bui, T., & Pelling, A. E. (2025). *Poly-L-Ornithine Coated Plant Scaffolds Support Motor Recovery in Rats after Traumatic Spinal Cord Injury*. https://doi.org/10.1101/2025.02.05.636658

Abstract:

Various biomaterials have been investigated as part of a therapeutic strategy to facilitate recovery from spinal cord injury. We hypothesize that cellulose scaffolds can be functionalized with a PLO coating and support recovery after SCI. The goal of this study is to confirm the biocompatibility of the PLO-coated plant scaffold and to test this scaffold in an animal model of complete spinal cord transection. We show that the scaffold supports hindlimb motor recovery in a rat model of SCI. In addition, histological analysis reveals neural cell infiltration and axonal sprouting inside the cellulose biomaterial. We assess tissue regeneration by neural tract tracing and find enhanced regeneration of sensory axons in animals with PLO-coated scaffolds compared to those without a scaffold. Our results highlight the potential tissue engineering applications of decellularized plant tissue.

3.1 In vivo biocompatibility of PLO-coated cellulose scaffolds

PLO-coated scaffolds were implanted subcutaneously in immunocompetent female rats to evaluate the immune response and integration with the surrounding tissue. This experiment was not performed in male rats, in alignment with our subsequent SCI model, which uses female rats exclusively for ease of post-operative care. Cell infiltration was observed by hematoxylin & eosin staining (Fig. 3.1) of fixed cellulose scaffolds at 2, 4, 8 and 12 weeks following their implantation. Interstitial fluids are stained in pink while nuclei (purple) can be seen infiltrating the scaffold. Following implantation, an acute foreign body reaction was observed in the PLO-coated scaffolds and uncoated scaffolds alike. This response resolved gradually, with no signs of persistent inflammation at the 12-week time point. Masson's Trichrome staining of fixed scaffolds at various timepoints post-implantation revealed extracellular matrix deposition within the PLO-coated scaffolds (Fig. 3.2).

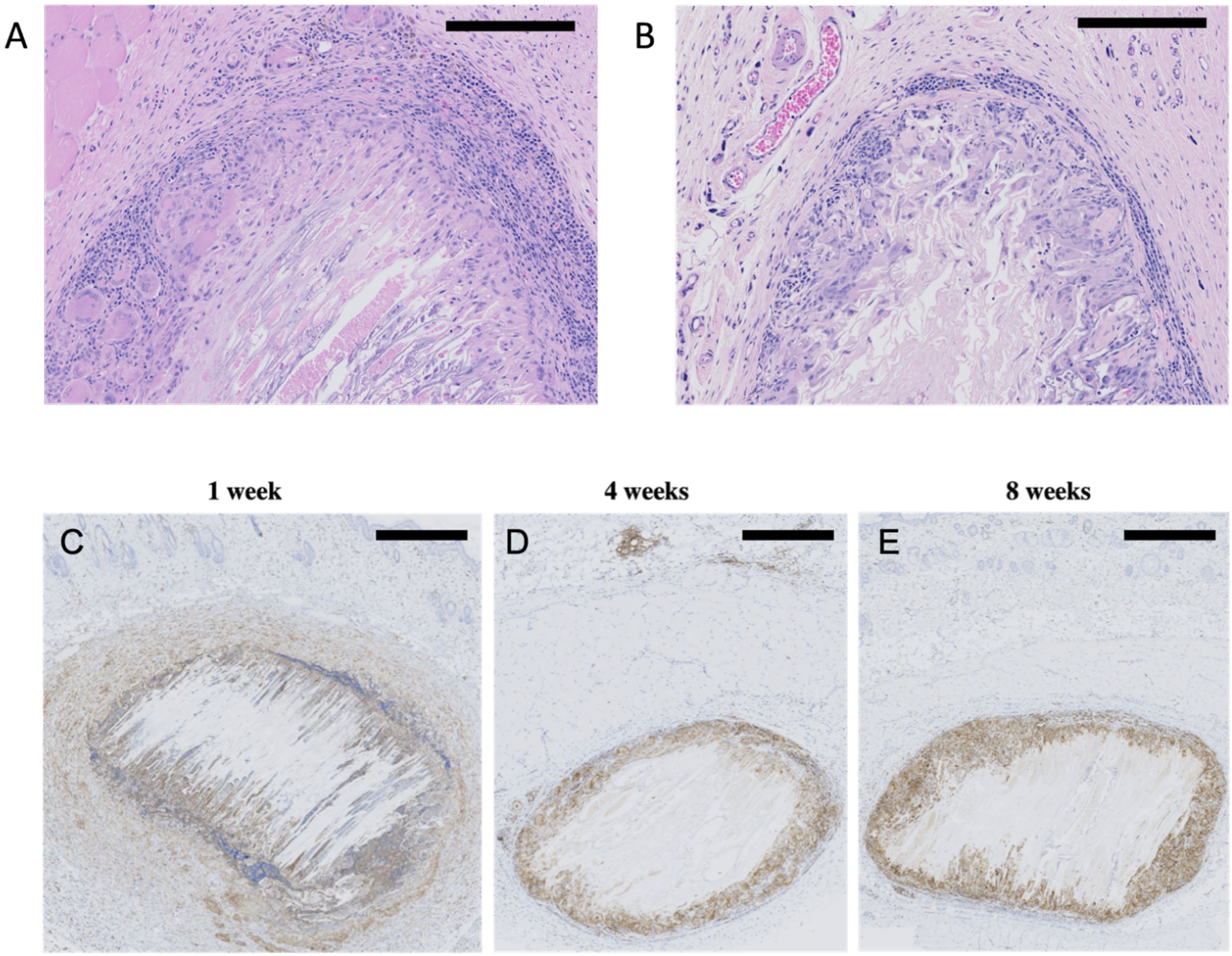

Figure 3.1 In vivo biocompatibility of PLO-coated cellulose implant (Hematoxylin & eosin, CD45). A. Hematoxylin & eosin staining of sagittal section of subcutaneous implant at 4 weeks post-implantation (Scale bar = 250µm). **B**. Hematoxylin & eosin staining of sagittal section of subcutaneous implant at 12 weeks post-implantation (scale bar = 250µm). **C**. CD45 immunohistochemistry staining of sagittal sections showing hematopoietic cells (in brown) infiltrating the biomaterial 1 week post-implantation (Scale bar = 900µm). **D**. CD45 immunohistochemistry staining of sagittal sections showing hematopoietic cells (in brown) infiltrating the biomaterial 4 weeks post-implantation (scale bar = 900µm). **E**. CD45 immunohistochemistry staining of sagittal sections showing hematopoietic cells (in brown) infiltrating the biomaterial 8 weeks post-implantation (scale bar = 900µm).

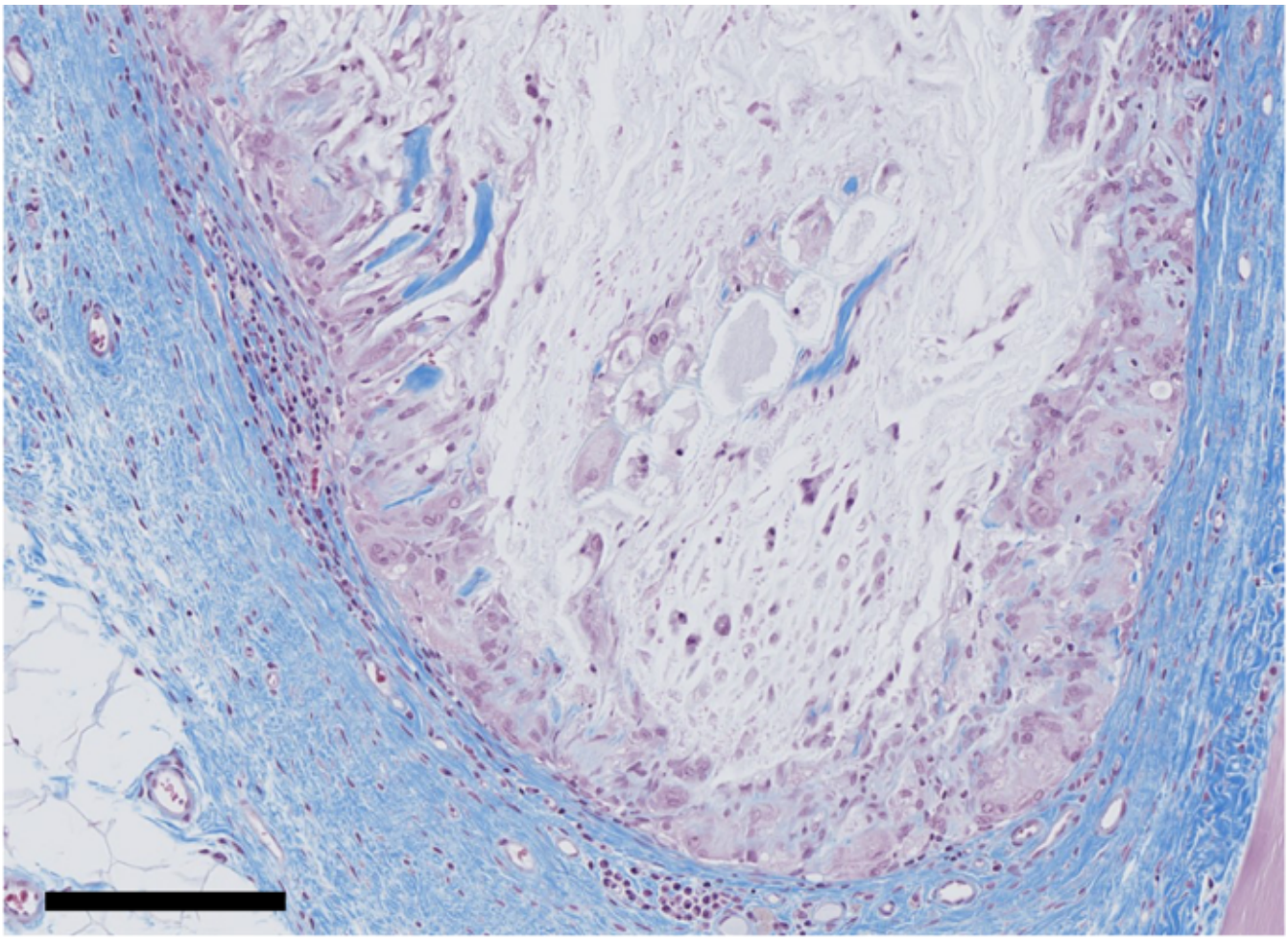

Figure 3.2 In vivo biocompatibility of PLO-coated cellulose implant (Masson's Trichrome). Masson's Trichrome staining of sagittal section of subcutaneous implant 12 weeks post-implantation (Scale bar = 300μm). Collagen is stained blue, nuclei in dark red and cytoplasm is stained pink.

3.2 Poly-L-Ornithine Coated Plant Scaffolds Support Motor Recovery in Rats after Traumatic Spinal Cord Injury

3.2.1 Abstract

Spinal cord injury (SCI) is a debilitating neurological condition with far-reaching consequences for patients, including loss of motor function and significant limitations to quality of life. Implantable biomaterials have emerged as a therapeutic strategy to modulate the SCI microenvironment and facilitate regeneration of axons. In this study, plant-derived cellulose scaffolds coated with poly-L-ornithine (PLO) are shown to support locomotor recovery and neural tissue repair in a rat model of spinal cord injury. Upon complete transection of the spinal cord, animals were implanted with a plant-derived scaffold coated in poly-L-ornithine, a positively charged amino acid chain that is known to promote neural stem cell differentiation into neurons and enhance myelin regeneration. Recovery of motor function was evaluated by the Basso, Beattie and Bresnahan (BBB) locomotor scale as well as the Karolinska Institutet Swim Assessment Tool (KSAT). Retrograde tracing of ascending sensory tracts revealed enhanced regeneration in animals that received the PLO-coated scaffold. Numerous β-III tubulin and neurofilament 200 positive fibers may indicate axonal sprouting within the cellulose scaffold and LFB staining highlights myelination around the PLO-coated scaffold. These results demonstrate the potential of plant-based biomaterials in a rat model of acute spinal cord injury and highlight their enhancement after PLO functionalization.

3.2.2 Introduction

The mammalian spinal cord has limited regenerative capacity after spinal cord injury (B. Zheng & Tuszynski, 2023). Failure of the adult central nervous system to regenerate can be attributed in part to the limited capacity of injured neurons to re-establish functional axons across the lesion (B. Zheng & Tuszynski, 2023). Mechanical trauma to the tissue elicits a range of cell responses, including increased proliferation of ependymal cells that line the central canal (C. B. Johansson et al., 1999). Upon activation, ependymal cells re-express neural stem cell properties and migrate to the site of injury, where they spontaneously differentiate into oligodendrocytes and astrocytes (Barnabé-Heider et al., 2010a; Lacroix

et al., 2014). Although ependymal cells can differentiate into neurons *in vitro*, the same has not been demonstrated following SCI *in vivo* (J. Li et al., 2023), though mature oligodendrocytes have been observed (Barnabé-Heider et al., 2010b; Meletis et al., 2008). After SCI, complex pathological mechanisms create a hostile microenvironment at the injury epicenter, which inhibits the regrowth of axons and damages surrounding tissue (Hachem & Fehlings, 2021). For instance, SCI-induced death of oligodendrocytes leads to an accumulation of myelin breakdown products at the injury site (Chambel & Cruz, 2023; J. K. Lee & Zheng, 2012; McKerracher & Rosen, 2015). Molecules such as Nogo-A and myelin-associated glycoprotein are released from damaged myelin into the extracellular matrix after SCI and represent an important group of axonal growth inhibitors (J. Wang et al., 2015). Many therapeutic strategies aim to establish a more permissive environment for regeneration by removing inhibitory molecules (Hyatt et al., 2010; Karimi-Abdolrezaee et al., 2012; Pakulska et al., 2017; Sartori et al., 2020), providing trophic support (Blesch & Tuszynski, 2003; Bradbury et al., 1998; Bregman et al., 2002; Díaz-Galindo et al., 2020), directing stem cell fate (L. Fan et al., 2018; Q. Liu et al., 2023), remyelinating axons (Keirstead et al., 2005; Sasaki et al., 2004), or implanting biomaterial scaffolds that can guide axonal growth (Álvarez et al., 2021; Chedly et al., 2017; Koffler et al., 2019; Pawar et al., 2015). In recent years, multimodal therapies have generated much attention since they address multiple aspects of SCI pathology and often produce greater benefit than their individual components (García et al., 2023; Guijarro-Belmar et al., 2022; Meshkini et al., 2024). Such therapeutic strategies have combined cell transplants, biomaterials, locomotor training, and neurotrophic factors with the goal of modulating the injury microenvironment to promote repair.

Developing biocompatible scaffolds to bridge the SCI has been at the forefront of tissue engineering strategies. Implantable biomaterials not only provide structural scaffolding to guide cell attachment and migration but can also be used to regulate the inflammatory response or deliver other

therapeutics such as stem cells and growth factors. Regenerative biomaterials for SCI are designed to replicate the properties of spinal cord tissue and should therefore have the mechanical strength, porosity and internal microstructures that are suitable for neurite extension across the injury site (S. Liu et al., 2019; Shen et al., 2022). Moreover, the surface chemistry of biomaterials is of particular importance, as it can be utilized to influence cell migration and differentiation (Flanagan et al., 2006; Ge et al., 2015; Joseph et al., 2021; Ren et al., 2009; J.-H. Wang et al., 2006).

Both degradable and non-degradable biomaterials have been investigated for SCI repair. In order for degradable scaffolds to act as extracellular matrix substitutes, it is essential that their rate of degradation aligns with the regeneration rate of axons (Kubinová & Syková, 2010). Synthetic materials are attractive candidates for spinal cord tissue engineering due to their controllable mechanical properties and high batch-to-batch consistency. For example, polyethylene glycol is a synthetic polymer that can be cross-linked to form injectable hydrogels that provide a framework for regenerating tissue and were shown to promote motor recovery in a rat model of SCI (Estrada et al., 2014). In addition, poly(lactic-co-glycolic acid)-based scaffolds have produced significant motor improvements and increased tissue remodelling in African green monkeys with an incomplete SCI (Slotkin et al., 2017). However, many synthetic biomaterials are limited by their hydrophobicity, which can impair cell attachment, or by their potential to release toxic by-products during degradation. By contrast, natural materials such as collagen, fibrin, alginate, chitosan and hyaluronic acid are widely studied as regenerative scaffolds for SCI due to their excellent biocompatibility and cell adhesion properties. In particular, collagen-based scaffolds are a promising SCI treatment that has been explored in diverse forms including collagen hydrogels (Breen et al., 2017b; Sugai et al., 2015), collagen sponges (Zou et al., 2022) or collagen scaffolds that deliver therapeutics to the injury (X. Li et al., 2018). Ongoing human clinical trials have reaffirmed the therapeutic potential of collagen scaffolds, notably in their ability to promote tissue regeneration and functional

recovery (Xiao et al., 2018). One common issue with scaffolds made from natural polymers is insufficient mechanical strength and durability *in vivo*, which multiple studies have aimed to resolve by adding cross-linkers (Davidenko et al., 2015) or combining natural and synthetic biomaterials.

Recently, plant-derived scaffolds have been investigated *in vivo* for various biomedical applications including skin (Dikici et al., 2019; Peng et al., 2022), tendon (Contessi Negrini et al., 2020), nerve (F. Chen et al., 2021) and bone (Balasundari et al., 2012; Contessi Negrini et al., 2020; J. Lee et al., 2019; Venkatesan & Kim, 2010) tissue engineering. Many different plant species can be decellularized with the help of detergents, sonication, enzymatic digestion, or freeze-thawing methods to produce cellulose-based scaffolds (Bilirgen et al., 2021) composed of β(1→4) linked D-glucose units. Plant cellulose scaffolds were shown to be biocompatible *in vivo* and supported extracellular matrix deposition when implanted subcutaneously (Modulevsky et al., 2016). In addition, these scaffolds became vascularized as early as one week post-implantation. Since cellulose is not biodegradable in humans, scaffolds made from this material are poised to offer long-term durability *in vivo* (Hickey & Pelling, 2019). Moreover, plant cellulose has proven to be a versatile material that can be combined with hydrogels to generate customizable macroscopic structures (Hickey et al., 2018a). Some groups have shown that cellulose scaffolds can be functionalized with chemical coatings to promote cell adhesion (Fontana et al., 2017a). For example, we have previously demonstrated that poly-L-ornithine-coated cellulose scaffolds produced from stalks of *Asparagus officinalis* can support attachment and proliferation of neural stem cells *in vitro* (Couvrette et al., 2023). In culture, rat neural stem cells form neurospheres that attach to the cellulose biomaterial and readily infiltrate its channels. Increased expression of neuron-specific beta-III tubulin and glial fibrillary acidic protein in cells grown on these scaffolds suggests they may promote differentiation of NSCs towards neurons and astrocytes, respectively, *in vitro*.

Here we investigate the ability of poly-L-ornithine-coated cellulose biomaterials to support neural tissue repair and functional recovery after traumatic SCI. We implanted poly-L-ornithine-coated scaffolds or uncoated scaffolds acutely following a complete spinal cord transection in rats housed in an enriched environment. Motor recovery was monitored by the Basso, Beattie and Bresnahan (BBB) open field assessment and Karolinska Institutet Swim Assessment Tool (KSAT). Sprouting and regeneration of the dorsal columns were analyzed by neural tract tracing with the retrograde tracer CTb injected into the sciatic nerve. The results of this experiment point to enhanced regeneration of the sensory tracts in animals that received PLO-coated implants compared to controls. In addition, the descending fibers of the corticospinal tracts (CST) were visualized with dextran amine injections in the motor cortex, which revealed CST axons projecting along the cellulose biomaterial. Finally, histological analysis showed host tissue integration with the scaffold and neural cell migration along its channels, which was enhanced by the PLO coating. In sum, we demonstrate the ability of PLO-modified plant-derived scaffolds to promote axonal sprouting in the lesion and induce motor recovery after SCI.

3.2.3 Results

3.2.3.1 Cellulose Scaffold Production and Implantation in Rodent Spinal Cord Injury

Stalks of Asparagus officinalis were cut into cylindrical sections with a biopsy punch and decellularized to produce cellulose scaffolds (Fig. 3.3A). Naturally occurring vascular bundles (VBs) cross the length of the cellulose scaffold, which has parenchyma with an average pore diameter of 39 ± 15µm (Fig. 3.3B). The aligned channels within the scaffold were characterized by scanning electron microscopy and the Young's modulus was measured parallel to the long axis as 128 ± 20 kPa (n = 5). In animals with a complete T8-T9 spinal cord transection, scaffolds were implanted into the gap between the stumps of the cord with the long axis of the VBs parallel to the spinal cord (Fig. 3.3D). The control group (n = 8) did not receive a scaffold, while the PLO group (n = 11) was implanted with a cellulose scaffold

coated with a 100µg/ml solution of poly-L-ornithine (PLO) and the ASP group (n = 9) received an uncoated cellulose scaffold. After 12 weeks *in vivo*, spinal cord tissue was collected, and histological analysis was performed to assess tissue integration with the scaffold. Immunohistochemistry staining for CD31 was performed to assess biomaterial vascularization (Fig. 3.3F and G). CD31 positive blood vessels were identified in the tissue surrounding the scaffold, including the dorsal, rostral, and caudal interfaces. As well, CD31 positive blood vessels were found inside the vascular bundles within the biomaterial. Hematoxylin & eosin staining revealed nuclei migrating along the channels of the cellulose biomaterial (Fig. 3.3E), which is consistent with our previous *in vitro* study (Couvrette et al., 2023). In particular, nuclei were observed within the vascular bundles of the biomaterial (Fig. 3.3C) and completely crossed the lesion. The scaffolds retained their structure and dimensions throughout the study and no signs of chronic foreign body reaction were observed, which aligns with the findings of previous studies (Modulevsky et al., 2016; Toker-Bayraktar et al., 2023). Prior to testing the biomaterial in a rat model of SCI, we examined its biocompatibility by subcutaneously implanting PLO-coated scaffolds in immunocompetent Sprague Dawley rats. Histological analysis performed at 1-, 4-, and 12-weeks post-implantation showed a gradual decrease in immune cell presence in the scaffold and surrounding dermis tissue. By the 12-week timepoint, low levels of foreign body multinucleated cells were observed at the periphery of the scaffold.

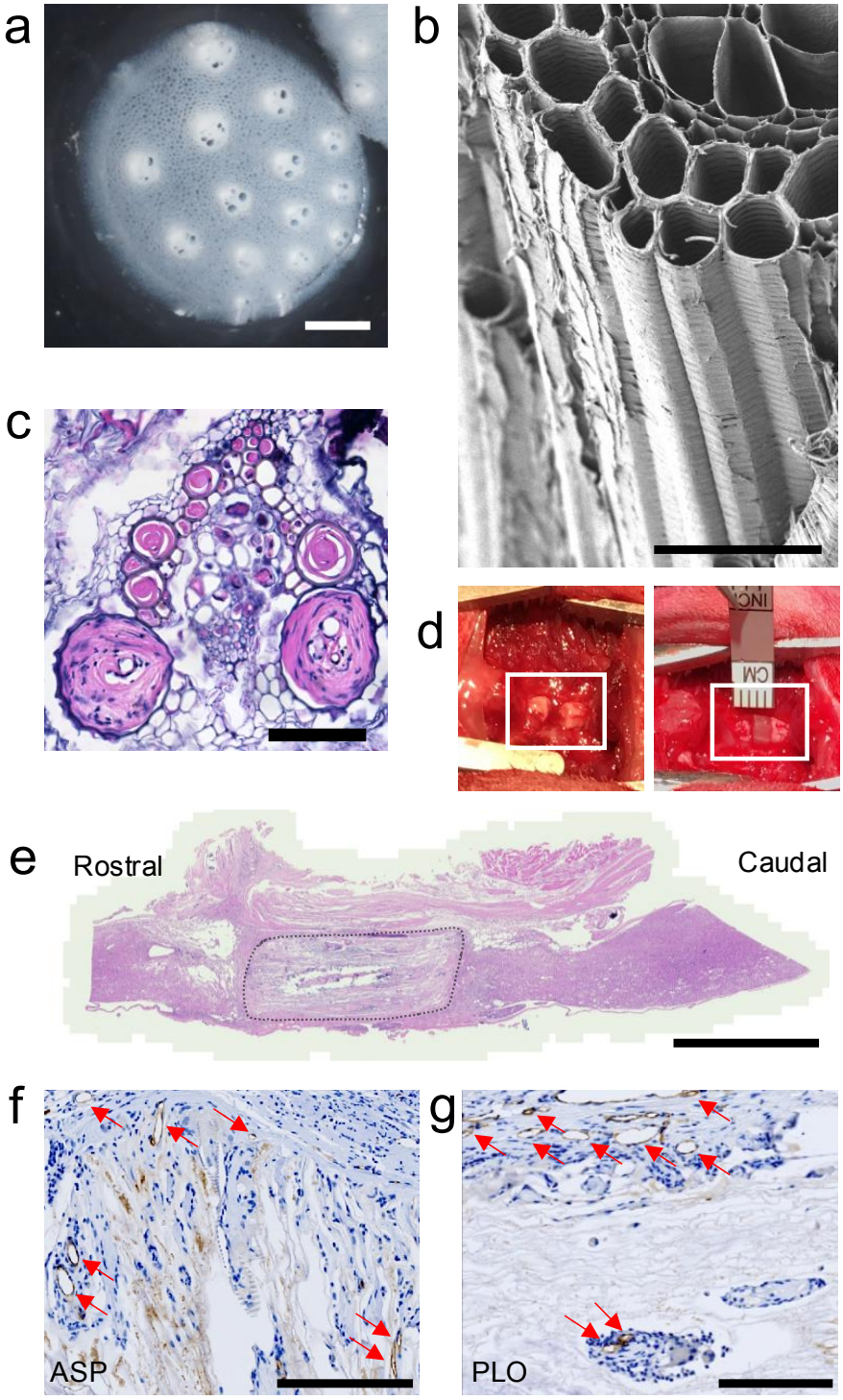

Figure 3.3 Plant-derived cellulose biomaterial in rodent model of complete transection spinal cord injury. **A**. A cross sectional view of decellularized plant-derived scaffold consisting of vascular bundles and parenchyma (scale bar = 1mm). **B**. SEM of cellulose scaffold microarchitecture (scale bar = 100µm). **C**. Hematoxylin & eosin staining of cross section of cellulose scaffold after 12 weeks *in vivo*. The scaffold's vascular bundles are infiltrated with host cells. (scale bar = 200µm). **D**. An exposed fully transected spinal cord (left box) and a scaffold after implantation (right box). **E**. Hematoxylin & eosin staining of sagittal section of spinal cord tissue with cellulose scaffold (outlined) after 12 weeks *in vivo* (scale bar = 2mm). **F**. Immunohistochemistry staining for CD31 (brown) in a sagittal section at the caudal biomaterial-tissue interface (representative image from the ASP group). CD31 positive blood vessels denoted by arrow (scale bar = 200µm). **G**. Immunohistochemistry staining for CD31 (brown) in a sagittal section at the caudal biomaterial-tissue interface (representative image from the PLO group). CD31 positive blood vessels denoted by arrow (scale bar = 200µm).

3.2.3.2 Hindlimb locomotor recovery after complete SCI

3.2.3.2.1 BBB Locomotor Assessment

Hindlimb motor function was assessed weekly using the Basso, Beattie and Bresnahan (BBB) locomotor scale, which ranges from 0 (complete hindlimb paralysis) to 21 (normal locomotion) points. Two weeks after complete transection of the spinal cord, the BBB assessment was performed to confirm total hindlimb paralysis. At this initial assessment, there were no significant differences in locomotor ability amongst the experimental groups: No Tx (transection with no scaffold, n = 8), ASP treated (cellulose implant only, n = 9), and PLO treated (PLO-coated cellulose implant, n = 11). Any animal that achieved a BBB score of above 5 at the 2-week post-operative timepoint was excluded from further locomotor evaluation. Out of 29 animals, a single rat was identified as an outlier, with a BBB score of 5.5 (average of 3 examiners) and was therefore excluded from the BBB motor recovery assessment. Over the 11-week recovery period, BBB scores increased significantly in animals that received PLO-coated scaffolds ($p < 0.0001$) as well as those implanted with uncoated scaffolds ($p = 0.0158$) (Fig. 3.4A). This was determined by comparing the average score at week 2 with the average score at week 11 for each experimental group. Whereas significant functional recovery was achieved in scaffold treated groups, animals that did not receive a scaffold had no significant change ($p = 0.3128$) in BBB scores throughout the recovery period. At week 11, the mean BBB score of rats treated with the PLO-coated scaffold was 5.6 ± 0.87 points, corresponding to slight movement in 2 joints and extensive movement of a third. The group receiving uncoated scaffolds had a mean score of 4.3 ± 0.96, indicating slight movement of all three joints of the hindlimb. By contrast, controls that did not receive a scaffold had a mean score of 3.35 ± 1.0, reflecting extensive movement in 2 joints. Importantly, no animals from the No Tx group attained scores of 6 or above, whereas several animals from the PLO and ASP groups achieved BBB scores of 7 (extensive movement of all three joints), 8 (plantar placement of the paw without weight support), and 9 (plantar placement of the paw with weight support in stance only).

3.2.3.2.2 KSAT Swimming Assessment

Motor recovery as assessed by the BBB can be influenced by the retraining effect (Battistuzzo et al., 2012; Burke et al., 2023; Rossignol et al., 2015; Starkey et al., 2014), whereby spontaneous "self-training" occurring in the cage contributes to functional recovery. Factors such as cage size and housing density can influence the activity level of the animals, which may impact the recovery of overground walking. By contrast, swimming performance is not affected by the retraining effect (Smith, Burke, et al., 2006), since animals are not normally exposed to swimming in a laboratory setting. Another potential confounding factor that may affect BBB scores is sensory feedback from below the injury, which can contribute to motor recovery during overground walking after SCI (Bouyer & Rossignol, 2003a; Courtine et al., 2009; Muir & Steeves, 1995; H. Park et al., 2019; Takeoka, 2020; Takeoka et al., 2014). During swimming, there is an important reduction in sensory feedback from the hindlimbs compared to overground walking (Smith, Burke, et al., 2006; Xu et al., 2015) since rats rely on buoyancy to support their bodyweight. The Karolinska Institutet Swim Assessment Tool (KSAT) evaluates swimming parameters including hindlimb movement, forelimb usage, trunk instability, and body angle. In this assessment, healthy animals achieve a maximum score of 19, based on intensity and frequency of limb and tail movement. At the first post-operative swim assessment, there were no differences amongst the experimental groups. After 11 weeks of recovery, rats with the PLO-coated scaffold showed significant improvements in swimming performance compared to their first post-operative assessment ($p = 0.0001$) (Fig. 3.4B). By contrast, the animals treated with uncoated scaffolds ($p = 0.0609$) and those without scaffolds ($p = 0.3361$) did not achieve statistically significant improvement over the course of the study. At the final swimming assessment, the average KSAT score of rats implanted with PLO-coated scaffolds was 3.79 ± 0.58 compared to 3.18 ± 0.64 with the uncoated scaffold (ASP group) and 2.25 ± 0.68 for those without scaffolds (No Tx group). Overall, animals from the PLO and ASP groups showed improvement

in hindlimb movement and trunk stability. Interestingly, the best performing animal from the PLO group attained a KSAT score of 8, while the highest score achieved in the ASP group was 6 and the highest score in the No Tx group was 5.

3.2.3.2.3 Inclined Plane test

Before the spinal cord injury, all animals were trained to perform the inclined plane test as described by Rivlin et al (Rivlin & Tator, 1977). Animals were placed on an inclined plane and the slope was adjusted to determine the maximum angle at which the animal could maintain its position without falling. Every 2 weeks after the spinal cord injury, the inclined plane test was performed to examine sensorimotor recovery. At the final week, there were no significant differences (p = 0.7915) in the performance of the three experimental groups (Fig. 3.4C). On average, animals reached a maximum angle of 26 ± 1 degrees in the PLO group (PLO-coated scaffolds), 28 ± 1 degrees in the ASP group (uncoated scaffolds), and 23 ± 3 degrees in the No Tx group (No scaffold).

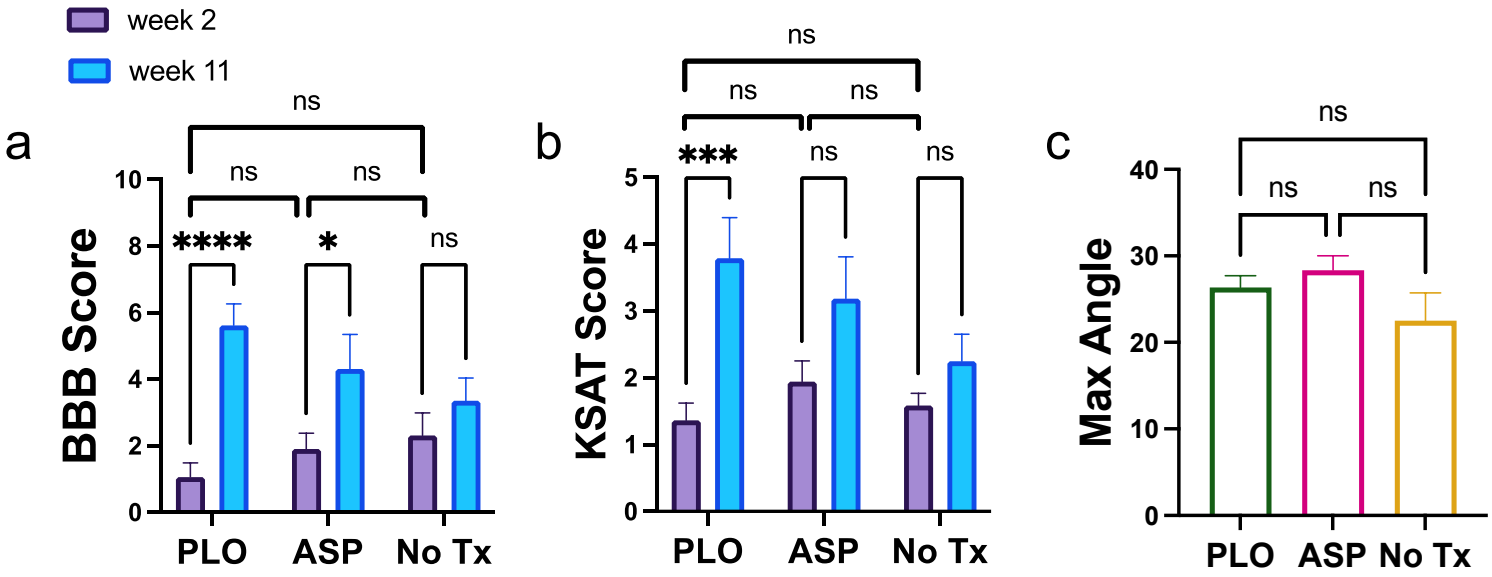

Figure 3.4 Locomotor assessments after complete spinal cord transection. **A**. Average BBB score of each experimental group at week 2 after SCI compared to week 11 after SCI (2-way ANOVA Uncorrected Fisher's LSD; **** $p < 0.0001$, * $p = 0.0158$; mean ± s.e.m, $n = 11$ PLO animals, $n = 9$ ASP animals, $n = 8$ No Tx animals). **B**. Average KSAT swim assessment score of each experimental group at week 2 after SCI compared to week 11 after SCI (2-way ANOVA Uncorrected Fisher's LSD; ***P = 0.0001; mean ± s.e.m, $n = 11$ PLO animals, $n = 9$ ASP animals, $n = 8$ No Tx animals). **C**. Average maximum angle achieved by each experimental group in inclined plane assessment at final week (mean ± s.e.m, n = 11 PLO animals, $n = 9$ ASP animals, $n = 8$ No Tx animals).

3.2.3.3 Retrograde tract tracing of ascending sensory fibers reveals enhanced regeneration

To elucidate possible mechanisms that may facilitate the observed motor recovery, retrograde tracing was performed on rats from each experimental group. Neuroanatomical tract tracing is commonly used to visualize sprouting or regeneration of axons after injury (Hellenbrand et al., 2013; Kim et al., 2013; Reiner et al., 2000; Saleeba et al., 2019). After the recovery period of 11 weeks, Cholera Toxin subunit B (CTb) conjugated to Alexa Fluor 647 was injected into the sciatic nerve to label sensory axons projecting along the dorsal column of the spinal cord. Cross sections of T10 spinal cord tissue caudal to the injury were imaged by confocal laser scanning microscopy and revealed a distinct CTb-positive signal in the dorsal column (Fig. 3.5B) which was not found in T6 sections rostral to the injury. Sagittal sections of spinal cord tissue showed CTb-labelled axons projecting into the caudal side of the scaffold towards the injury epicenter (Fig. 3.5C, D & E). Compared to animals without a scaffold, those with PLO-coated scaffolds had on average a significantly smaller distance ($p = 0.0264$) between the furthest rostral CTb-traced axons and the injury epicenter (Fig. 3.5A). This result suggests that the PLO-coated scaffold enhanced regeneration of axons and/or reduced axon retraction. In animals treated with PLO-coated scaffolds (Fig. 3.5E), the furthest rostral CTb-labelled axons were identified at an average of 3.2 ± 0.2 mm from the injury epicenter. By contrast, control animals that did not receive a scaffold had CTb-traced axons at an average distance of 4.8 ± 0.4 mm from the epicenter (Fig. 3.5C). In animals treated with the uncoated scaffold, the average distance of CTb-traced axons from the epicenter was 3.2 ± 0.3 mm. This tract tracing experiment reveals that sensory axons extend further rostrally in animals with PLO-coated scaffolds compared to those without a scaffold. However, it is unclear whether those sensory fibers are regenerated axons or spared fibers that may result from reduced cystic cavitation after injury.

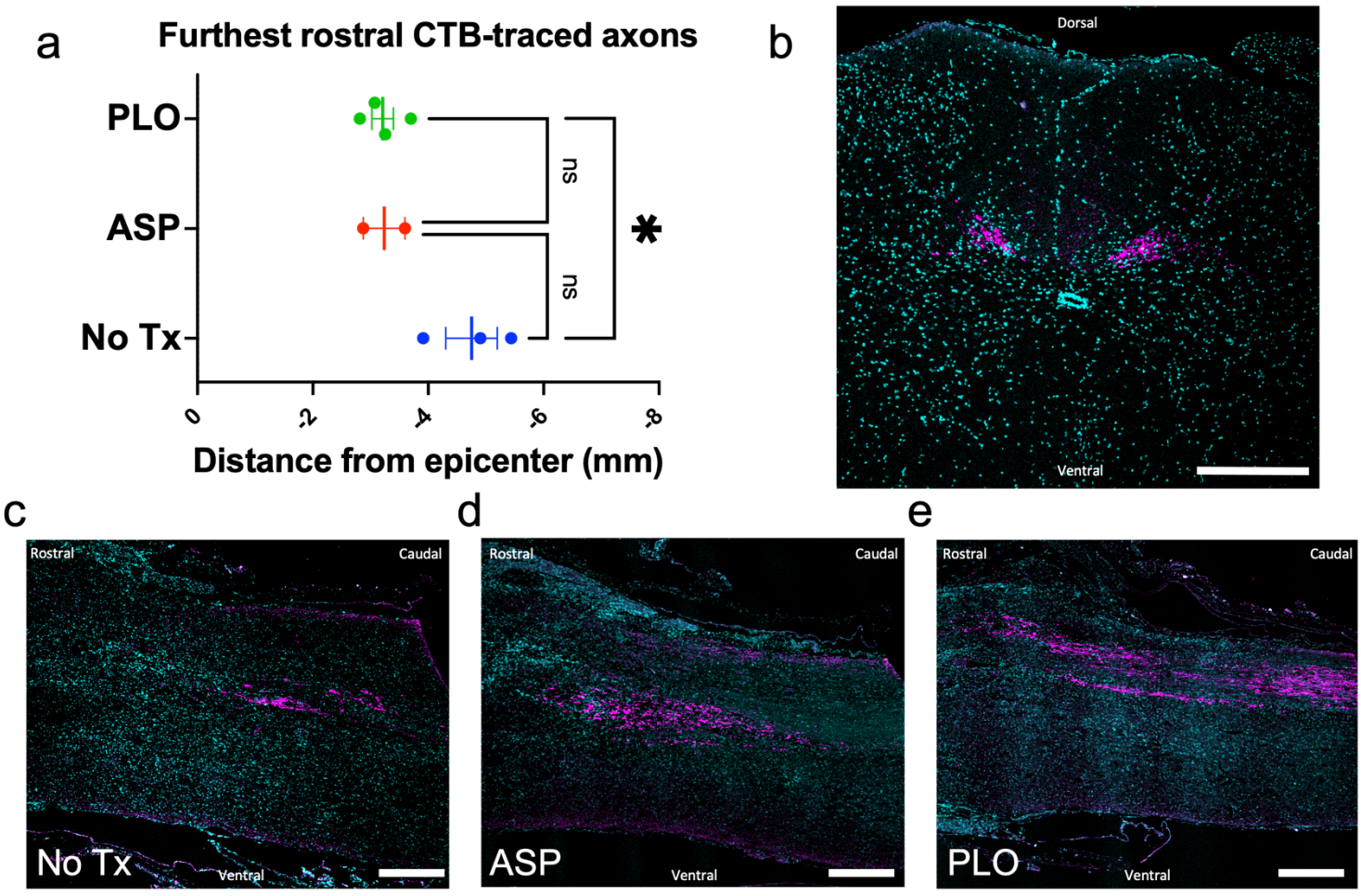

Figure 3.5 Retrograde tract tracing of ascending sensory afferents by CTb injection into sciatic nerve
A. Furthest rostral CTb-traced axons. Each point represents the distance (mm) between the injury epicenter and the furthest rostral CTb-traced axon in one animal. Bar represents the mean ± s.e.m of each group (One-way ANOVA; * P = 0.0264, *n* = 4 PLO animals, *n* = 2 ASP animals, *n* = 3 No Tx animals). **B**. Hoescht (cyan) stained cross section of spinal cord at T10 (caudal to the injury) confirms presence of CTb (magenta) in dorsal column and lamina 4 (scale bar = 300µm). **C**. Hoescht (cyan) stained sagittal section of spinal cord from SCI animal with no scaffold at T9 (caudal side of the injury). CTb-traced axons (magenta) can be seen in the dorsal column (scale bar = 500µm). **D**. Hoescht (cyan) stained sagittal section of spinal cord from SCI animal with uncoated scaffold at T9 (caudal side of the injury). CTb-traced axons (magenta) can be seen in the dorsal column (scale bar =500µm). **E**. Hoescht (cyan) stained sagittal section of spinal cord from SCI animal implanted with PLO-coated cellulose scaffold at T9 (caudal side of the injury). CTb-traced axons (magenta) can be seen in the dorsal column (scale bar = 500µm).

3.2.3.4 Anterograde labeling of the corticospinal tract

Another tract tracing experiment was performed to investigate the regeneration of the hindlimb corticospinal tract (CST), which is involved in the control of voluntary movement in mammals (Schieber, 2007; Ueno et al., 2018). After the recovery period of 11 weeks, stereotaxic injections of dextran amine (DA) conjugated to Alexa Fluor 488 were made into the hindlimb motor cortex, which has descending projections in the spinal cord. Successful tracer uptake was confirmed by confocal laser scanning microscopy of T6 spinal cord cross-sections rostral to the injury, which showed strong positive dextran amine labelling of axons in the corticospinal tract (Fig. 3.6B). In sagittal sections, dextran amine-labeled axons were identified at the rostral interface between the biomaterial and spinal cord (Fig. 3.6D & E), though none were present in T10 cord sections caudal to the injury. The most caudal DA-labelled axons were identified at an average distance of 0.33 ± 0.4 mm from the epicenter for animals with PLO-coated scaffolds (Fig. 3.6E), 0.45 ± 0.3 mm from the epicenter for those with the uncoated scaffold (Fig. 3.6D), and 1.6 ± 0.1 mm from the epicenter for animals without a scaffold (Fig. 3.6C). Although no significant difference in CST axon extension was found between the experimental groups, DA-traced axons were seen projecting along the dorsal side of the PLO-coated cellulose biomaterial towards the caudal spinal cord (Fig. 3.6E).

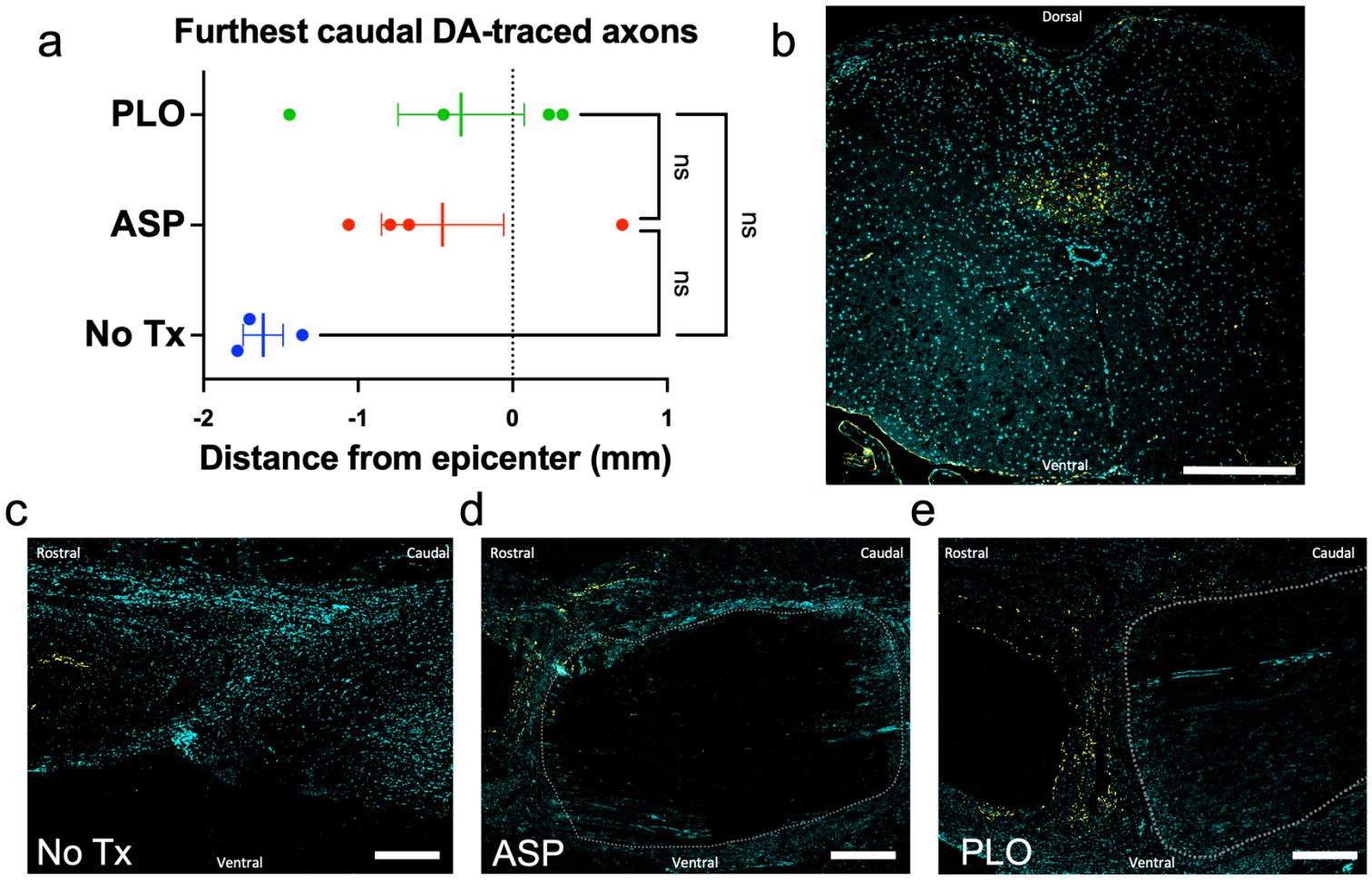

Figure 3.6 Anterograde labeling of the corticospinal tract by injection of dextran amine into hindlimb motor cortex. A. Furthest caudal dextran amine-traced axons. Each point represents the distance (mm) between the injury epicenter and the furthest caudal DA-traced axon in one animal. Bar represents the mean ± s.e.m of each group (One-way ANOVA; P = 0.0903, *n* = 4 PLO animals, n = 4 ASP animals, *n* = 3 No Tx animals). **B**. Hoescht (cyan) stained cross section of spinal cord at T6 (rostral to the injury) confirms presence of dextran amine (yellow) in corticospinal tract (scale bar = 300µm). **C**. Hoescht (cyan) stained sagittal section of spinal cord from SCI animal with no scaffold. DA-traced axons (yellow) can be seen in the corticospinal tract (rostral aspect on the left, scale bar = 500µm). **D**. Hoescht (cyan) stained sagittal section of spinal cord from SCI animal implanted with uncoated cellulose scaffold (outlined by white dotted line). DA-traced axons (yellow) can be seen in the corticospinal tract (rostral aspect on the left, scale bar = 500µm). **E**. Hoescht (cyan) stained sagittal section of spinal cord from SCI animal implanted with PLO-coated cellulose scaffold (outlined by white dotted line). DA-traced axons (yellow) can be seen in the corticospinal tract (rostral aspect on the left, scale bar =500 µm)**.**

3.2.3.5 Neural cell infiltration and axonal sprouting inside cellulose biomaterial

Histological analysis of spinal cord tissue revealed host cell infiltration into the scaffolds from the rostral and caudal interface. Within the scaffold, both cell bodies and axonal projections expressing β-III tubulin, an early neuronal marker, were identified (Fig. 3.7A & B). This finding suggests that endogenous adult neural stem cells infiltrated the biomaterial and initiated differentiation towards neural lineages. In addition, a substantial number of NF200-positive cells were observed inside the scaffold and surrounding tissue (Fig. 3.7C). In both PLO-coated and uncoated scaffolds, NF200-positive cells densely clustered at the outermost edge of the scaffold and some NF200-positive neurites extended into its channels. To determine the effect of PLO coating on infiltration of NF200-positive cells, the distance of infiltration into the channels was measured from the scaffold edge towards the injury epicenter in NF200-stained sagittal sections. NF200-positive cells penetrated significantly further into the channels of PLO-coated scaffolds compared to those without the coating ($p = 0.0286$, Fig. 3.7F). On average, the longest distance of NF200-positive cell infiltration was 388.8 ± 154.5 μm into the PLO-coated scaffolds and 215.6 ± 22.3 μm in the uncoated scaffolds. However, the percentage of channels infiltrated by cells did not differ between the two conditions ($p = 0.8286$). In PLO coated scaffolds, 93 ± 0.8% of the channels were infiltrated by NF200-positive cells, on average, and uncoated scaffolds had 93 ± 2% of their channels infiltrated. Interestingly, at the rostral and caudal interfaces of the biomaterial we observed a cluster of neurofilament-positive projections branching from the dorsal to ventral aspect of the spinal cord, perpendicular to the axis of the tracts (Fig. 3.7D).

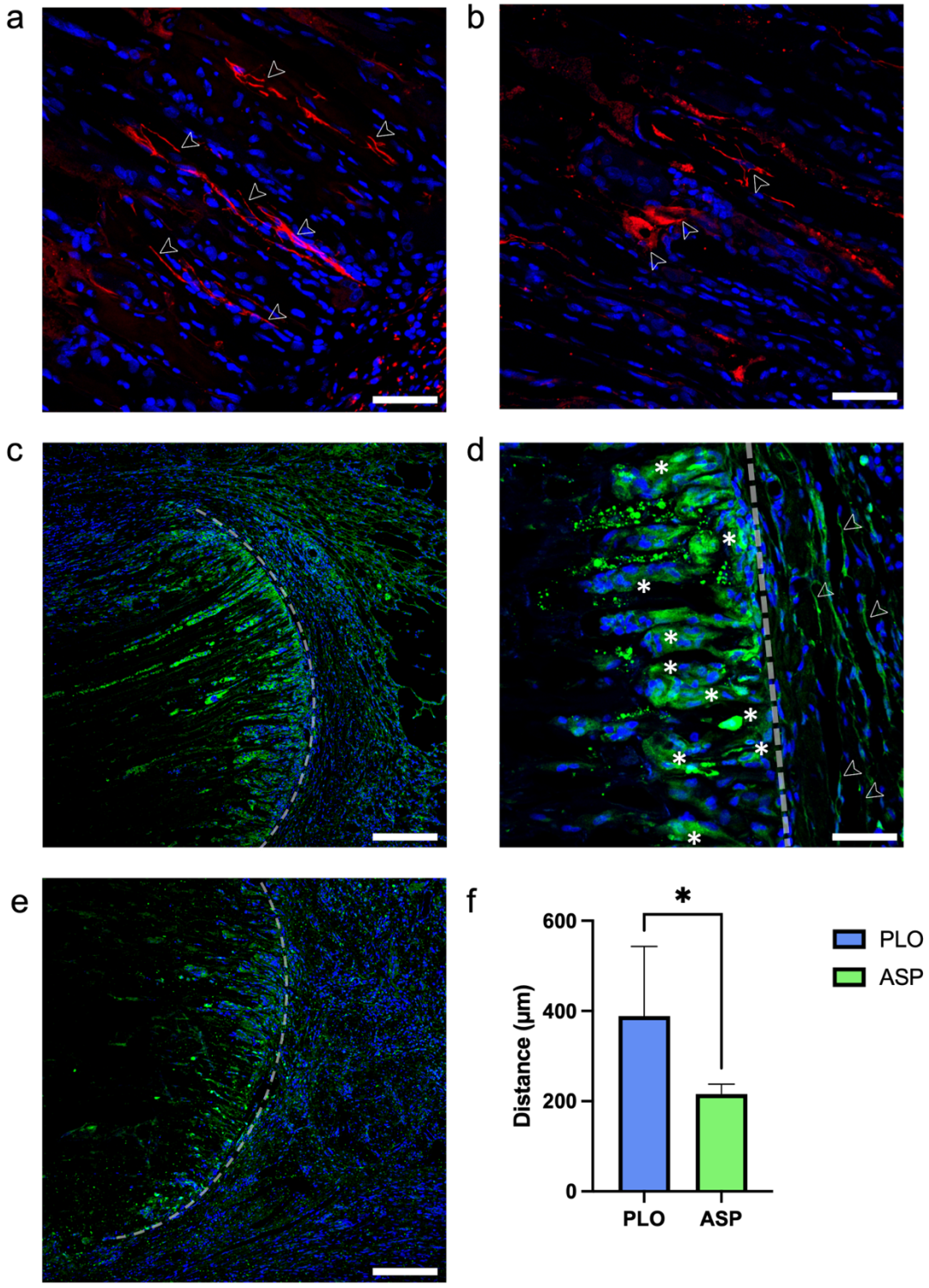

Figure 3.7 Immunostaining for ß-III tubulin and neurofilament-200 reveals neural cells attaching to scaffold and migrating along channels. A. ß-III tubulin (red) and Hoescht (blue) staining of sagittal section within PLO-coated biomaterial. Cell bodies (identified by arrow) can be seen inside the scaffold (scale bar = 50µm). **B**. ß-III tubulin (red) and Hoescht (blue) staining of sagittal section within PLO-coated biomaterial. Axons (identified by arrow) can be seen sprouting inside the scaffold (scale bar = 50 µm). **C**. Neurofilament 200 (green) and Hoescht (blue) staining of sagittal section at the interface (dashed line) between PLO-coated biomaterial and spinal cord (scale bar = 200µm). **D**. Neurofilament 200 (green) and Hoescht (blue) staining of sagittal section at the interface (dashed line) between PLO-coated biomaterial and spinal cord. NF200 positive cells can be seen infiltrating the biomaterial (asterisk) & NF200 axon projections extend from the dorsal to ventral aspect of the biomaterial (arrow) (scale bar = 50µm). **E**. Neurofilament 200 (green) and Hoescht (blue) staining of sagittal section at the interface (dashed line) between uncoated biomaterial and spinal cord (scale bar 200µm). **F**. Longest distance of infiltration of NF200-cells into the scaffold for each experimental group. The mean ± SD of each group is shown (unpaired T-test Mann Whitney; $p = 0.0286$, $n = 4$ PLO animals, $n = 4$ ASP animals).

Finally, tissue sections from each experimental group were stained with luxol fast blue (LFB) to evaluate axon myelination in the injury site (Fig. 3.8 and 3.9). As expected with a traumatic spinal cord injury, severe degeneration of myelin was observed in the perilesional tissue, consistent with Wallerian degeneration. However, in animals that received a PLO-coated scaffold, dark blue bands of LFB staining were consistently observed at the rostral and caudal interface of the PLO-coated scaffold and tissue, indicating possible remyelination induced by the poly-L-ornithine (Fig. 3.8A). Although we did not quantify this observation, several images from different animals are provided in Figure 3.9.

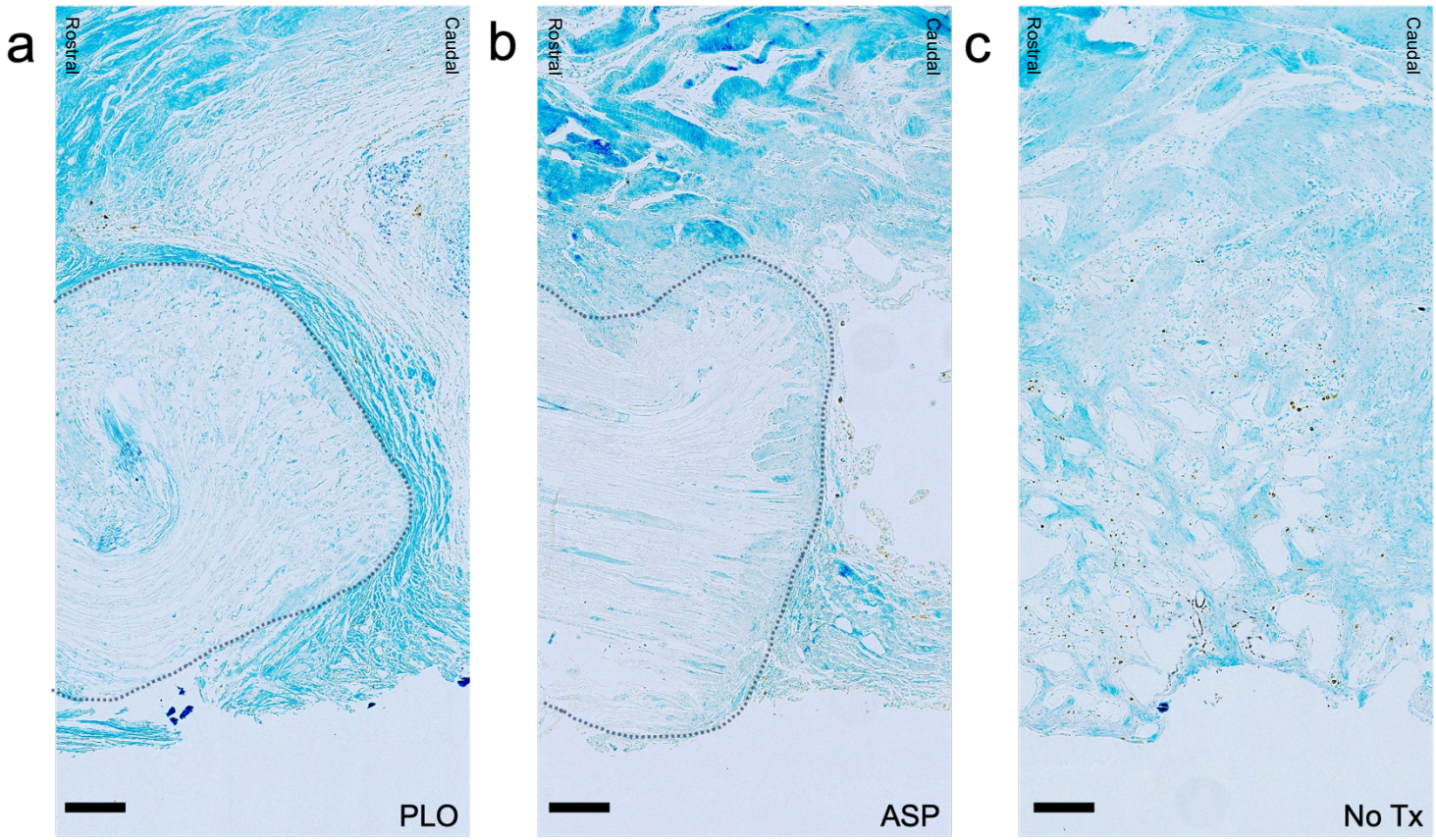

Figure 3.8 Luxol fast blue (LFB) staining of sagittal tissue sections for assessment of myelin at the site of spinal cord injury. A. Representative LFB staining at scaffold-tissue interface in animals implanted with PLO coated cellulose scaffold. Outline denotes cellulose scaffold (scale bar = 200µm). **B**. LFB staining at scaffold-tissue interface in animals implanted with uncoated cellulose scaffold (outlined) (scale bar = 200µm). **C**. LFB staining at cyst-tissue interface in animals with no scaffold (scale bar = 200µm).

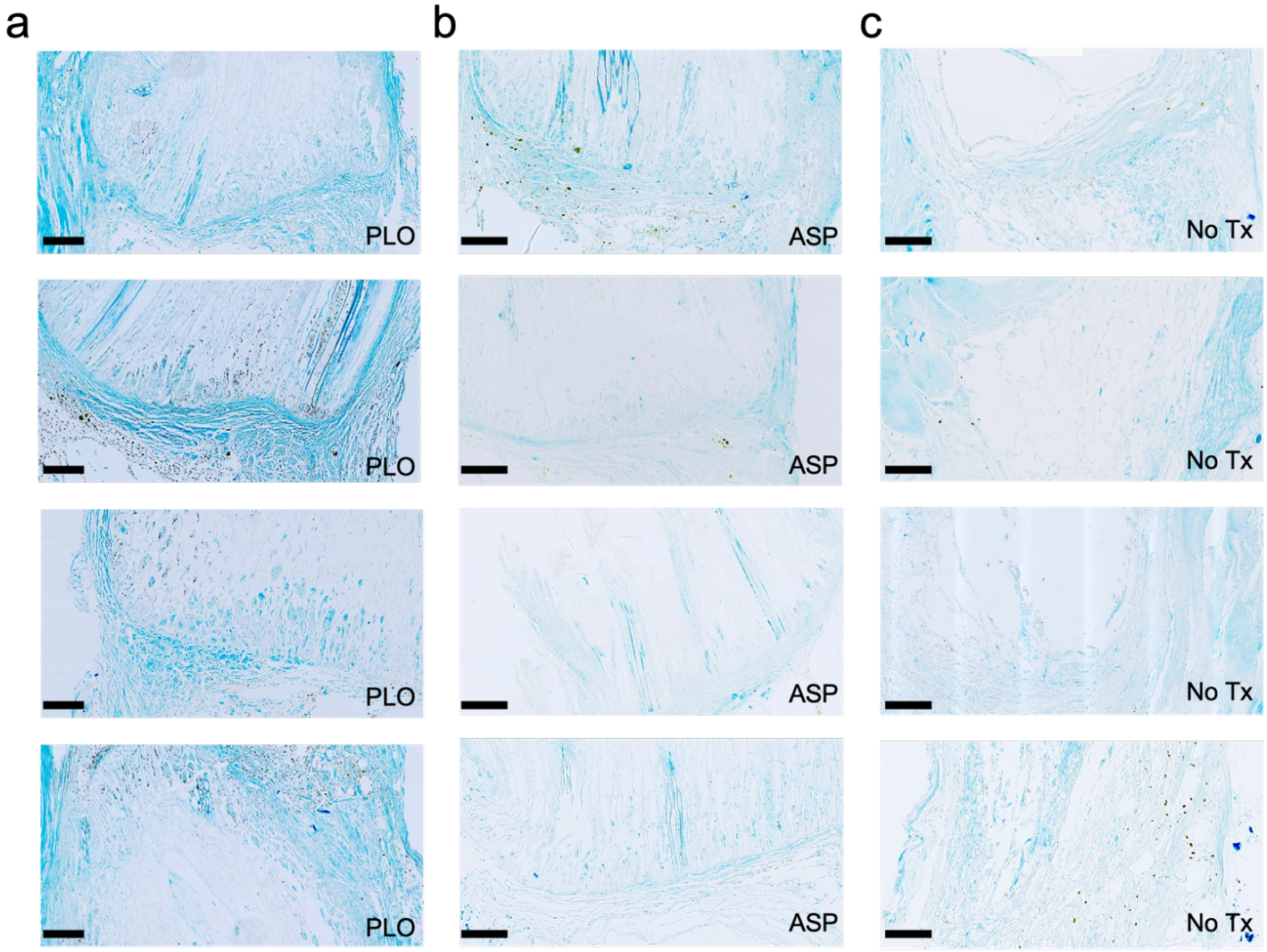

Figure 3.9 Luxol fast blue (LFB) staining of sagittal tissue sections for assessment of myelin at the site of spinal cord injury. A. Representative LFB staining at scaffold-tissue interface in animals (n = 4) implanted with PLO coated cellulose scaffold. Outline denotes cellulose scaffold (scale bar = 200µm). **B**. LFB staining at scaffold-tissue interface in animals (n = 4) implanted with uncoated cellulose scaffold (outlined) (scale bar = 200µm). **C**. LFB staining at cyst-tissue interface in animals (n = 4) with no scaffold (scale bar = 200µm).

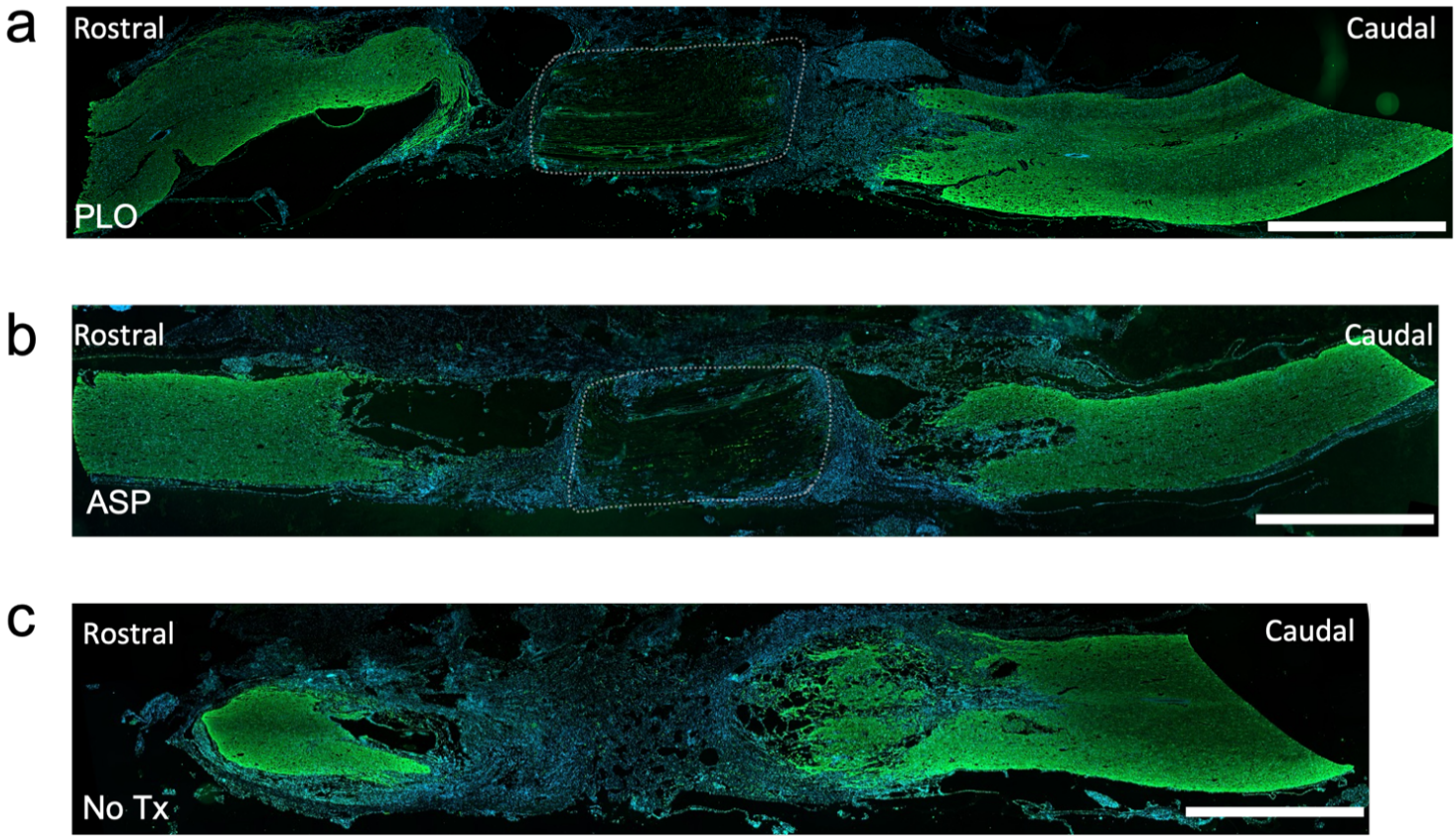

Figure 3.10 Immunostaining for glial fibrillary acidic protein (GFAP) in sagittal spinal cord sections after SCI. A. GFAP (green) stained cord section from animal implanted with PLO coated cellulose scaffold. Nuclei stained with dapi (blue). Outline denotes cellulose scaffold (scale bar = 200µm). **B**. GFAP (green) stained cord section from animal implanted with uncoated cellulose scaffold (outlined). Nuclei stained with dapi (blue) (scale bar = 200µm). **C**. GFAP (green) stained cord section from animal with no scaffold. Nuclei stained with dapi (blue) (scale bar = 200µm).

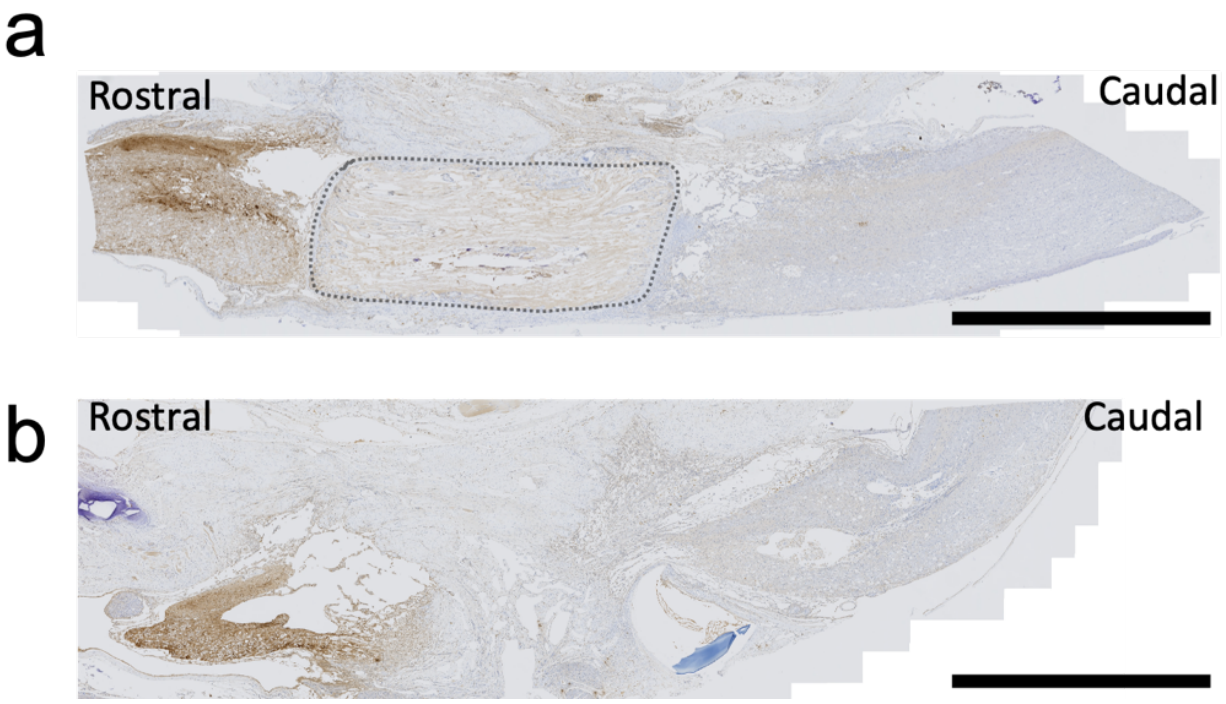

Figure 3.11 5-HT immunohistochemistry staining of sagittal section of T8-T9 spinal cord injury. A. 5-HT staining of spinal cord implanted with ASP scaffold (outlined). IHC was performed using DAB as the chromogen (brown) (scale bar = 2mm). **B**. 5-HT staining of spinal cord with no implant. IHC was performed using DAB as the chromogen (brown) (scale bar = 2mm).

3.2.4 Discussion

Complete SCI leads to the loss of both sensorimotor and autonomic function distal to the injury site due to the interruption of ascending and descending pathways. Regrowth of axons and restoration of appropriate synaptic connectivity after SCI remains a major medical challenge. Various therapeutic strategies have attempted to induce sprouting of the corticospinal tract or to establish relay neural circuits that can mediate functional recovery (Jin et al., 2015; Lai et al., 2021). Neural circuits in the injured spinal cord are known to exhibit plasticity after treadmill training (Shah et al., 2013) or electrical epidural stimulation (Ichiyama et al., 2005) that can produce some degree of motor recovery. However, irregular synaptic connectivity after SCI can be maladaptive and lead to spasticity or neuropathic pain (West et al., 2015). In recent decades, biomaterial-based therapeutic strategies for SCI have been explored as a means to support axonal growth and deliver cells or pharmaceuticals locally to modulate the inhibitory milieu of the lesion. For instance, some groups have produced bioactive scaffolds that use cell signaling molecules to enhance axonal regrowth, myelination, and functional recovery (Álvarez et al., 2021) while others have 3D printed scaffolds with microarchitectures that mimic the structures in the spinal cord to support the formation of neural relays (Koffler et al., 2019). As well, several scaffolds have been used as carriers to deliver various types of stem cells to the injured cord to promote repair (Gong et al., 2020).

In the present study, we investigated the ability of naturally occurring microarchitectures found in plant-derived scaffolds to provide physical support to regenerating axons and guide their extension across a lesion in the spinal cord. Our results show that plant cellulose can become vascularized after implantation into the spinal cord and that endogenous neural cells expressing β-III tubulin and NF200 readily migrate into the channels of the scaffold in a linear orientation along the rostral-to-caudal axis.

Aside from directing the extension of regenerating axons, the biomaterial may have contributed to motor recovery by its interaction with astrocytes, which are known to play a key role in SCI pathology. The presence of channels at the surface of the cellulose scaffolds may have affected the alignment and

morphology of astrocytes in the injury site, as previous reports have shown that cytoskeletal modulation in astrocytes can be induced by microgrooves (Singh et al., 2015). After SCI, reactive astrogliosis causes changes in the gene expression and morphology of astrocytes surrounding the lesion, leading to the formation of a dense glial scar (X. Li et al., 2020). Glial fibrillary acidic protein (GFAP) is commonly used as a marker for the glial scar, which is known to play a protective role by separating healthy CNS tissue from injured tissue (Okada et al., 2018), while also contributing to regeneration failure. We found positive immunostaining for GFAP in sagittal spinal cord sections from each experimental group (Figure 3.10). In all animals, GFAP expression was observed in the tissue rostral and caudal to the injury, with little to no GFAP visible in the injury epicenter. By occupying space in the injury site, the cellulose scaffold may have reduced the number of reactive astrocytes migrating into the lesion and interfered with signaling mechanisms involved in the propagation of reactive astrogliosis, thereby attenuating tissue damage and enhancing motor ability. Importantly, expression of GFAP was likely influenced by the animals' exposure to environmental enrichment, as has previously been demonstrated (Saur et al., 2014).

Though some SCI therapeutic approaches aim to minimize scar formation, in the present study, no observable difference in GFAP expression was found. Importantly, recent studies found that eliminating the glial scar by ablation of astrocytes resulted in worse functional outcomes (M. A. Anderson et al., 2016b; Bellver-Landete et al., 2019; Perez-Gianmarco & Kukley, 2023). Their findings also suggest the involvement of multiple other cell types and other non-neural components such as chondroitin sulphate proteoglycans in the glial scar (M. A. Anderson et al., 2016a; Gu et al., 2019). Given recent findings, future studies should investigate the impact of cellulose biomaterials on these other scar components.

We tested the ability of plant-derived cellulose scaffolds to support repair in combination with a coating of poly-L-ornithine, a positively charged synthetic amino acid that adheres to cellulose by electrostatic interactions. PLO is commonly used in neural stem cell culture and previous studies have

demonstrated its ability to improve cell attachment and migration (Ge et al., 2016; Schackel et al., 2019). Specifically, PLO was shown to promote filopodia formation in neural progenitors *in vitro* (Ge et al., 2016) by increasing the expression of α-Actinins 4, a critical effector of structural plasticity. Based on this, we hypothesized that PLO may have a similar effect *in vivo* after SCI and that increased sprouting of severed axons could assist in establishing neural relays across the scaffold, thereby mediating functional recovery.

We found that animals implanted with the uncoated cellulose scaffold had a modest recovery of motor function in the BBB assessment and this recovery was enhanced by the addition of the poly-L-ornithine coating. By contrast, no significant recovery of motor function was observed amongst the No Tx animals during the recovery period. Despite the motor improvements seen in biomaterial-treated animals, we did not find evidence of serotonergic activity below the injury. Immunohistochemistry staining for 5-HT revealed some sprouting of serotonergic axons, though positive 5-HT staining was limited to tissue on the rostral side of the complete transection in all experimental groups (Figure 3.11). Serotonin (5-HT) plays a key role in the activation of spinal networks that control locomotion. Complete SCI typically results in depletion of 5-HT below the injury, accompanied by an increase in the expression of certain 5-HT receptors (Ghosh et al., 2015). After SCI, it has been suggested that 5-HT receptors become constitutively active in the absence of 5-HT & could contribute to spontaneous recovery of motoneuron excitability (Murray et al., 2011). Future work could investigate whether the biomaterial-treated animals in our study have increases in activity of 5-HT receptors, which could enable intrinsic spinal circuits to partially compensate for lost serotonergic input. The cellulose scaffold's effect on 5-HT receptor activity below the injury may be one of the mechanisms by which the biomaterial supports motor recovery.

To investigate possible axon regeneration which may contribute to the observed motor recovery, we performed retrograde tract tracing by injecting CTb into the sciatic nerve. This neural tract tracing experiment demonstrated that sensory axons extended a greater distance into the injury site in animals with PLO-coated scaffolds compared to those without a scaffold. Our findings are consistent with those of Schackel et al, who found that PLO/laminin-coated hydrogels implanted in animals with a cervical hemisection had increased host cell migration and a slight increase in neurite growth (Schackel et al., 2019). Further experiments may elucidate the mechanism by which the PLO-coated scaffold produced this effect. It is unclear whether the CTb-traced sensory fibers in the injury site are regenerated axons or spared fibers that may result from reduced axonal retraction after injury. We speculate that the presence of the cellulose scaffold in the injury site may slightly reduce cystic cavitation, thereby mitigating further axon retraction after injury. In addition, it is possible that the PLO coating promoted neurite extension, as demonstrated by other works (Ge et al., 2016; Schackel et al., 2019; Setien et al., 2020). Similarly, the immunostaining experiments we performed on sagittal sections of the scaffold after 12-weeks *in vivo* revealed NF200-positive cells migrating further into the channels of scaffolds with the PLO coating compared to the uncoated biomaterial. Taken together, our results highlight the potential of plant-derived scaffolds, though further work is necessary to optimize therapeutic strategies using these biomaterials with PLO or other peptides to further enhance neural cell infiltration to potentially enable communication between circuits below and above the injury.

The differences we identified in the sensory axons in PLO-treated animals could possibly have contributed to their recovery in motor ability, given the importance of sensory feedback in motor function (Courtine et al., 2009; Takeoka, 2020; Takeoka et al., 2014; Takeoka & Arber, 2019). To test whether these axons serve as the substrate for functional recovery, further experiments could be performed to assess the functionality of theses regenerated sensory fibers and to identify whether they have relevant

synaptic contacts. In addition to sprouting of sensory axons, we found enhanced myelination in the injury site of animals with PLO-coated scaffolds, as evidenced by the luxol fast blue staining showing myelin in the scaffold periphery. In a recent study, the ability of PLO to enhance myelin repair was demonstrated in an animal model of focal demyelination (Xiong et al., 2023). We speculate that myelin repair may be a contributing mechanism underlying PLO-induced motor recovery in our SCI model. Further, the positive effect of PLO on myelination in the injury site may be two-fold, as myelin breakdown products are known to be inhibitors of neuronal plasticity. Hence, by enhancing remyelination, PLO may also be creating a more permissive environment for axonal sprouting, consistent with our observations. In future experiments, plant cellulose scaffolds could be seeded with stem cells, functionalized with neurotrophins or axon guidance molecules such as netrins or ephrins to further promote regeneration of axons through the scaffold.

Environmental enrichment (EE) was included as part of our multifaceted neurorehabilitation strategy due to its ability to enhance neuroplasticity and attenuate SCI-induced neuropathic pain (Berrocal et al., 2007; De Virgiliis et al., 2020; Koopmans et al., 2012). Environmental enrichment is a housing manipulation that includes novel toys, tunnels, nesting materials, puzzles, and running wheels along with opportunities for socialization with conspecifics. By enhancing plasticity, enriched environments support functional improvements in animal models of stroke and SCI (Berrocal et al., 2007; Clemenson et al., 2015; De Virgiliis et al., 2020; Hutson et al., 2019; Koopmans et al., 2012; McDonald et al., 2018; Neves et al., 2023; Tai et al., 2021). Studies have indicated that EE promotes plasticity through various mechanisms including increased production of neurotrophic factors and changes in dendritic-spine density (Rossi et al., 2006). In rodent SCI models, enrichment potentiates the regenerative ability of neurons via Creb-binding protein-mediated histone acetylation, which increases expression of regeneration-associated genes (Hutson et al., 2019). Many groups have reported that environmental enrichment substantially

improves sensory and motor recovery after contusive SCI (Berrocal et al., 2007; Koopmans et al., 2012). Similarly, in animal models of stroke, exposure to an enriched environment causes neuroanatomical changes including dendritic remodeling, axonal sprouting, and the release of growth factors (B. B. Johansson & Belichenko, 2002). It has also been reported that environmental enrichment may promote white matter recovery after stroke by reducing microglia activation (Y.-S. Guo et al., 2022). Altogether, environmental enrichment shows great promise as part of a multimodal SCI therapeutic strategy. In the present study, all animals were housed with EE and no standard housing (SH) controls were included, since SH is an impoverished environment that is not representative of the conditions of human SCI patients. In addition to improving animal welfare throughout the study, we speculate that the enriched environment may have contributed to the growth of axons after SCI by expanding the regenerative ability of sensory neurons, as previously reported (De Virgiliis et al., 2020). Enrichment has been explored as a therapeutic modality for stroke and traumatic brain injury, with results suggesting it may act synergistically with other treatments to enhance functional outcomes (Maegele et al., 2005). However, it is possible that enrichment in our study overshadowed the benefits of the PLO-coated scaffold alone.

This study demonstrated the potential of plant-derived cellulose scaffolds to be functionalized with peptides and used in a multimodal SCI therapeutic strategy that includes environmental enrichment. We found that coating the biomaterial with poly-L-ornithine supported hindlimb motor recovery and neural tissue repair in a rat model of complete transection. The biomaterial was infiltrated by endogenous neural cells, which migrated along the linearly oriented channels of the plant scaffold. Retrograde neural tracing highlighted regeneration of sensory tracts in the spinal cord after treatment with PLO-coated scaffolds. Results from experimental SCI models must be interpreted cautiously when attempting to translate them to human applications, as some key differences exist between species. In particular, post-injury immune responses and neuroplasticity are species-dependent factors that impact disease progression (Filipp et al.,

2019; Sharif-Alhoseini et al., 2017). For instance, the formation of fluid-filled cysts is common after injury in humans and rats, but not in mice (Hachem & Fehlings, 2021; Ma et al., 2001; METZ et al., 2000). Overall, our results point to exciting potential patient-treatment strategies that use plant-derived scaffolds in combination with other therapeutics.

3.2.5 Methods

Biomaterial production: Cellulose scaffolds were prepared using a 4 mm diameter biopsy punch to cut Asparagus officinalis sections which were then placed into a 50ml Falcon tube containing 0.1% sodium dodecyl sulphate (SDS) (Sigma-Aldrich). Samples were shaken for 72 hours at 180 RPM at room temperature. The resulting cellulose scaffolds were then transferred into new sterile microcentrifuge tubes, washed and incubated for 12 hours in phosphate-buffered saline (PBS). Following the PBS washing steps, the asparagus were then incubated in 100 mM CaCl2 for 24 hours at room temperature and washed 3 times with dH2O. Samples were then sterilized in 70% ethanol overnight. Finally, scaffolds were washed 12 times in a sterile saline solution before incubating overnight in a 100µg/ml solution of poly-L-ornithine (30-70kDa, Sigma-Aldrich, P3655).

Animal Housing and Environmental Enrichment: All procedures described in this study were approved and performed in accordance with standards set out by the University of Ottawa Animal Care and Veterinary Services ethical review committee. Methods and results are reported in accordance with ARRIVE guidelines. Juvenile female Sprague Dawley rats were purchased from Charles River. Rat tickling was performed with the juvenile rats as a habituation technique to improve welfare. Experimenters followed the Panksepp method (Burgdorf & Panksepp, 2001) of rat tickling which consists of 15 sec rest followed by 15 sec of dorsal contacts and pins for a total of 2 minutes for 4 days of training. Upon completing tickle training, every rat was tickled before every procedure. Clicker training was performed

with the juvenile rats to encourage cooperation in all behavioral assays and to develop positive affect with experimenters. Briefly, rats were encouraged to step onto a plastic platform and given food rewards upon successful completion, accompanied by a 'click'. Clicker training was done for 5 days (4 mins daily). All rats were housed in pairs throughout the study and got 20 minutes of daily group play with conspecifics. During group play, up to 10 rats were placed in a 1-meter diameter arena with climbing structures, tunnels, foraging toys, food enrichment and nesting material. Enrichment was provided in all rats' home cages, including a wooden block, nylon bone (Bio-Serv, K3580), bunny block (Bio-Serv, F05274) and metal swing. In addition to a diet of standard rat chow, all rats were given daily food enrichment including mini yogurt drops (Cedarlane Bio-Serve, F7577), banana chips (Cedarlane Bio-Serve F7161), fruity bites (Cedarlane Bio-Serve F6038), ABC fruit blend (Cedarlane Bio-Serve F7228), Mealworms (Cedarlane Bio-Serve 9264), veggie-bites (Cedarlane Bio-Serve F5158) and pumpkin (E.D. Smith).

Spinal Cord Transection Surgical Procedure: Once rats reach a weight of 250-300g, they are anesthetized with isoflurane USP-PPC and injected subcutaneously with normal saline (Baxter) and enrofloxacin (Baytril). Laminectomies were performed at the T8-T9 level to expose the spinal cord, followed by a dorsal midline durotomy. The entire cord was gently lifted by a hook before cutting with micro scissors. Surgifoam 1972 (Ethicon) was used to establish hemostatic control, then the gap was measured after 10 minutes to select the appropriately sized cellulose implant. Prior to surgery, animals were be split into four groups: sham (laminectomy only, $n = 2$), No Tx (full transection only, no scaffold, $n = 8$), ASP treated (cellulose implant only, $n = 9$), and PLO treated (PLO-coated cellulose implant, $n = 11$). PLO-coated scaffolds were rinsed twice with sterile water before implantation. While implanting the scaffold, ARTISS fibrin sealant (Baxter) was be applied into the cavity. The muscle and adipose tissue are reapproximated with 3-0 Vicryl sutures (Johnson & Johnson) and the skin was closed with Michel

clips (Fine Science Tools). Rats received post-operative care including bladder expressions 4 times daily, pain monitoring and management with buprenorphine HCl, when necessary, weight loss and dehydration tracking.

BBB Locomotor Assessment: Functional recovery of the hindlimbs was assessed by a weekly BBB open field assessment.(BASSO et al., 1995) Each rat was placed in a 1-meter diameter arena covered with a non-slippery floor and recorded by 5 cameras. The 4-minute videos were then scored by three blinded observers and the average of three examiners was calculated for each animal at each timepoint. Spasticity and movement occurring simultaneously with urination was ignored and confirmed with repeated views of the videos. Two weeks after receiving the spinal cord injury, one animal was excluded based on their BBB score, which was above 5.

KSAT Swim Assessment: Before SCI, all rats were acclimatized to the pool daily (up to 5 minutes) for 5 days. During this pre-training, each rat was placed into a clear acrylic swim tank (depth 20cm, length 150cm) filled with water (27-30˚C) and encouraged to swim via clicker training. Animals with poor performance were excluded from the study before the SCI surgery. After rats sustained a SCI, the swim assessment was performed every 2 weeks to assess functional recovery. Each animal was allowed three runs across the swim tank with 20 second rests between runs. Swimming was recorded by 4 cameras and videos were scored by 3 blind observers using the Karolinska Institutet Swim Assessment Tool (KSAT) (Xu et al., 2015).

Inclined Plane Assessment: Before the spinal cord injury, all animals were trained to perform the inclined plane test as described by Rivlin et al (Rivlin & Tator, 1977). Each rat was placed on an inclined plane while adjusting the slope to determine the maximum angle at which the animal can maintain its position without falling. Every 2 weeks after the spinal cord injury, the inclined plane test was performed to examine sensorimotor recovery.

Retrograde Tract Tracing of Ascending Sensory Afferents: Animals also received 2uL of Cholera Toxin Subunit B conjugated to Alexa Fluor 647 (CTb, ThermoFisher, cat. C34778, 1% solution in sterile PBS) injected bilaterally into their sciatic nerves (4uL total per rat). Rats were anesthetized with 3% isoflurane, a linear incision was made along the femur, and the gluteus maximus was separated from the gluteus medius to expose the sciatic nerve. Using a surgical microscope, a nick was made in the proximal portion of the exposed nerve. The CTb solution was loaded into a Hamilton syringe, and the needle was inserted 5mm into the sciatic nerve. CTb was injected in increments of 0.5µL, waiting 30 seconds and withdrawing the needle by 1mm per injection. Once the injection was complete, a sterile Q-tip was used to remove any CTb that was expelled from the nerve and the incision was sutured using 4-0 Prolene sutures. Post-operatively, 2% bupivacaine was applied topically and animals were given buprenorphine (0.05mg/kg subcutaneously) and Gabapentin (Chiron, 50mg/kg subcutaneously) for analgesia. Pain was assessed TID and additional buprenorphine was administered as necessary. To prevent infections, Enrofloxacin (Bayer, 10mg/kg subcutaneously) was administered daily for 3 days peri-operatively.

Anterograde Labeling of the Corticospinal Tract: 11 weeks post-operatively, rats from each group were injected with neural tracers to visualize axons in and around the injury site. Animals were anesthetized with 3% isoflurane and placed into a stereotactic frame. After a surgical scrub, a sagittal

incision was made to expose the top of the skull and the periosteum was scraped off. Using a Zeiss surgical microscope, the skull was levelled by measuring the Dorsal-Ventral axis at 4 random points and ensuring they are within 0.05mm of each other. Bregma was located and its coordinates were used to calculate the target location of each injection. Using a surgical drill (Micro Drill, Harvard Apparatus) attached to the stereotactic frame, 8 holes were drilled into the cranium. Stereotactic injections were made into the right and left motor cortex at coordinates: Injection 1: Anterior-posterior (AP) -0.5mm, Medial-lateral (ML) ±2mm, Dorsal-Ventral (DV) 1.5mm. Injection 2: Anterior-posterior (AP) -1mm, Medial-lateral (ML) ±2.5mm, Dorsal-Ventral (DV) 1.5mm. Injection 3: Anterior-posterior (AP) -1.5mm, Medial-lateral (ML) ±2mm, Dorsal-Ventral (DV) 1.5mm. Injection 4: Anterior-posterior (AP) -2mm, Medial-lateral (ML) ±2.5mm, Dorsal-Ventral (DV) 1.5mm. Injections were made using a 5uL Hamilton syringe. After a 2-minute delay, a volume of 0.5µL of 10% Dextran Amine Alexa Fluor 488 (ThermoFisher, cat. D22910, 10,000 MW) was injected into each location at a rate of 250nl/min for a total injection volume of 4µL per rat. Each injection was followed by a 2-minute delay to ensure diffusion into the tissue. Once all 8 injections were complete, the scalp was sutured with 4-0 Prolene sutures and 2% transdermal bupivacaine was applied to the incision. Animals had 2 weeks of recovery time before euthanasia to allow for transport of neural tracers. For tissue collection, animals were deeply anesthetized with isoflurane USP-PPC and euthanized by cardiac perfusion with 500ml of 1xPBS followed by 500ml of 4% paraformaldehyde. The brain and spinal cord were dissected out and fixed overnight in 4% paraformaldehyde at 4°C, then stored in 70% ethanol at 4°C until embedding and sectioning.

Quantification of neuroanatomical tract tracing: Cross-sections of spinal cord tissue above and below the injury site were imaged by confocal laser scanning microscopy to confirm successful tracer uptake. For retrograde tracing, CTb-traced axons were seen in the dorsal columns of T10 cross-sections. For

anterograde tracing, dextran amine labelled axons were identified within the corticospinal tract of T6 cross-sections. For each animal, 3 sagittal sections in the middle of the cord were imaged by confocal laser scanning microscopy and the distance between the tracers and the injury epicenter was measured using ImageJ. For retrograde tracing with CTb (n = 4 PLO animals, n = 2 ASP animals, n = 3 No Tx animals), the distance (mm) was measured between the furthest rostral CTb-traced axon and the injury epicenter. For anterograde tracing with dextran amine (n = 4 PLO animals, n = 4 ASP animals, n = 3 No Tx animals), the distance (mm) was measured between the furthest caudal dextran amine-traced axon and the injury epicenter. Averages were calculated for each group and a one-way ANOVA was performed.

GFAP Immunostaining: Paraformaldehyde-fixed paraffin-embedded tissue sections (5µm thick) were deparaffinized and pre-treated using heat-mediated antigen retrieval with Sodium Citrate buffer (pH 6.0). Slides were then rehydrated in 1X TBST buffer and blocked for 30 minutes with Rodent Block R (Biocare RBR962H). Sections were then incubated with Rabbit GFAP (1:3000, Sigma AB5804) at room temperature for 1.5 hours. Sections were washed with 1XTBST and then incubated with the Goat anti-Rabbit-488 antibody for 2 hours in the dark at room temperature. This was followed by incubation with a quencher (Vector TrueView Autofluorescence Quenching Kit #SP-8400, Vector Labs) to decrease autofluorescence. Sections were then washed, incubated with 5 ug/ml of DAPI (ThermoScientific #62248) and coverslipped.

β-III Tubulin Immunostaining: Paraformaldehyde-fixed paraffin-embedded tissue sections (5µm thick) were deparaffinized and tissue was permeabilized at room temperature (5 mins) the following buffer: 0.5% Triton-X, 20mM HEPES, 300mM Sucrose, 50mM NaCl, 3mM MgCl2, 0.05% sodium azide. Sections were incubated in blocking buffer (6% Normal Goat Serum in 1xPBS) for 10 minutes. Sections were

rinsed twice in 1xPBS before incubation at 4˚C overnight in mouse anti-β-III tubulin antibody (10ug/ml, MAB1195, R&D systems). The following day, after 2 washes of 1xPBS, sections were incubated at room temperature (2.5 hours) in goat anti-mouse alexa Fluor 594 polyclonal antibody (1:200, A11005, Thermofisher) and counterstained with Hoescht (1:2000).

Neurofilament 200 Immunostaining: Paraformaldehyde-fixed paraffin-embedded tissue sections (5µm thick) were deparaffinized and tissue was permeabilized at room temperature (3x 5 minutes) in 1X TBST. Sections were incubated in blocking buffer (5% Normal Goat Serum in 1X TBST) for 30 minutes followed by 3 washes in 1X TBST. Tissue was incubated at 4˚C overnight in rabbit anti-NF200 (1:3000 dilution in 1X PBS, cat. N4142 Sigma). The following day, after 2 washes of 1X PBS, sections were incubated at room temperature (2 hours) in goat anti-rabbit alexa fluor 488 (cat. A11008 Thermofisher) and counterstained with Hoescht (1:2000).

5-HT Immunohistochemistry: Paraformaldehyde-fixed paraffin-embedded tissue sections (5µm thick) were deparaffinized and incubated in rabbit anti-serotonin antibody (1:2500 dilution in 1X PBS, Sigma S5545) for 2 hours. Immunohistochemistry was performed using DAB as the chromogen and counterstained with Hoescht (1:2000).

Luxol Fast Blue Staining: Paraformaldehyde-fixed paraffin-embedded tissue sections (5µm thick) were deparaffinized and stained following the protocol from Carson, Freida L., and Christa Hladik Cappellano. Histotechnology: A Self-Instructional Text. ASCP, 2020. ISBN 13: 9780891896760.

Statistical Analysis: Experimental data were analyzed using GraphPad Prism. For the distance of infiltration of NF200-positive cells, the differences between two groups were compared utilizing the Student's t-test at a significance level of $P < 0.05$ & the Mann Whitney test was performed. Differences between multiple groups were compared by one way ANOVA followed by Tukey's multiple comparisons test (for neuroanatomical tract tracing) or the uncorrected Fisher's LSD (for BBB locomotor assessment) at a significance level of $P < 0.05$.

Chapter 4: dI3s Mediate Sensory-Dependent Motor Recovery After Complete Spinal Cord Injury

This chapter was adapted from a research paper (in preparation) written by Lauren J. Couvrette, Emam Khan, Alex M. Laliberté, Sara Goltash, Krystal L. A. Walker, Andrew E. Pelling and Tuan V. Bui

4.1 Abstract

Cutaneous sensory inputs have been implicated in facilitating recovery of proper locomotor activity in spinalized animals. dI3 neurons are a population of spinal neurons that integrate propriospinal and low-threshold cutaneous sensory inputs and have been implicated in the recovery of locomotor activity after spinal cord injury. In this study, we investigate whether exposing spinalized mice to a textured surface selected to increase low-threshold mechanoreceptor stimuli to the hindlimbs increases locomotor activity through dI3 neuron activity. Mice expressing an inhibitory DREADD receptor, hM4Di, in spinal dI3 neurons, underwent a complete spinal cord transection at the lower thoracic level. Hindlimb motor ability was evaluated using both the standard Basso Mouse Scale (BMS) and a novel crinkle paper locomotor assessment designed to increase low-threshold cutaneous stimuli. Over the course of six weeks, significant improvements in hindlimb activity were observed in the crinkle paper assessment, including plantar paw placement and dorsal stepping. In contrast, no such improvement was observed in the BMS scores of animals placed on a flat, untextured surface. Electromyographic recordings at six weeks revealed increased EMG activity during the crinkle paper test, suggesting that sensory feedback facilitated spinal locomotor circuitry. To distinguish the contribution of cutaneous input from proprioceptive input, lidocaine was used to selectively block cutaneous afferents, leading to a marked reduction in motor activity. Finally, silencing of dI3 neurons impaired the recovery facilitated by crinkle paper, implicating

this population of spinal interneurons in sensory-mediated motor reactivation. These results suggest that cutaneous inputs may serve as a driving force to initiate hindlimb motor activity after injury and reveal the role played by dI3 neurons in modulating spinal locomotor circuits after SCI.

4.2 Introduction

Spinal locomotor circuits underlie the rhythmic and patterned activation of limb muscles to generate locomotor behaviors such as walking (Grillner & Kozlov, 2021). These spinal circuits rely on descending supraspinal inputs as a principal source of driving commands and sensory feedback to adjust motor patterns to the dynamically changing environment (Oliver et al., 2021; Pearson, 2004). Complete transection of the spinal cord abolishes the descending drive to spinal locomotor circuits, leading to hindlimb paralysis. Despite the significant focus on descending pathways as a target for motor recovery after spinal cord injury, few interventions have achieved meaningful axon regeneration in such pathways (X. Li et al., 2019).

Below the level of injury, intraspinal locomotor circuits are often spared and undergo spontaneous remodelling after SCI (Hollis et al., 2015; Onifer et al., 2011; H. Wang et al., 2015; Y. Wang et al., 2018). Without supraspinal input, sensory feedback becomes the primary source of excitation in these motor circuits. Therefore, sensory afferents are a potential therapeutic target which could be manipulated in order to activate motor circuitry after SCI. For instance, epidural electrical stimulation (EES) recruits sensory afferents to activate motoneurons in spinal circuits caudal to an injury (Capogrosso et al., 2013; Courtine et al., 2009; Formento et al., 2018; Lavrov et al., 2008; Musienko et al., 2007). Likewise, treadmill training is known to activate spinal locomotor circuits and produce hindlimb stepping in SCI animals (Kobravi et al., 2017; Leblond et al., 2003) and in humans with SCI (Hicks et al., 2003), likely by recruiting proprioceptive and low-threshold mechanoreceptive inputs. Mounting evidence indicates that hindlimb

sensory afferents can activate spinal circuitry and elicit movement after SCI without the need for supraspinal input (Courtine et al., 2009; Takeoka, 2020).

The role of cutaneous feedback in motor recovery after SCI was investigated via swimming assessments in chicks (Muir & Steeves, 1995) and rats (Smith, Shum-Siu, et al., 2006b) with incomplete injuries. In the absence of limb loading, stimulation of cutaneous receptors resulted in improvements in hindlimb function during swimming in both animals. Moreover, cutaneous feedback was shown to enhance plantar stepping in spinal rats (Sławińska et al., 2012). *Sławińska et al.* found that the upright posture facilitates plantar stepping in rats with SCI. This improvement was reversed by local anesthesia of the hindpaw, demonstrating that cutaneous feedback from the plantar surface of the paw is largely responsible. Likewise, studies performed on spinalized cats also suggest a role for cutaneous inputs in recovery of locomotion. *Bouyer et al* found that cutaneous denervation of the hind paws before spinal transection impairs recovery of both paw placement and weight support in cats (Bouyer & Rossignol, 2003a, 2003b). Further, in transected cats that had recovered some hindlimb locomotion, subsequent cutaneous denervation of hind paws caused the loss of proper paw placement and a reduction in weight support. By contrast, other work in cats with spinal cord injuries shows that cutaneous stimulation of the dorsal lumbar region has an inhibitory effect on locomotion (Frigon et al., 2012; Merlet et al., 2020).

There is a pressing need to identify the mechanisms by which spinal locomotor circuits are regulated after SCI. Determining the role of precise cell types in this phenomenon will help advance therapeutic strategies that rely on the automaticity of lumbar neural circuitry to restore motor function. Reorganization of propriospinal circuits is believed to play a role in the activation of lumbar CPGs after SCI (J. Cheng & Guan, 2023; Laliberte et al., 2019b). Propriospinal neurons propagate sensorimotor input and transmit information between segments of the cord, making them well-positioned to participate in plasticity of spinal circuits. In particular, dI3 neurons are a population of excitatory spinal neurons that

relay cutaneous and proprioceptive information to motoneurons and putatively to spinal locomotor circuits (T. V Bui et al., 2016). In the intermediate spinal cord, dI3 neurons can be identified by the expression of the Islet-1 (Isl1) transcription factor and they are known to project ipsilaterally within the spinal cord (T. V Bui et al., 2016). Silencing of dI3s blunts locomotor recovery in spinalized mice (T. V. Bui et al., 2013; T. V Bui et al., 2016).

We hypothesize that dI3 neurons mediate enhanced signaling between cutaneous afferents and spinal locomotor circuit motoneurons after SCI, thereby enabling low threshold mechanoreceptive inputs to increase excitability of spinal motor circuits. To test this hypothesis, spinally transected mice performed a series of motor assessments with varying degrees of sensory input and chemogenetic manipulation of dI3 activity while placed on a textured surface (crinkle paper) or on a smooth surface.

4.3 Results

4.3.1 Sensory stimulation promotes increased hindlimb motor activity after complete SCI

Seven mice expressing an inhibitory DREADD receptor in spinal dI3 neurons underwent complete transection of the spinal cord (n = 4 transgenic Isl1-Cre; Vglut2-Flp; Cre^{ON}-Flp^{ON} hM4Di mice & n = 3 Isl1-Cre; Vglut2-Flp mice with lumbar intraspinal injection of an AAV carrying hM4Di under the control of Cre and Flp expression). Following surgery, hindlimb motor ability was evaluated weekly using the Basso Mouse Scale (BMS) and the mean of both hindlimbs was used to yield a single BMS score per mouse. BMS scores were attributed based on the following parameters: no ankle movement results in a score of 0, slight ankle movement (less than half of the ankle joint excursion) corresponds to a score of 1, and extensive ankle movement (more than half of the joint excursion) corresponds to a score of 2. A BMS score of 3 is given for plantar placing of the paw, where the paw is actively placed with both the thumb and the last toe touching the ground, with or without weight support. Dorsal stepping (regardless of

frequency) also results in a BMS score of 3 and is defined by weight support at lift off, forward limb advancement and re-establishment of weight support. Occasional plantar stepping results in a BMS score of 4. Two weeks after complete transection (wpi) of the spinal cord, the average BMS score of the group was 0.43 ± 0.35 (n = 7) when animals were observed while placed on flat sterilization wrap (Fig. 4.1A).

To study the effect of additional sensory stimulus on motor ability after complete SCI, the same mice were also placed on a testing area covered in 1/8-inch strips of crinkled paper strands (Fig. 4.1B) that provide enhanced sensory stimulus to the hindlimbs and trunk. The average score of the BMS assessment for mice on the crinkle paper at 2 wpi was 0.78 ± 0.27 (N = 7) (Fig. 4.1C). There was no significant difference in motor ability between the two locomotor assays at 2 wpi (p = 0.3790). Over the 6-week recovery period, BMS scores did not change significantly when animals were tested on the flat sterilization wrap (p = 0.4977, n = 7). By contrast, we found a significant improvement in hindlimb motor ability in the crinkle paper assessment over the same recovery period (p = 0.0006, n = 7) (Fig. 4.1C). Starting at 3 wpi, we found a significant difference in hindlimb motor ability in the crinkle paper locomotor assay compared to the standard BMS (p = 0.0006). By 6 wpi, the average score was 0.64 ± 0.47 in the standard BMS compared to 2.71 ± 0.49 in the crinkle paper motor assessment (Fig. 4.1C).

At 6 wpi, electromyographic (EMG) recordings of activity in the gastrocnemius muscles were performed in mice when placed on the flat sterilization wrap or on crinkle paper. All mice seemed to have a higher mean EMG amplitude in randomly selected 120-second EMG recordings when mice were placed on crinkle paper compared to 120-second recordings when mice were placed on sterilization wrap, though statistical significance was not achieved (p = 0.0677, n = 4) (Fig. 4.1D). Activity bursts were extracted from the 120 second recordings and the maximum peak amplitude of each burst was calculated. The

average of maximum peak amplitudes was calculated for each animal. In all mice, EMG recordings of activity in the gastrocnemius muscles seemed to have higher average peak maximum amplitudes on crinkle paper compared to recordings on sterilization wrap, though statistical significance was not achieved ($p = 0.1029$, $n = 4$) (Fig. 4.1E). This may be due to the small sample size and high variability in percent change.

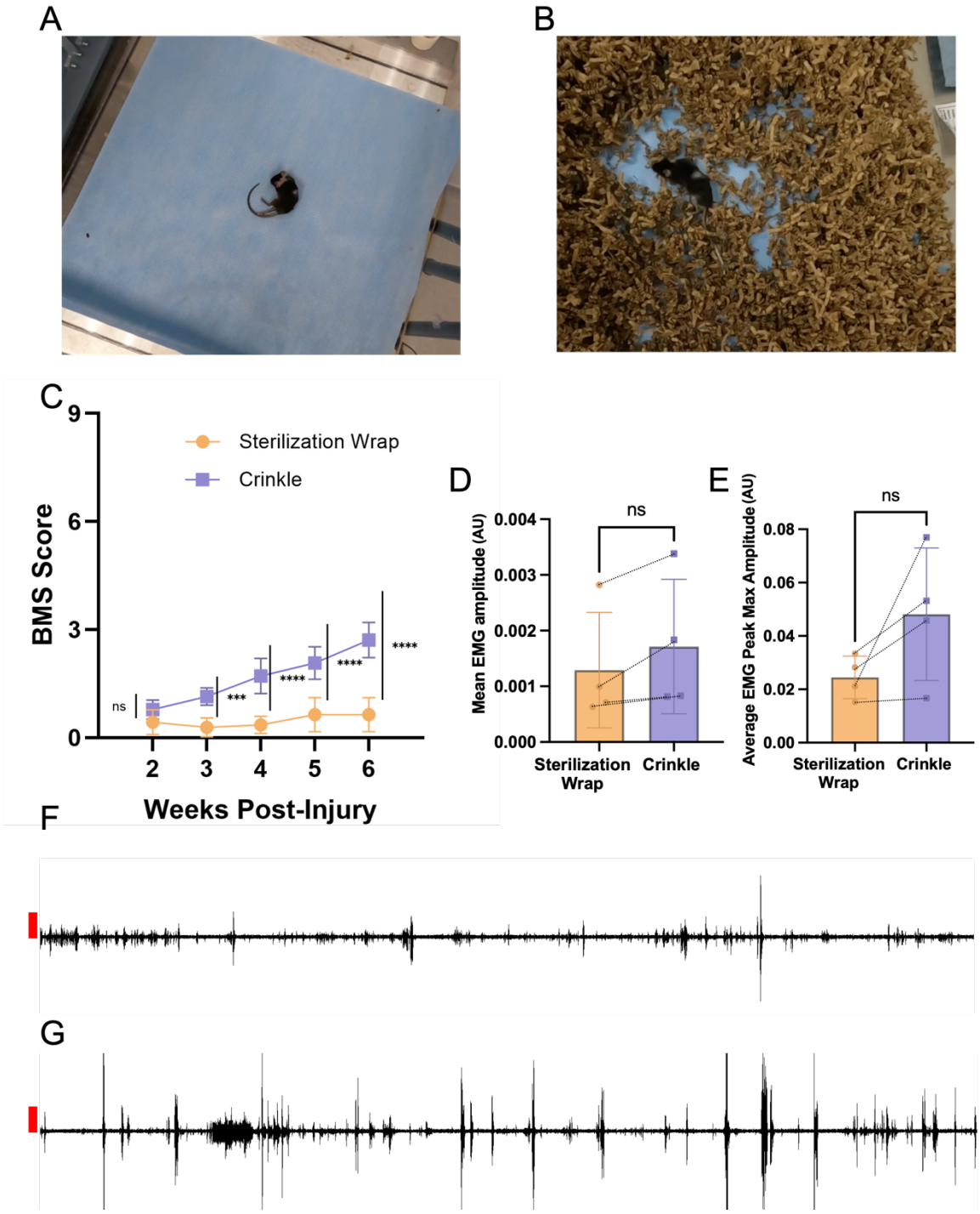

Figure 4.1 Cutaneous sensory stimulation promotes increased hindlimb motor activity after complete SCI. A. Representative photograph of mouse during locomotor assessment on sterilization wrap. **B**. Representative photograph of mouse during locomotor assessment on crinkle paper. **C**. Average BMS scores in the locomotor assessment performed on sterilization wrap (in orange) and on crinkle paper (in purple) as a function of time since complete spinal cord transection (weeks post-injury). Each data point represents the weekly mean for all animals ($N = 7$). ***P = 0.0006, ****P < 0.0001 by two-way ANOVA and Šídák's multiple comparisons test. **D**. Average EMG amplitude (AU = arbitrary units) in 120-second recordings of gastrocnemius activity on crinkle paper compared to sterilization wrap at 6 wpi (ratio paired t-test with dotted line connecting data points from the same animal, P = 0.0677, $n = 4$). **E**. Average peak maximum amplitude (AU = arbitrary units) in 120-second EMG recordings of gastrocnemius activity on crinkle paper compared to sterilization wrap at 6 wpi (ratio paired t-test with dotted line connecting data points from the same animal, P = 0.1029, $n = 4$). **F**. Representative photograph of electromyographic activity of gastrocnemius muscle during locomotor assessment on sterilization wrap (scale bar

in red = 0.1 AU). **G**. Representative photograph of electromyographic activity of gastrocnemius muscle during locomotor assessment on crinkle paper (scale bar in red = 0.1 AU).

4.3.2 Cutaneous stimulation contributes to sensory-mediated motor recovery after complete SCI

To determine the contribution of different types of sensory feedback to the reactivation of CPGs after SCI, we aimed to isolate cutaneous input from proprioceptive input (Fig. 4.2A). At 6 wpi, lidocaine was injected intradermally to selectively block cutaneous tactile afferents originating from the skin of the footpad, while preserving intact proprioceptive afferent signaling from muscles. When injected into the dermis, lidocaine blocks sodium ion channels, thereby preventing conduction of neuronal impulses in cutaneous low-threshold mechanoreceptors found in the skin. Importantly, hindlimb muscle afferents located in muscle spindles and Golgi tendon organs are not affected by the intradermal lidocaine injection. As previously described, crinkle paper was used to provide enhanced sensory stimulus to the hindlimbs and trunk as mice performed the locomotor assay. Lidocaine injections (Fig. 4.2A) led to a significant reduction in hindlimb motor ability, resulting in an average BMS score of 0.71 ± 0.39 in the 'lidocaine and crinkle paper' assessment ($p < 0.0001$, $n = 7$). Despite the presence of crinkle paper, mice were unable to achieve plantar paw placement or dorsal stepping after lidocaine was administered. Similarly, after xylocaine was applied topically to the hindlimb, we found a significant reduction in BMS scores in the 'xylocaine and crinkle paper' assessment ($p < 0.0001$, $n = 7$) (Fig. 4.2A). On average, mice obtained a score of 1.14 ± 0.38 while xylocaine was blocking tactile afferents from the skin. There was no significant difference in BMS scores between the 'xylocaine and crinkle paper' and the 'lidocaine and crinkle paper' assessments ($p = 0.3962$, $n = 7$).

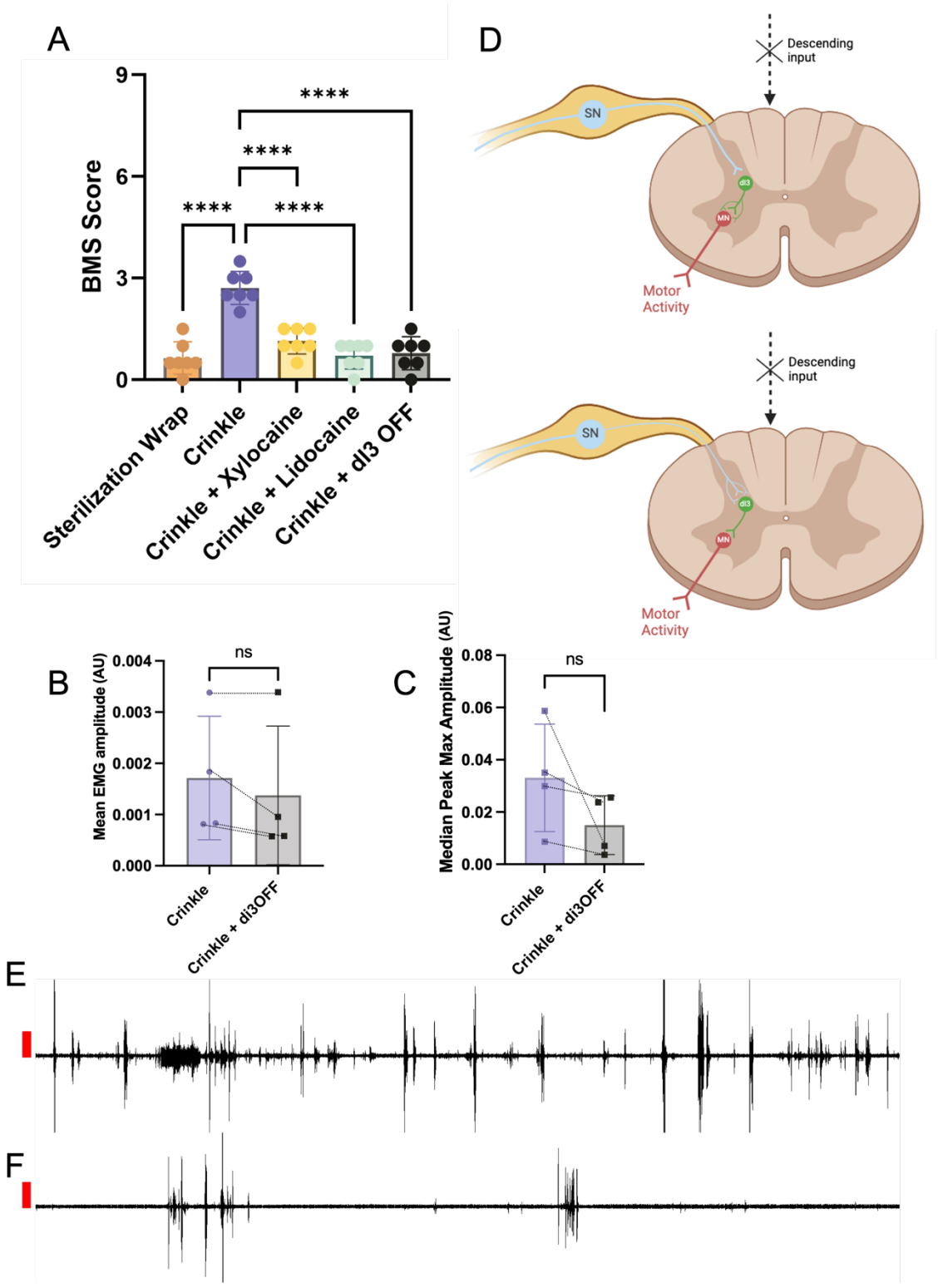

Figure 4.2. dI3 neurons mediate activation of spinal locomotor circuits by cutaneous afferents after SCI. A. Average BMS score 6 weeks post-SCI when performing the locomotor assessment on sterilization wrap (in orange), on crinkle paper (in purple), with xylocaine (in yellow), with lidocaine (in green) and with JHU37160 to silence dI3 (in grey). Plotted data are the mean ± SD. (One-way ANOVA with Tukey's multiple comparisons test; ****P < 0.0001, *n* = 7). **B**. Average EMG amplitude (AU = arbitrary units) in 120-second recordings of gastrocnemius activity on crinkle paper before and after JHU37160 administration (dI3-OFF) at 6 wpi (ratio paired t-test with dotted line connecting data points from the same animal P = 0.0853, *n* = 4). **C**. Median peak maximum amplitude (AU = arbitrary units) in in 120-second EMG recordings of gastrocnemius activity on crinkle paper before and after JHU37160

administration (dI3-OFF) at 6 wpi (ratio paired t-test with dotted line connecting data points from the same animal P = 0.1366, n = 4). **D**. Diagram of proposed mechanisms. **E**. Representative photograph of electromyographic activity of gastrocnemius muscle during locomotor assessment on crinkle paper (scale bar in red = 0.1 AU). **F**. Representative photograph of electromyographic activity of gastrocnemius muscle during locomotor assessment on crinkle paper after JHU37160 administration (dI3-OFF) (scale bar in red = 0.1 AU).

4.3.3 dI3 neurons mediate activation of spinal locomotor circuits by cutaneous afferents after SCI

Next, we examined the role of dI3 neurons in the improved BMS scores when spinalized mice were assessed on crinkle paper. Expression of the inhibitory DREADD receptor hM4Di in spinal dI3 neurons enabled chemogenetic manipulation of dI3 neuron activity during locomotor assessments. Silencing of dI3 neuron neurotransmission was achieved by administering the designer drug, JHU37160. Mice with JHU37160 were placed on crinkle paper and hindlimb motor ability was scored using the BMS. The average BMS score for this group was 0.79 ± 0.49 (Fig. 4.2A, n = 7). Despite the enhanced sensory stimulus from the crinkle paper, mice with JHU37160 displayed significantly reduced hindlimb motor activity compared to that seen in the crinkle paper assessment without any drug administration (p < 0.0001, n = 7) (Fig. 4.2A). There was no significant difference in BMS scores between the mice with JHU37160 on crinkle paper and the 'lidocaine and crinkle paper' assessments (p = 0.9982, n = 7).

To examine the role of dI3 neurons in hindlimb muscle activation after SCI, we performed EMG recordings of gastrocnemius activity at 6 wpi after administering JHU37160. In 3 out of 4 animals with reduced di3 neuron activity, we found a decrease in the mean EMG amplitude over the 120-second recording, although statistical significance was not achieved (p = 0.0853, n = 4) (Fig. 4.2B). Activity bursts were extracted from the 120 second recordings and the maximum peak amplitude of each burst was calculated. The average of maximum peak amplitudes was calculated for each animal. In EMG recordings of gastrocnemius activity in mice on crinkle paper, peaks had lower maximum amplitudes when dI3

neurotransmission was silenced, although statistical significance was not achieved ($p = 0.1366$, $n = 4$) (Fig. 4.2C).

4.4 Discussion

Promising results from rehabilitative training and electrical stimulation therapies have demonstrated that sensory inputs can re-engage neural networks in the injured spinal cord and produce improvements in swimming, walking, bladder control and thermoregulatory functions (Gill et al., 2018; Harkema et al., 2011; Rowald et al., 2022). However, is it largely unknown how excitability is re-established in these spinal circuits and which neuronal subtypes facilitate motor activity after SCI (Eisdorfer et al., 2020; Furlan et al., 2022). It is believed that epidural stimulation activates sensory afferents, which then recruit neurons and motoneurons to generate motor output (Eisdorfer et al., 2020; Formento et al., 2018; Lavrov et al., 2008). In this study, we investigated the contribution of cutaneous afferents to hindlimb motor recovery in a mouse model of complete SCI. We find that providing additional cutaneous sensory input via contact with crinkle paper significantly increases hindlimb motor activity in mice with complete SCI, suggesting that enhancing cutaneous inputs may be a promising therapeutic approach to promote motor recovery after SCI.

Six weeks after complete SCI, hindlimb motor activity was positively affected by enhancing sensory stimulus. Mice that had only slight ankle movement in one hindlimb when placed on a flat surface were capable of extensive ankle movement, plantar paw placement and dorsal stepping when placed on crinkle paper. The increase in observable movements was supported by increased EMG activity in ankle flexor and extensor muscles. We did not find evidence for sex differences in this experiment, which included both male and female mice. However, given the small sample size, future cohorts are needed to evaluate the impact of sex as a biological variable and determine if there is an effect on the increase in hindlimb motor activity with enhanced cutaneous inputs.

The precise mechanism by which sensory feedback contributes to motor recovery after a complete injury has yet to be fully elucidated. Sensory inputs have been proposed to facilitate neuroplasticity in spinal motor networks (Côté & Gossard, 2004; Frigon et al., 2021; Merlet et al., 2021; Smith, Shum-Siu, et al., 2006a; Takeoka, 2020; Takeoka et al., 2014; Takeoka & Arber, 2019; Yen et al., 2014). As fMRI studies in both rats and humans have demonstrated, spinal processing of sensory input is altered after SCI (Cadotte et al., 2012; Endo et al., 2008). These studies report a significant increase in responsiveness in spinal circuits to activation of sensory inputs caudal to the injury (Cadotte et al., 2012; Endo et al., 2008). Strengthened synaptic connections between afferent fibers and spinal neurons of motor circuits in nearby spinal cord segments might compensate for the loss of supraspinal drive after SCI (Eisdorfer et al., 2020). In the present study, the benefits of providing a textured surface was absent in the first 3 weeks post injury. The changing influence of sensory stimulus on hindlimb motor activity suggests a dependency on intraspinal plasticity during the recovery period. We propose that plasticity occurring below the level of complete injury caused spinal locomotor circuits to become responsive to sensory stimulus in a feed-forward manner. Plasticity among propriospinal neurons is one possible explanation for the heightened effect of sensory input on excitability of locomotor circuits after SCI (Fig. 4.2D). For instance, increased connectivity between dI3s and spinal motoneurons could amplify cutaneous inputs to the CPGs. At the same time, sprouting of cutaneous and/or proprioceptive afferents may also be a contributing factor. The synaptic competition model proposes that the removal of supraspinal input may stimulate sprouting in sensory afferents, which would usurp the space left by transected corticospinal fibers (Jiang et al., 2016; Merlet et al., 2021). Reports of SCI-induced sprouting in cutaneous afferents reveal that sprouting can extend into territories which are not innervated in normal animals. For example, in a rat model of SCI, cutaneous Aδ fibers expand their projection area and increase synaptic termination in the dorsal horn (H. J. Lee et al., 2019). Previous work from our lab found changes in VGLUT1+ sensory inputs to dI3 neurons

after SCI as well as changes in presynaptic inhibition which modulates the gain of those sensory inputs (Goltash et al., 2023).

In this study, we aimed to isolate the contribution of cutaneous afferents from that of proprioceptive afferents by selectively blocking cutaneous input to the spinal cord. Intradermal lidocaine injections blocked cutaneous signals from the skin of the footpad, whereas the topical xylocaine reduced cutaneous input from the skin of the entire hindlimb. Importantly, proprioceptive signals from muscle afferents were intact in both conditions. Mice with reduced cutaneous input performed a locomotor assessment in crinkle paper. We found that when cutaneous input was blocked, the tactile sensory stimulus from crinkle paper failed to elicit extensive ankle movement or plantar paw placement that was previously observed in the crinkle paper assessment. This loss in hindlimb motor activity suggests that input from cutaneous mechanoreceptors was instrumental to the re-activation of spinal motoneurons as seen in the crinkle paper assessment. Other research groups have previously established a role for proprioceptive afferents in motor recovery after SCI (Takeoka & Arber, 2019). Through activity-dependent reorganization, group Ia proprioceptive afferents form new synaptic contacts with hindlimb motoneuron pools (Takeoka & Arber, 2019).

Next, we asked how hindlimb cutaneous afferents were recruiting lumbar spinal motoneurons. We hypothesized that dI3 neurons may participate, due to their involvement in spinal sensory processing and their critical role in motor recovery after SCI (Brownstone & Bui, 2010; T. V. Bui et al., 2013; T. V Bui et al., 2016; Goltash et al., 2023). This population of propriospinal neurons resides in the intermediate spinal cord and the dorsal horn, where they integrate proprioceptive and cutaneous sensory input that is relayed to motoneurons and putatively spinal locomotor circuits (T. V. Bui et al., 2013; Laliberte et al., 2022). To determine if dI3 neurons are involved in sensory-mediated activation of CPGs, we used a mouse model that expresses an inhibitory DREADD receptor in spinal dI3 neurons. The designer drug was

administered, putatively resulting in temporary silencing of dI3s. Mice with reduced dI3 activity had significantly lower BMS scores, despite the enhanced sensory stimulus from the crinkle paper. This result supports a role for dI3 neurons in the transmission of excitatory drive from cutaneous afferents to spinal locomotor circuits after SCI.

Here, we show that increasing cutaneous sensory input to spinal circuits through a simple application of a textured surface can contribute to re-engaging spinal motor circuits in a rat model of complete SCI. Our findings could inform the design of SCI therapies that rely on locomotor circuits in the lumbar spinal cord to restore motor function. For instance, rehabilitative training is widely used to facilitate motor recovery after SCI, though the underlying mechanisms have only been partially demonstrated (Khalki et al., 2018; Kiss Bimbova et al., 2022; Q. Liu et al., 2017; P. Yu et al., 2019). In light of our results, we speculate that treadmill training and other forms of physical rehabilitation may produce greater functional recovery if performed in conjunction with enhanced cutaneous stimulation. In addition, SCI treatment strategies targeting propriospinal neurons (Gao et al., 2021; Laliberte et al., 2019a) could also benefit from a better understanding of the key players in spinal locomotor circuit regulation after SCI. Our results may also contribute to a more complete mechanistic understanding of electrical epidural stimulation. It has been demonstrated that, in human patients, EES stimulation protocols must preserve proprioceptive information to restore locomotion (Formento et al., 2018). Elucidating the contribution of cutaneous input could guide the development of EES stimulation parameters and may facilitate the application of electrical stimulation in combinatorial strategies.

4.5 Methods

Animals: All procedures described were approved and performed in accordance with standards set out by the University of Ottawa Animal Care and Veterinary Services ethical review committee (BL-3945). Experiments were performed in 2 groups of mice expressing an inhibitory DREADD (Designer Receptors Exclusively Activated by Designer Drugs) receptor, hM4Di, which was introduced using a Cre-mediated strategy. 'Transgenic hM4Di mice' (n = 4; 2 male, 2 female) conditionally express the hM4Di receptor in cells that are Isl1+ and VGLUT2+, which corresponds to spinal dI3 neurons and some sensory neurons involved in mechanical nociception (Lagerström et al., 2010). In another group of mice (n = 3; 2 male, 1 female), dI3 expression of the hM4Di receptor was achieved by intraspinal infection via a viral vector that targets Isl1+ and VGLUT2+ cells. In these mice, the AAV viral vector (expressing the hM4Di receptor) was injected intraspinally into lumbar segments controlling hindlimb movements, in order to limit hM4Di expression to spinal dI3 neurons only. The 6 injections were performed between L1 and L6 spinal cord segments bilaterally. Upon subcutaneous administration of the designer drug, JHU37160, the hM4Di receptor is activated, leading to hyperpolarization of the cell membrane.

Spinal Cord Transection Surgical Procedure: Mice were anesthetized using 2% isoflurane and complete transections were performed at T9-T10. Sterile surgical foam (Surgifoam, Johnson & Johnson Medtech) was implanted into the cavity in the spinal column to prevent any axon regeneration across the lesion. Post-operatively, buprenorphine was administered subcutaneously (0.1mg/kg injection, Ceva Animal Health) for three days. Animals were monitored thrice daily, and bladders were expressed manually thrice daily. Humane endpoints were defined as self-mutilation or loss of body weight >20%. All mice were allowed to recover for at least one week before behavioral testing. For animals receiving implanted chronic EMG electrodes (n = 4), a second surgery was performed one-week after spinal cord

transection as described previously (Goltash et al., 2025). Mice were anesthetized with isoflurane and implanted with EMG electrodes in the left lateral gastrocnemius and tibialis anterior. Incisions were made into the skin at the neck area and at the hindlimbs. The electrodes were led under the skin from the neck to the leg incisions and implanted into the left and right ankle flexor tibialis anterior and ankle extensor gastrocnemius muscles using an attached 27 G needle. Following insertion into the muscle, the electrodes were anchored in place by knotting the paired wires at the distal end of the muscle and removing the attached needle. The incisions on the hindlimbs were closed with 7-0 polypropylene sutures (Ethicon) and the attachment was stitched to the skin near the neck incision by 5-0 silk sutures (Ethicon) and mice were given analgesic and allowed to recover for 3 days.

BMS Locomotor Assessment: Starting 2 weeks after transection of the spinal cord, the BMS open field motor assessment was performed weekly. Each mouse was placed in an empty plexiglass arena and allowed to move around freely for 4 minutes. A single layer of flat sterilization wrap was placed over the surface to prevent slipping. For statistical analysis, the mean of the left and right hindlimb scores was used to yield a single BMS score per mouse. A second open field locomotor assessment was performed weekly to determine the effect of additional sensory stimulus on motor ability after SCI. Crinkle paper (Enviro-dri) was placed inside the plexiglass arena (approx. 2 inches in depth) to cover the surface of the testing area and provide enhanced sensory stimulus to the hindlimbs and trunk. Enviro-dri consists of 1/8-inch strips of crinkled, 3 layer-thick, natural paper strands. Animals were allowed to freely move around the loose crinkle paper strands for 4 minutes. Animals hindlimb movement was scored using the BMS. For statistical analysis, the average of the left and right hindlimb scores was used as single BMS score per mouse.

Xylocaine and Crinkle Paper Locomotor Assessment: On the 6th post-operative week, topical xylocaine (2%, transdermal, total volume per animal 0.5 ml) was applied to both hindlimbs to reduce sensory input to the spinal cord. A 5-minute waiting period was allowed to ensure absorption of the xylocaine. The animal was then placed into the arena with crinkle paper covering the surface as described above and allowed to freely move around for 4 minutes. Movement was scored using the BMS. For statistical analysis, the average of the left and right hindlimb scores was used as single BMS score per mouse.

Lidocaine and Crinkle Paper Locomotor Assessment: On a separate day during the 6th post-operative week, lidocaine injections were made into the plantar side of each hind paw (foot pad). Injections were performed according to the protocol of *Sławińska et al*. (2013) to block cutaneous feedback from the plantar surface of the hind paws. Bilateral injections of 5mg/ml lidocaine (DIN 02422026, Hikma, total injection = 0.03ml, split between two footpads) were performed. The animal was then placed into the arena with crinkle paper covering the surface as described above and allowed to freely move around for 4 minutes. Movement was scored using the BMS. For statistical analysis, the average of the left and right hindlimb scores was used as single BMS score per mouse.

Locomotor Assessment with chemogenetic silencing: The designer drug, JHU37160, was injected subcutaneously (0.5 mg/kg). A 10-minute waiting period was allowed after injection before starting the assessment. The animal was then placed into the arena with crinkle paper covering the surface, as described above, and allowed to freely move around for 4 minutes. Hindlimb movement was scored using the BMS. For statistical analysis, the average of the left and right hindlimb scores was used as single BMS score per mouse.

Electromyograph recordings: EMG recordings were performed using chronically implanted electrodes in the gastrocnemius muscle. Mice (n = 4) were lightly anesthetized using 2% isoflurane to attach to a differential AC Amplifier (Model 1700, AM Systems) to the attachment on the mouse. Frequencies below 300Hz and above 500Hz were filtered out. Recordings of 120 continuous seconds were taken in both of the following conditions: mice on flat sterilization wrap and mice on 1/8-inch strips of crinkled paper strands. In each recording, activity bursts were extracted (a burst is defined as contiguous signal at least 3 standard deviations from baseline level of EMG signal) and the maximum peak amplitude of each burst was calculated. The average maximum peak amplitude of all of the bursts within a recording was calculated for each animal. Immediately after these recordings, the designer drug JHU37160 was injected subcutaneously (0.5 mg/kg). A 10-minute waiting period was allowed after injection before starting the next EMG recording. Recordings of 120 continuous seconds were taken in the following conditions: mice on flat sterilization wrap with JHU37160 injection and mice on 1/8-inch strips of crinkled paper strands with JHU37160 injection. One outlier EMG recording had to be non-continuous to avoid EMG artifacts.

Statistical: Experimental data were analyzed using GraphPad Prism. Power analysis showed that a sample size of 8 mice would be needed to reach a power of 80%. For motor assessments at the same timepoint, the average BMS scores with and without crinkle paper were compared using the Mann Whitney test was performed. For comparisons across time (Fig. 4.1C), the average BMS scores of different conditions were compared by two-way ANOVA and Šídák's multiple comparisons test. Conditions in figure 4.2 were compared by one-way ANOVA with Tukey's multiple comparisons test. In EMG recordings, the medians and averages of peak maximum amplitudes from different conditions were compared by ratio paired t-tests.

Chapter 5: Conclusion

The Pelling lab and others in the field have previously demonstrated the potential of plant tissue to be processed into biocompatible scaffolds with tissue engineering applications (Bilirgen et al., 2021; Indurkar et al., 2021; Modulevsky et al., 2014). This thesis explores various biomedical applications of plant-derived cellulose scaffolds, with a particular emphasis on regeneration of the CNS. We first characterized scaffolds' physical properties and demonstrated their utility as a platform for 3D culture of neural stem cells. Our findings illustrate that not only can cellulose biomaterials support proliferation of NSCs, but they also have the ability to direct NSC differentiation. Next, we show that cellulose scaffolds have potential as a therapeutic biomaterial for spinal cord injury. *In vivo*, endogenous neural cells infiltrated the biomaterial and migrated along its microchannels. The scaffold supported hindlimb motor recovery in a rat model of SCI and the addition of a peptide coating led to enhanced axon regeneration with possible remyelination. Finally, we investigate endogenous SCI repair mechanisms that involve changes in sensory processing below the injury. In a mouse model of SCI, we find that cutaneous sensory stimulation caudal to the injury enhances motor ability in the hindlimbs. Further, we identify dI3 neurons as an important player in the facilitation of spinal locomotor circuitry via cutaneous input.

The findings in this thesis have potential applications in the fields of disease modelling, stem cell replacement therapy, drug discovery, tissue engineering, biomaterial-based therapeutics, spinal motor control, and electrical neuromodulatory interventions. The cellulose scaffolds from chapter 2 have potential as 3D *in vitro* models of neurodegenerative diseases such as Alzheimer's or amyotrophic lateral sclerosis. Such cell culture systems could be used to study the molecular defects specific to CNS diseases or to test therapeutic drugs in a more realistic environment. In relation to stem cell replacement therapy, plant-derived biomaterials may be useful in scaffold-based delivery of stem cells for various diseases. As demonstrated in the present thesis, cellulose scaffolds guide neural stem cell differentiation into the

neuronal lineage, which is a key issue in the field of NSC therapies. In future work, these cellulose scaffolds could be optimized for use as a substrate for the 3D culture of human NSCs.

The *in vivo* experiments in chapter 3 are a proof-of-concept study that highlights a potential therapeutic application for plant biomaterials. Our results also suggest enhanced re-myelination in animals with PLO-coated scaffolds, which could be investigated more thoroughly in future experiments. Next steps could include optimizing the concentration and delivery of PLO to further enhance its positive effect. However, one important limitation with this study is the reliance on the rodent SCI model. Despite the similarities between rodent and human SCI pathology, certain differences may represent an obstacle for translatability of these studies. Species differences in metabolic speed, comorbidities and injury characteristics including size can make it difficult to extrapolate between species. Another limitation of the study is the use of the complete transection injury model, which is not representative of the most common injury type in humans. Nonetheless, this study is a starting point for the development of more refined plant scaffolds for SCI which could eventually be translated into human clinical research. Currently, Spiderwort Biotechnologies is working towards regenerative medicine applications using plant cellulose-based biomaterials.

The results of chapter 4 contribute to the understanding of spinal locomotor circuit regulation after SCI. Highlighting the importance of an understudied spinal neuron population will broaden the understanding of intrinsic spinal mechanisms of motor recovery after SCI. Our findings could inform the design of SCI therapies that rely on preserved spinal circuits to restore motor function such as rehabilitative training, electrical epidural stimulation or treatment strategies targeting propriospinal neurons (Gao et al., 2021; Laliberte et al., 2019a). For example, there may be implications for EES stimulation parameters. Moreover, understanding intrinsic spinal repair mechanisms after SCI may also inform the development and evaluation of biomaterial therapeutics. It is not uncommon for groups testing

SCI biomaterials to report motor recovery without considerable cross-lesion regeneration of axons (Fouad et al., 2005; B.-L. He et al., 2013). We theorize that some functional recovery may be due to biomaterials' impact on spinal plasticity caudal to the injury as opposed to their effect on cross-lesion regeneration. Our findings in chapter 4 may bring clarity to the mechanism of action of such SCI biomaterials. Considering the effect of a biomaterial on sensory processing below the injury could help to resolve whether movement in the hindlimbs is the result of increased supraspinal input or increased sensory feedback.

After CNS injury, axon regeneration and the formation of functional relay circuits remain two of the major obstacles to achieving significant recovery of lost function due to injury. It is widely believed that a combinatorial therapeutic approach is the ideal strategy to address various aspects of SCI pathophysiology. In order for this area of research to progress, it will be crucial to consider the interplay between neurorehabilitation, pharmacologic interventions, trophic support, cell transplants, biomaterial-based treatments, and endogenous SCI repair mechanisms. Overall, my thesis reveals potential biomedical applications of plant-derived scaffolds and demonstrates their ability to be functionalized in the context of combinatorial SCI treatments. Future studies should explore different forms of plant biomaterials that could be used in a contusion injury model or in a chronic SCI model.

Despite hundreds of preclinical studies transitioning into the clinical trials stage, reproducing results in human patients has proven to be extremely difficult. This is partially due to the use of overly simplified animal models that do not accurately represent the clinical setting. For instance, up to 47% of SCI patients have concomitant traumatic brain injury, though preclinical studies using this co-presentation are scarce (Valbuena Valecillos et al., 2022). To address the translational gap, preclinical SCI models could be expanded to account for factors such as concomitant injuries, diet, age, sex, and lifestyle (Gliksten & Yip, 2023).

Further, we propose that the SCI research community should refine the standard housing conditions for rodent models, to be more representative of the conditions of human SCI patients and to improve animal wellbeing. Research rodents used as SCI models are routinely singly housed in small cages that restrict their natural behaviours. Mounting evidence demonstrates that standard rodent housing increases stress and compromises the animals' health, leading to higher morbidity and mortality (Cait et al., 2022; Manouze et al., 2019; Ratuski et al., 2024). The enhanced animal care protocol implemented throughout this thesis includes advanced handling techniques, social enrichment, and environmental enrichment such as chew toys, balls, food enrichment, improved nesting material, and climbing structures. To better meet their social needs, our rats were co-housed and were given a daily group play session, which is currently being adopted by many animal care facilities around the world. Overall, we believe that improving the standard housing conditions for rodent SCI models will benefit the animals and enhance the predictive value of preclinical studies.

Recent advances in the field of SCI research have offered new hope to patients living with severe SCI. Several promising treatments are currently in clinical trials, including implantable biomaterials, stem cell therapies, neuroprotective drugs and electrical stimulation devices (Lorach et al., 2023; Moritz et al., 2024). Given the significant long-term burden of SCI for patients and healthcare systems, this research is fundamentally important to the wellbeing of Canadians.

References

Abraira, V. E., & Ginty, D. D. (2013). The Sensory Neurons of Touch. *Neuron*, *79*(4), 618–639. https://doi.org/10.1016/j.neuron.2013.07.051

Ahmed, R. U., Alam, M., & Zheng, Y.-P. (2019). Experimental spinal cord injury and behavioral tests in laboratory rats. *Heliyon*, *5*(3), e01324. https://doi.org/10.1016/j.heliyon.2019.e01324

Ahuja, C. S., Wilson, J. R., Nori, S., Kotter, M. R. N., Druschel, C., Curt, A., & Fehlings, M. G. (2017). Traumatic spinal cord injury. *Nature Reviews Disease Primers*, *3*(1), 17018. https://doi.org/10.1038/nrdp.2017.18

Akay, T., Tourtellotte, W. G., Arber, S., & Jessell, T. M. (2014). Degradation of mouse locomotor pattern in the absence of proprioceptive sensory feedback. *Proceedings of the National Academy of Sciences*, *111*(47), 16877–16882. https://doi.org/10.1073/pnas.1419045111

Allison, D. J., & Ditor, D. S. (2015). Immune dysfunction and chronic inflammation following spinal cord injury. *Spinal Cord*, *53*(1), 14–18. https://doi.org/10.1038/sc.2014.184

Álvarez, Z., Kolberg-Edelbrock, A. N., Sasselli, I. R., Ortega, J. A., Qiu, R., Syrgiannis, Z., Mirau, P. A., Chen, F., Chin, S. M., Weigand, S., Kiskinis, E., & Stupp, S. I. (2021). Bioactive scaffolds with enhanced supramolecular motion promote recovery from spinal cord injury. *Science*, *374*(6569), 848–856. https://doi.org/10.1126/science.abh3602

Amrein, I. (2015). Adult Hippocampal Neurogenesis in Natural Populations of Mammals. *Cold Spring Harbor Perspectives in Biology*, *7*(5), a021295. https://doi.org/10.1101/cshperspect.a021295

Anderson, K. D., Gunawan, A., & Steward, O. (2005). Quantitative assessment of forelimb motor function after cervical spinal cord injury in rats: Relationship to the corticospinal tract. *Experimental Neurology*, *194*(1), 161–174. https://doi.org/10.1016/j.expneurol.2005.02.006

Anderson, M. A., Burda, J. E., Ren, Y., Ao, Y., O'Shea, T. M., Kawaguchi, R., Coppola, G., Khakh, B. S., Deming, T. J., & Sofroniew, M. V. (2016a). Astrocyte scar formation aids central nervous system axon regeneration. *Nature*, *532*(7598), 195–200. https://doi.org/10.1038/nature17623

Anderson, M. A., Burda, J. E., Ren, Y., Ao, Y., O'Shea, T. M., Kawaguchi, R., Coppola, G., Khakh, B. S., Deming, T. J., & Sofroniew, M. V. (2016b). Astrocyte scar formation aids central nervous system axon regeneration. *Nature*, *532*(7598), 195–200. https://doi.org/10.1038/nature17623

Anjum, A., Yazid, M. D., Fauzi Daud, M., Idris, J., Ng, A. M. H., Selvi Naicker, A., Ismail, O. H. R., Athi Kumar, R. K., & Lokanathan, Y. (2020). Spinal Cord Injury: Pathophysiology, Multimolecular Interactions, and Underlying Recovery Mechanisms. *International Journal of Molecular Sciences*, *21*(20), 7533. https://doi.org/10.3390/ijms21207533

Asboth, L., Friedli, L., Beauparlant, J., Martinez-Gonzalez, C., Anil, S., Rey, E., Baud, L., Pidpruzhnykova, G., Anderson, M. A., Shkorbatova, P., Batti, L., Pagès, S., Kreider, J., Schneider, B. L., Barraud, Q., & Courtine, G. (2018a). Cortico–reticulo–spinal circuit reorganization enables functional recovery after severe spinal cord contusion. *Nature Neuroscience*, *21*(4), 576–588. https://doi.org/10.1038/s41593-018-0093-5

Asboth, L., Friedli, L., Beauparlant, J., Martinez-Gonzalez, C., Anil, S., Rey, E., Baud, L., Pidpruzhnykova, G., Anderson, M. A., Shkorbatova, P., Batti, L., Pagès, S., Kreider, J., Schneider, B. L., Barraud, Q., & Courtine, G. (2018b). Cortico–reticulo–spinal circuit reorganization enables functional recovery after severe spinal cord contusion. *Nature Neuroscience*, *21*(4), 576–588. https://doi.org/10.1038/s41593-018-0093-5

Ashammakhi, N., Kim, H.-J., Ehsanipour, A., Bierman, R. D., Kaarela, O., Xue, C., Khademhosseini, A., & Seidlits, S. K. (2019). Regenerative Therapies for Spinal Cord Injury. *Tissue Engineering Part B: Reviews*, *25*(6), 471–491. https://doi.org/10.1089/ten.teb.2019.0182

Baek, J., Cho, S.-Y., Kang, H., Ahn, H., Jung, W.-B., Cho, Y., Lee, E., Cho, S.-W., Jung, H.-T., & Im, S. G. (2018). Distinct Mechanosensing of Human Neural Stem Cells on Extremely Limited Anisotropic Cellular Contact. *ACS Applied Materials & Interfaces*, *10*(40), 33891–33900. https://doi.org/10.1021/acsami.8b10171

Balasundari, R., Bishi, D. K., Mathapati, S., Naser, S. B., Cherian, K. M., & Guhathakurta, S. (2012). Nanocoated Botanical Scaffold in Salvage for Human Tissue Regeneration. *Journal of Biomaterials and Tissue Engineering*, *2*(4), 330–335. https://doi.org/10.1166/jbt.2012.1058

Ballermann, M., & Fouad, K. (2006). Spontaneous locomotor recovery in spinal cord injured rats is accompanied by anatomical plasticity of reticulospinal fibers. *European Journal of Neuroscience*, *23*(8), 1988–1996. https://doi.org/10.1111/j.1460-9568.2006.04726.x

Banerjee, A., Arha, M., Choudhary, S., Ashton, R. S., Bhatia, S. R., Schaffer, D. V., & Kane, R. S. (2009). The influence of hydrogel modulus on the proliferation and differentiation of encapsulated neural stem cells. *Biomaterials*, *30*(27), 4695–4699. https://doi.org/10.1016/j.biomaterials.2009.05.050

Bao, M., Xie, J., & Huck, W. T. S. (2018). Recent Advances in Engineering the Stem Cell Microniche in 3D. *Advanced Science*, *5*(8), 1800448. https://doi.org/10.1002/advs.201800448

Barbeau, H., & Rossignol, S. (1987). Recovery of locomotion after chronic spinalization in the adult cat. *Brain Research*, *412*(1), 84–95. https://doi.org/10.1016/0006-8993(87)91442-9

Bareyre, F. M., Kerschensteiner, M., Raineteau, O., Mettenleiter, T. C., Weinmann, O., & Schwab, M. E. (2004). The injured spinal cord spontaneously forms a new intraspinal circuit in adult rats. *Nature Neuroscience*, *7*(3), 269–277. https://doi.org/10.1038/nn1195

Barnabé-Heider, F., Göritz, C., Sabelström, H., Takebayashi, H., Pfrieger, F. W., Meletis, K., & Frisén, J. (2010a). Origin of New Glial Cells in Intact and Injured Adult Spinal Cord. *Cell Stem Cell*, *7*(4), 470–482. https://doi.org/10.1016/j.stem.2010.07.014

Barnabé-Heider, F., Göritz, C., Sabelström, H., Takebayashi, H., Pfrieger, F. W., Meletis, K., & Frisén, J. (2010b). Origin of New Glial Cells in Intact and Injured Adult Spinal Cord. *Cell Stem Cell*, *7*(4), 470–482. https://doi.org/10.1016/j.stem.2010.07.014

BASSO, D. M., BEATTIE, M. S., & BRESNAHAN, J. C. (1995). A Sensitive and Reliable Locomotor Rating Scale for Open Field Testing in Rats. *Journal of Neurotrauma*, *12*(1), 1–21. https://doi.org/10.1089/neu.1995.12.1

Battistuzzo, C. R., Callister, R. J., Callister, R., & Galea, M. P. (2012). A Systematic Review of Exercise Training To Promote Locomotor Recovery in Animal Models of Spinal Cord Injury. *Journal of Neurotrauma*, *29*(8), 1600–1613. https://doi.org/10.1089/neu.2011.2199

Belfiore, L., Aghaei, B., Law, A. M. K., Dobrowolski, J. C., Raftery, L. J., Tjandra, A. D., Yee, C., Piloni, A., Volkerling, A., Ferris, C. J., & Engel, M. (2021). Generation and analysis of 3D cell culture models for drug discovery. *European Journal of Pharmaceutical Sciences*, *163*, 105876. https://doi.org/10.1016/j.ejps.2021.105876

Bellver-Landete, V., Bretheau, F., Mailhot, B., Vallières, N., Lessard, M., Janelle, M.-E., Vernoux, N., Tremblay, M.-È., Fuehrmann, T., Shoichet, M. S., & Lacroix, S. (2019). Microglia are an essential component of the neuroprotective scar that forms after spinal cord injury. *Nature Communications*, *10*(1), 518. https://doi.org/10.1038/s41467-019-08446-0

Berrocal, Y., Pearse, D. D., Singh, A., Andrade, C. M., McBroom, J. S., Puentes, R., & Eaton, M. J. (2007). Social and Environmental Enrichment Improves Sensory and Motor Recovery after Severe

Contusive Spinal Cord Injury in the Rat. *Journal of Neurotrauma*, *24*(11), 1761–1772. https://doi.org/10.1089/neu.2007.0327
Bilirgen, A. C., Toker, M., Odabas, S., Yetisen, A. K., Garipcan, B., & Tasoglu, S. (2021). Plant-Based Scaffolds in Tissue Engineering. *ACS Biomaterials Science & Engineering*, *7*(3), 926–938. https://doi.org/10.1021/acsbiomaterials.0c01527
Blesch, A., & Tuszynski, M. H. (2003). Cellular GDNF delivery promotes growth of motor and dorsal column sensory axons after partial and complete spinal cord transections and induces remyelination. *Journal of Comparative Neurology*, *467*(3), 403–417. https://doi.org/10.1002/cne.10934
Böhm, U. L., & Wyart, C. (2016). Spinal sensory circuits in motion. *Current Opinion in Neurobiology*, *41*, 38–43. https://doi.org/10.1016/j.conb.2016.07.007
Bolton, D. A. E., & Misiaszek, J. E. (2009). Contribution of Hindpaw Cutaneous Inputs to the Control of Lateral Stability During Walking in the Cat. *Journal of Neurophysiology*, *102*(3), 1711–1724. https://doi.org/10.1152/jn.00445.2009
Bouyer, L. J. G., & Rossignol, S. (2003a). Contribution of Cutaneous Inputs From the Hindpaw to the Control of Locomotion. I. Intact Cats. *Journal of Neurophysiology*, *90*(6), 3625–3639. https://doi.org/10.1152/jn.00496.2003
Bouyer, L. J. G., & Rossignol, S. (2003b). Contribution of Cutaneous Inputs From the Hindpaw to the Control of Locomotion. II. Spinal Cats. *Journal of Neurophysiology*, *90*(6), 3640–3653. https://doi.org/10.1152/jn.00497.2003
Bozza, A., Coates, E. E., Incitti, T., Ferlin, K. M., Messina, A., Menna, E., Bozzi, Y., Fisher, J. P., & Casarosa, S. (2014). Neural differentiation of pluripotent cells in 3D alginate-based cultures. *Biomaterials*, *35*(16), 4636–4645. https://doi.org/10.1016/j.biomaterials.2014.02.039
Bradbury, E. J., King, V. R., Simmons, L. J., Priestley, J. V., & McMahon, S. B. (1998). NT-3, but not BDNF, prevents atrophy and death of axotomized spinal cord projection neurons. *European Journal of Neuroscience*, *10*(10), 3058–3068. https://doi.org/10.1046/j.1460-9568.1998.00307.x
Bradke, F., Fawcett, J. W., & Spira, M. E. (2012). Assembly of a new growth cone after axotomy: the precursor to axon regeneration. *Nature Reviews Neuroscience*, *13*(3), 183–193. https://doi.org/10.1038/nrn3176
Breen, B. A., Kraskiewicz, H., Ronan, R., Kshiragar, A., Patar, A., Sargeant, T., Pandit, A., & McMahon, S. S. (2017a). Therapeutic Effect of Neurotrophin-3 Treatment in an Injectable Collagen Scaffold Following Rat Spinal Cord Hemisection Injury. *ACS Biomaterials Science & Engineering*, *3*(7), 1287–1295. https://doi.org/10.1021/acsbiomaterials.6b00167
Breen, B. A., Kraskiewicz, H., Ronan, R., Kshiragar, A., Patar, A., Sargeant, T., Pandit, A., & McMahon, S. S. (2017b). Therapeutic Effect of Neurotrophin-3 Treatment in an Injectable Collagen Scaffold Following Rat Spinal Cord Hemisection Injury. *ACS Biomaterials Science & Engineering*, *3*(7), 1287–1295. https://doi.org/10.1021/acsbiomaterials.6b00167
Bregman, B. S., Coumans, J.-V., Dai, H. N., Kuhn, P. L., Lynskey, J., McAtee, M., & Sandhu, F. (2002). *Chapter 18 Transplants and neurotrophic factors increase regeneration and recovery of function after spinal cord injury* (pp. 257–273). https://doi.org/10.1016/S0079-6123(02)37020-1
Breslin, S., & O'Driscoll, L. (2013). Three-dimensional cell culture: the missing link in drug discovery. *Drug Discovery Today*, *18*(5–6), 240–249. https://doi.org/10.1016/j.drudis.2012.10.003
Brown, A. R., & Martinez, M. (2019). From cortex to cord: motor circuit plasticity after spinal cord injury. *Neural Regeneration Research*, *14*(12), 2054–2062. https://doi.org/10.4103/1673-5374.262572

Brownstone, R. M., & Bui, T. V. (2010). *Spinal interneurons providing input to the final common path during locomotion* (pp. 81–95). https://doi.org/10.1016/B978-0-444-53613-6.00006-X

Bui, T. V., Akay, T., Loubani, O., Hnasko, T. S., Jessell, T. M., & Brownstone, R. M. (2013). Circuits for Grasping: Spinal dI3 Interneurons Mediate Cutaneous Control of Motor Behavior. *Neuron*, *78*(1), 191–204. https://doi.org/10.1016/j.neuron.2013.02.007

Bui, T. V, Stifani, N., Akay, T., & Brownstone, R. M. (2016). Spinal microcircuits comprising dI3 interneurons are necessary for motor functional recovery following spinal cord transection. *ELife*, *5*. https://doi.org/10.7554/eLife.21715

Burgdorf, J., & Panksepp, J. (2001). Tickling induces reward in adolescent rats. *Physiology & Behavior*, *72*(1–2), 167–173. https://doi.org/10.1016/S0031-9384(00)00411-X

Burke, D. A., Morehouse, J. R., Saraswat Ohri, S., & Magnuson, D. S. K. (2023). Unintentional Effects from Housing Enhancement Resulting in Functional Improvement in Spinal Cord–Injured Mice. *Neurotrauma Reports*, *4*(1), 71–81. https://doi.org/10.1089/neur.2022.0059

Buss, A., Pech, K., Kakulas, B. A., Martin, D., Schoenen, J., Noth, J., & Brook, G. A. (2009). NG2 and phosphacan are present in the astroglial scar after human traumatic spinal cord injury. *BMC Neurology*, *9*(1), 32. https://doi.org/10.1186/1471-2377-9-32

Cadotte, D. W., Bosma, R., Mikulis, D., Nugaeva, N., Smith, K., Pokrupa, R., Islam, O., Stroman, P. W., & Fehlings, M. G. (2012). Plasticity of the Injured Human Spinal Cord: Insights Revealed by Spinal Cord Functional MRI. *PLoS ONE*, *7*(9), e45560. https://doi.org/10.1371/journal.pone.0045560

Cait, J., Cait, A., Scott, R. W., Winder, C. B., & Mason, G. J. (2022). Conventional laboratory housing increases morbidity and mortality in research rodents: results of a meta-analysis. *BMC Biology*, *20*(1), 15. https://doi.org/10.1186/s12915-021-01184-0

Cao, Q., Benton, R. L., & Whittemore, S. R. (2002). Stem cell repair of central nervous system injury. *Journal of Neuroscience Research*, *68*(5), 501–510. https://doi.org/10.1002/jnr.10240

Capogrosso, M., Wenger, N., Raspopovic, S., Musienko, P., Beauparlant, J., Bassi Luciani, L., Courtine, G., & Micera, S. (2013). A Computational Model for Epidural Electrical Stimulation of Spinal Sensorimotor Circuits. *The Journal of Neuroscience*, *33*(49), 19326–19340. https://doi.org/10.1523/JNEUROSCI.1688-13.2013

Chambel, S. S., & Cruz, C. D. (2023). Axonal growth inhibitors and their receptors in spinal cord injury: from biology to clinical translation. *Neural Regeneration Research*, *18*(12), 2573–2581. https://doi.org/10.4103/1673-5374.373674

Chaplan, S. R., Bach, F. W., Pogrel, J. W., Chung, J. M., & Yaksh, T. L. (1994). Quantitative assessment of tactile allodynia in the rat paw. *Journal of Neuroscience Methods*, *53*(1), 55–63. https://doi.org/10.1016/0165-0270(94)90144-9

Chedly, J., Soares, S., Montembault, A., von Boxberg, Y., Veron-Ravaille, M., Mouffle, C., Benassy, M.-N., Taxi, J., David, L., & Nothias, F. (2017). Physical chitosan microhydrogels as scaffolds for spinal cord injury restoration and axon regeneration. *Biomaterials*, *138*, 91–107. https://doi.org/10.1016/j.biomaterials.2017.05.024

Chen, F., Wu, M., Wu, P., Xiao, A., Ke, M., Huselstein, C., Cai, L., Tong, Z., & Chen, Y. (2021). Natural *Flammulina velutipes* -Based Nerve Guidance Conduit as a Potential Biomaterial for Peripheral Nerve Regeneration: In Vitro and In Vivo Studies. *ACS Biomaterials Science & Engineering*, *7*(8), 3821–3834. https://doi.org/10.1021/acsbiomaterials.1c00304

Chen, K., Yu, W., Zheng, G., Xu, Z., Yang, C., Wang, Y., Yue, Z., Yuan, W., Hu, B., & Chen, H. (2024). Biomaterial-based regenerative therapeutic strategies for spinal cord injury. *NPG Asia Materials*, *16*(1), 5. https://doi.org/10.1038/s41427-023-00526-4

Chen, W., Shao, Y., Li, X., Zhao, G., & Fu, J. (2014). Nanotopographical surfaces for stem cell fate control: Engineering mechanobiology from the bottom. *Nano Today*, *9*(6), 759–784. https://doi.org/10.1016/j.nantod.2014.12.002

Cheng, J., & Guan, N. N. (2023). A fresh look at propriospinal interneurons plasticity and intraspinal circuits remodeling after spinal cord injury. *IBRO Neuroscience Reports*, *14*, 441–446. https://doi.org/10.1016/j.ibneur.2023.04.001

Cheng, Y.-W., Shiwarski, D. J., Ball, R. L., Whitehead, K. A., & Feinberg, A. W. (2020a). Engineering Aligned Skeletal Muscle Tissue Using Decellularized Plant-Derived Scaffolds. *ACS Biomaterials Science & Engineering*, *6*(5), 3046–3054. https://doi.org/10.1021/acsbiomaterials.0c00058

Cheng, Y.-W., Shiwarski, D. J., Ball, R. L., Whitehead, K. A., & Feinberg, A. W. (2020b). Engineering Aligned Skeletal Muscle Tissue Using Decellularized Plant-Derived Scaffolds. *ACS Biomaterials Science & Engineering*, *6*(5), 3046–3054. https://doi.org/10.1021/acsbiomaterials.0c00058

Cheriyan, T., Ryan, D. J., Weinreb, J. H., Cheriyan, J., Paul, J. C., Lafage, V., Kirsch, T., & Errico, T. J. (2014). Spinal cord injury models: a review. *Spinal Cord*, *52*(8), 588–595. https://doi.org/10.1038/sc.2014.91

Chopek, J. W., Nascimento, F., Beato, M., Brownstone, R. M., & Zhang, Y. (2018). Sub-populations of Spinal V3 Interneurons Form Focal Modules of Layered Pre-motor Microcircuits. *Cell Reports*, *25*(1), 146-156.e3. https://doi.org/10.1016/j.celrep.2018.08.095

Clarke, L. E., & Barres, B. A. (2013). Emerging roles of astrocytes in neural circuit development. *Nature Reviews Neuroscience*, *14*(5), 311–321. https://doi.org/10.1038/nrn3484

Clemenson, G. D., Deng, W., & Gage, F. H. (2015). Environmental enrichment and neurogenesis: from mice to humans. *Current Opinion in Behavioral Sciences*, *4*, 56–62. https://doi.org/10.1016/j.cobeha.2015.02.005

Contessi Negrini, N., Toffoletto, N., Farè, S., & Altomare, L. (2020). Plant Tissues as 3D Natural Scaffolds for Adipose, Bone and Tendon Tissue Regeneration. *Frontiers in Bioengineering and Biotechnology*, *8*. https://doi.org/10.3389/fbioe.2020.00723

Côté, M.-P., Detloff, M. R., Wade, R. E., Lemay, M. A., & Houlé, J. D. (2012). Plasticity in ascending long propriospinal and descending supraspinal pathways in chronic cervical spinal cord injured rats. *Frontiers in Physiology*, *3*. https://doi.org/10.3389/fphys.2012.00330

Côté, M.-P., & Gossard, J.-P. (2004). Step Training-Dependent Plasticity in Spinal Cutaneous Pathways. *The Journal of Neuroscience*, *24*(50), 11317–11327. https://doi.org/10.1523/JNEUROSCI.1486-04.2004

Courtine, G., Gerasimenko, Y., van den Brand, R., Yew, A., Musienko, P., Zhong, H., Song, B., Ao, Y., Ichiyama, R. M., Lavrov, I., Roy, R. R., Sofroniew, M. V, & Edgerton, V. R. (2009). Transformation of nonfunctional spinal circuits into functional states after the loss of brain input. *Nature Neuroscience*, *12*(10), 1333–1342. https://doi.org/10.1038/nn.2401

Courtine, G., Song, B., Roy, R. R., Zhong, H., Herrmann, J. E., Ao, Y., Qi, J., Edgerton, V. R., & Sofroniew, M. V. (2008). Recovery of supraspinal control of stepping via indirect propriospinal relay connections after spinal cord injury. *Nature Medicine*, *14*(1), 69–74. https://doi.org/10.1038/nm1682

Couvrette, L. J., Walker, K. L. A., Bui, T. V., & Pelling, A. E. (2023). Plant Cellulose as a Substrate for 3D Neural Stem Cell Culture. *Bioengineering*, *10*(11), 1309. https://doi.org/10.3390/bioengineering10111309

Currie, L. J., Sharpe, J. R., & Martin, R. (2001). The Use of Fibrin Glue in Skin Grafts and Tissue-Engineered Skin Replacements: A Review. *Plastic and Reconstructive Surgery*, *108*(6), 1713–1726. https://doi.org/10.1097/00006534-200111000-00045

Czeisler, C., Short, A., Nelson, T., Gygli, P., Ortiz, C., Catacutan, F. P., Stocker, B., Cronin, J., Lannutti, J., Winter, J., & Otero, J. J. (2016). Surface topography during neural stem cell differentiation regulates cell migration and cell morphology. *Journal of Comparative Neurology*, *524*(17), 3485–3502. https://doi.org/10.1002/cne.24078

Dai, Y., Qiao, K., Li, D., Isingizwe, P., Liu, H., Liu, Y., Lim, K., Woodfield, T., Liu, G., Hu, J., Yuan, J., Tang, J., & Cui, X. (2023). Plant-Derived Biomaterials and Their Potential in Cardiac Tissue Repair. *Advanced Healthcare Materials*, *12*(20). https://doi.org/10.1002/adhm.202202827

Davidenko, N., Schuster, C. F., Bax, D. V., Raynal, N., Farndale, R. W., Best, S. M., & Cameron, R. E. (2015). Control of crosslinking for tailoring collagen-based scaffolds stability and mechanics. *Acta Biomaterialia*, *25*, 131–142. https://doi.org/10.1016/j.actbio.2015.07.034

De Virgiliis, F., Hutson, T. H., Palmisano, I., Amachree, S., Miao, J., Zhou, L., Todorova, R., Thompson, R., Danzi, M. C., Lemmon, V. P., Bixby, J. L., Wittig, I., Shah, A. M., & Di Giovanni, S. (2020). Enriched conditioning expands the regenerative ability of sensory neurons after spinal cord injury via neuronal intrinsic redox signaling. *Nature Communications*, *11*(1), 6425. https://doi.org/10.1038/s41467-020-20179-z

Dias, D. O., Kim, H., Holl, D., Werne Solnestam, B., Lundeberg, J., Carlén, M., Göritz, C., & Frisén, J. (2018). Reducing Pericyte-Derived Scarring Promotes Recovery after Spinal Cord Injury. *Cell*, *173*(1), 153-165.e22. https://doi.org/10.1016/j.cell.2018.02.004

Díaz-Galindo, M. del C., Calderón-Vallejo, D., Olvera-Sandoval, C., & Quintanar, J. L. (2020). Therapeutic approaches of trophic factors in animal models and in patients with spinal cord injury. *Growth Factors*, *38*(1), 1–15. https://doi.org/10.1080/08977194.2020.1753724

Dikici, S., Claeyssens, F., & MacNeil, S. (2019). Decellularised baby spinach leaves and their potential use in tissue engineering applications: Studying and promoting neovascularisation. *Journal of Biomaterials Applications*, *34*(4), 546–559. https://doi.org/10.1177/0885328219863115

Ding, Y., Kastin, A., & Pan, W. (2005). Neural Plasticity After Spinal Cord Injury. *Current Pharmaceutical Design*, *11*(11), 1441–1450. https://doi.org/10.2174/1381612053507855

Doblado, L. R., Martínez-Ramos, C., & Pradas, M. M. (2021). Biomaterials for Neural Tissue Engineering. *Frontiers in Nanotechnology*, *3*. https://doi.org/10.3389/fnano.2021.643507

Donnelly, D. J., & Popovich, P. G. (2008). Inflammation and its role in neuroprotection, axonal regeneration and functional recovery after spinal cord injury. *Experimental Neurology*, *209*(2), 378–388. https://doi.org/10.1016/j.expneurol.2007.06.009

Dovedytis, M., Liu, Z. J., & Bartlett, S. (2020). Hyaluronic acid and its biomedical applications: A review. *Engineered Regeneration*, *1*, 102–113. https://doi.org/10.1016/j.engreg.2020.10.001

Du, D., Furukawa, K. S., & Ushida, T. (2009). 3D culture of osteoblast-like cells by unidirectional or oscillatory flow for bone tissue engineering. *Biotechnology and Bioengineering*, *102*(6), 1670–1678. https://doi.org/10.1002/bit.22214

Dumont, R. J., Okonkwo, D. O., Verma, S., Hurlbert, R. J., Boulos, P. T., Ellegala, D. B., & Dumont, A. S. (2001). Acute Spinal Cord Injury, Part I: Pathophysiologic Mechanisms. *Clinical Neuropharmacology*, *24*(5), 254–264. https://doi.org/10.1097/00002826-200109000-00002

Edelbrock, A. N., Clemons, T. D., Chin, S. M., Roan, J. J. W., Bruckner, E. P., Álvarez, Z., Edelbrock, J. F., Wek, K. S., & Stupp, S. I. (2021). Superstructured Biomaterials Formed by Exchange Dynamics and Host–Guest Interactions in Supramolecular Polymers. *Advanced Science*, *8*(8), 2004042. https://doi.org/10.1002/advs.202004042

Edgerton, V. R., Tillakaratne, N. J. K., Bigbee, A. J., de Leon, R. D., & Roy, R. R. (2004). PLASTICITY OF THE SPINAL NEURAL CIRCUITRY AFTER INJURY. *Annual Review of Neuroscience*, *27*(1), 145–167. https://doi.org/10.1146/annurev.neuro.27.070203.144308

Edmondson, R., Broglie, J. J., Adcock, A. F., & Yang, L. (2014). Three-dimensional cell culture systems and their applications in drug discovery and cell-based biosensors. *Assay and Drug Development Technologies*, *12*(4), 207–218. https://doi.org/10.1089/adt.2014.573

Eilfort, A. M., Rasenack, M., Zörner, B., Curt, A., & Filli, L. (2024a). Evidence for reticulospinal plasticity underlying motor recovery in Brown-Séquard-plus Syndrome: a case report. *Frontiers in Neurology*, *15*. https://doi.org/10.3389/fneur.2024.1335795

Eilfort, A. M., Rasenack, M., Zörner, B., Curt, A., & Filli, L. (2024b). Evidence for reticulospinal plasticity underlying motor recovery in Brown-Séquard-plus Syndrome: a case report. *Frontiers in Neurology*, *15*. https://doi.org/10.3389/fneur.2024.1335795

Eisdorfer, J. T., Smit, R. D., Keefe, K. M., Lemay, M. A., Smith, G. M., & Spence, A. J. (2020). Epidural Electrical Stimulation: A Review of Plasticity Mechanisms That Are Hypothesized to Underlie Enhanced Recovery From Spinal Cord Injury With Stimulation. *Frontiers in Molecular Neuroscience*, *13*. https://doi.org/10.3389/fnmol.2020.00163

Endo, T., Spenger, C., Westman, E., Tominaga, T., & Olson, L. (2008). Reorganization of sensory processing below the level of spinal cord injury as revealed by fMRI. *Experimental Neurology*, *209*(1), 155–160. https://doi.org/10.1016/j.expneurol.2007.09.017

Engler, A. J., Sen, S., Sweeney, H. L., & Discher, D. E. (2006). Matrix Elasticity Directs Stem Cell Lineage Specification. *Cell*, *126*(4), 677–689. https://doi.org/10.1016/j.cell.2006.06.044

Estrada, V., Brazda, N., Schmitz, C., Heller, S., Blazyca, H., Martini, R., & Müller, H. W. (2014). Long-lasting significant functional improvement in chronic severe spinal cord injury following scar resection and polyethylene glycol implantation. *Neurobiology of Disease*, *67*, 165–179. https://doi.org/10.1016/j.nbd.2014.03.018

Fallica, B., Maffei, J. S., Villa, S., Makin, G., & Zaman, M. (2012). Alteration of Cellular Behavior and Response to PI3K Pathway Inhibition by Culture in 3D Collagen Gels. *PLoS ONE*, *7*(10), e48024. https://doi.org/10.1371/journal.pone.0048024

Fan, L., Liu, C., Chen, X., Zou, Y., Zhou, Z., Lin, C., Tan, G., Zhou, L., Ning, C., & Wang, Q. (2018). Directing Induced Pluripotent Stem Cell Derived Neural Stem Cell Fate with a Three-Dimensional Biomimetic Hydrogel for Spinal Cord Injury Repair. *ACS Applied Materials & Interfaces*, *10*(21), 17742–17755. https://doi.org/10.1021/acsami.8b05293

Fan, P., Li, S., Yang, J., Yang, K., Wu, P., Dong, Q., & Zhou, Y. (2024). Injectable, self-healing hyaluronic acid-based hydrogels for spinal cord injury repair. *International Journal of Biological Macromolecules*, *263*, 130333. https://doi.org/10.1016/j.ijbiomac.2024.130333

Farhy-Tselnicker, I., & Allen, N. J. (2018). Astrocytes, neurons, synapses: a tripartite view on cortical circuit development. *Neural Development*, *13*(1), 7. https://doi.org/10.1186/s13064-018-0104-y

Fawcett, J. W., & Verhaagen, J. (2018). Intrinsic Determinants of Axon Regeneration. *Developmental Neurobiology*, *78*(10), 890–897. https://doi.org/10.1002/dneu.22637

Ferguson, A. R., Huie, J. R., Crown, E. D., Baumbauer, K. M., Hook, M. A., Garraway, S. M., Lee, K. H., Hoy, K. C., & Grau, J. W. (2012). Maladaptive spinal plasticity opposes spinal learning and recovery in spinal cord injury. *Frontiers in Physiology*, *3*. https://doi.org/10.3389/fphys.2012.00399

Filipp, M., Travis, B., Henry, S., Idzikowski, E., Magnuson, S., Loh, M., Hellenbrand, D., & Hanna, A. (2019). Differences in neuroplasticity after spinal cord injury in varying animal models and humans. *Neural Regeneration Research*, *14*(1), 7. https://doi.org/10.4103/1673-5374.243694

Filli, L., & Schwab, M. (2015). Structural and functional reorganization of propriospinal connections promotes functional recovery after spinal cord injury. *Neural Regeneration Research*, *10*(4), 509. https://doi.org/10.4103/1673-5374.155425

Flanagan, L. A., Rebaza, L. M., Derzic, S., Schwartz, P. H., & Monuki, E. S. (2006). Regulation of human neural precursor cells by laminin and integrins. *Journal of Neuroscience Research*, *83*(5), 845–856. https://doi.org/10.1002/jnr.20778

Fontana, G., Gershlak, J., Adamski, M., Lee, J., Matsumoto, S., Le, H. D., Binder, B., Wirth, J., Gaudette, G., & Murphy, W. L. (2017a). Biofunctionalized Plants as Diverse Biomaterials for Human Cell Culture. *Advanced Healthcare Materials*, *6*(8), 1601225. https://doi.org/10.1002/adhm.201601225

Fontana, G., Gershlak, J., Adamski, M., Lee, J.-S., Matsumoto, S., Le, H. D., Binder, B., Wirth, J., Gaudette, G., & Murphy, W. L. (2017b). Decellularized Plants: Biofunctionalized Plants as Diverse Biomaterials for Human Cell Culture (Adv. Healthcare Mater. 8/2017). *Advanced Healthcare Materials*, *6*(8). https://doi.org/10.1002/adhm.201770038

Fontoura, J. C., Viezzer, C., dos Santos, F. G., Ligabue, R. A., Weinlich, R., Puga, R. D., Antonow, D., Severino, P., & Bonorino, C. (2020). Comparison of 2D and 3D cell culture models for cell growth, gene expression and drug resistance. *Materials Science and Engineering: C*, *107*, 110264. https://doi.org/10.1016/j.msec.2019.110264

Formento, E., Minassian, K., Wagner, F., Mignardot, J. B., Le Goff-Mignardot, C. G., Rowald, A., Bloch, J., Micera, S., Capogrosso, M., & Courtine, G. (2018). Electrical spinal cord stimulation must preserve proprioception to enable locomotion in humans with spinal cord injury. *Nature Neuroscience*, *21*(12), 1728–1741. https://doi.org/10.1038/s41593-018-0262-6

Fouad, K., Pedersen, V., Schwab, M. E., & Brösamle, C. (2001). Cervical sprouting of corticospinal fibers after thoracic spinal cord injury accompanies shifts in evoked motor responses. *Current Biology*, *11*(22), 1766–1770. https://doi.org/10.1016/S0960-9822(01)00535-8

Fouad, K., Schnell, L., Bunge, M. B., Schwab, M. E., Liebscher, T., & Pearse, D. D. (2005). Combining Schwann Cell Bridges and Olfactory-Ensheathing Glia Grafts with Chondroitinase Promotes Locomotor Recovery after Complete Transection of the Spinal Cord. *The Journal of Neuroscience*, *25*(5), 1169–1178. https://doi.org/10.1523/JNEUROSCI.3562-04.2005

Francos-Quijorna, I., Sánchez-Petidier, M., Burnside, E. R., Badea, S. R., Torres-Espin, A., Marshall, L., de Winter, F., Verhaagen, J., Moreno-Manzano, V., & Bradbury, E. J. (2022). Chondroitin sulfate proteoglycans prevent immune cell phenotypic conversion and inflammation resolution via TLR4 in rodent models of spinal cord injury. *Nature Communications*, *13*(1), 2933. https://doi.org/10.1038/s41467-022-30467-5

Frigon, A., Akay, T., & Prilutsky, B. I. (2021). Control of Mammalian Locomotion by Somatosensory Feedback. In *Comprehensive Physiology* (pp. 2877–2947). Wiley. https://doi.org/10.1002/cphy.c210020

Frigon, A., & Rossignol, S. (2006a). *Functional plasticity following spinal cord lesions* (pp. 231–398). https://doi.org/10.1016/S0079-6123(06)57016-5

Frigon, A., & Rossignol, S. (2006b). *Functional plasticity following spinal cord lesions* (pp. 231–398). https://doi.org/10.1016/S0079-6123(06)57016-5

Frigon, A., Thibaudier, Y., Johnson, M. D., Heckman, C. J., & Hurteau, M.-F. (2012). Cutaneous inputs from the back abolish locomotor-like activity and reduce spastic-like activity in the adult cat following complete spinal cord injury. *Experimental Neurology*, *235*(2), 588–598. https://doi.org/10.1016/j.expneurol.2012.03.013

Führmann, T., Anandakumaran, P. N., & Shoichet, M. S. (2017). Combinatorial Therapies After Spinal Cord Injury: How Can Biomaterials Help? *Advanced Healthcare Materials*, *6*(10), 1601130. https://doi.org/10.1002/adhm.201601130

Furlan, J. C., Pakosh, M., Craven, B. C., & Popovic, M. R. (2022). Insights on the Potential Mechanisms of Action of Functional Electrical Stimulation Therapy in Combination With Task-Specific Training: A Scoping Review. *Neuromodulation: Technology at the Neural Interface*, *25*(8), 1280–1288. https://doi.org/10.1111/ner.13403

Gabel, B. C., Curtis, E. I., Marsala, M., & Ciacci, J. D. (2017). A Review of Stem Cell Therapy for Spinal Cord Injury: Large Animal Models and the Frontier in Humans. *World Neurosurgery*, *98*, 438–443. https://doi.org/10.1016/j.wneu.2016.11.053

Gage, F. H. (2000). Mammalian Neural Stem Cells. *Science*, *287*(5457), 1433–1438. https://doi.org/10.1126/science.287.5457.1433

Gao, Z., Yang, Y., Feng, Z., Li, X., Min, C., Zhu, Z., Song, H., Hu, Y., Wang, Y., & He, X. (2021). Chemogenetic stimulation of proprioceptors remodels lumbar interneuron excitability and promotes motor recovery after SCI. *Molecular Therapy*, *29*(8), 2483–2498. https://doi.org/10.1016/j.ymthe.2021.04.023

García, E., Sánchez-Noriega, S., González-Pacheco, G., González-Vázquez, A. N., Ibarra, A., & Rodríguez-Barrera, R. (2023). Recent advances in the combination of cellular therapy with stem cells and nanoparticles after a spinal cord injury. *Frontiers in Neurology*, *14*. https://doi.org/10.3389/fneur.2023.1127878

Gaudet, A. D., & Popovich, P. G. (2014). Extracellular matrix regulation of inflammation in the healthy and injured spinal cord. *Experimental Neurology*, *258*, 24–34. https://doi.org/10.1016/j.expneurol.2013.11.020

Ge, H., Tan, L., Wu, P., Yin, Y., Liu, X., Meng, H., Cui, G., Wu, N., Lin, J., Hu, R., & Feng, H. (2015). Poly-L-ornithine promotes preferred differentiation of neural stem/progenitor cells via ERK signalling pathway. *Scientific Reports*, *5*(1), 15535. https://doi.org/10.1038/srep15535

Ge, H., Yu, A., Chen, J., Yuan, J., Yin, Y., Duanmu, W., Tan, L., Yang, Y., Lan, C., Chen, W., Feng, H., & Hu, R. (2016). Poly-L-ornithine enhances migration of neural stem/progenitor cells via promoting α-Actinin 4 binding to actin filaments. *Scientific Reports*, *6*(1), 37681. https://doi.org/10.1038/srep37681

Gershlak, J. R., Hernandez, S., Fontana, G., Perreault, L. R., Hansen, K. J., Larson, S. A., Binder, B. Y. K., Dolivo, D. M., Yang, T., Dominko, T., Rolle, M. W., Weathers, P. J., Medina-Bolivar, F., Cramer, C. L., Murphy, W. L., & Gaudette, G. R. (2017). Crossing kingdoms: Using decellularized plants as perfusable tissue engineering scaffolds. *Biomaterials*, *125*, 13–22. https://doi.org/10.1016/j.biomaterials.2017.02.011

Ghosh, Mousumi, and Damien D. Pearse. “The Role of the Serotonergic System in Locomotor Recovery after Spinal Cord Injury.” Frontiers in Neural Circuits, vol. 8, Feb. 2015. https://doi.org/10.3389/fncir.2014.00151.

Gill, M. L., Grahn, P. J., Calvert, J. S., Linde, M. B., Lavrov, I. A., Strommen, J. A., Beck, L. A., Sayenko, D. G., Van Straaten, M. G., Drubach, D. I., Veith, D. D., Thoreson, A. R., Lopez, C., Gerasimenko, Y. P., Edgerton, V. R., Lee, K. H., & Zhao, K. D. (2018). Neuromodulation of lumbosacral spinal networks enables independent stepping after complete paraplegia. *Nature Medicine*, *24*(11), 1677–1682. https://doi.org/10.1038/s41591-018-0175-7

Gliksten, L., & Yip, P. K. (2023). Current Spinal Cord Injury Animal Models are Too Simplistic for Clinical Translation. *Journal of Experimental Neurology*, *4*(1), 6–10. https://doi.org/10.33696/Neurol.4.068

Goltash, S., Khodr, R., Bui, T. V., & Laliberte, A. M. (2025). An optogenetic mouse model of hindlimb spasticity after spinal cord injury. *Experimental Neurology*, *386*, 115157. https://doi.org/10.1016/j.expneurol.2025.115157

Goltash, S., Stevens, S. J., Topcu, E., & Bui, T. V. (2023). Changes in synaptic inputs to dI3 INs and MNs after complete transection in adult mice. *Frontiers in Neural Circuits*, *17*. https://doi.org/10.3389/fncir.2023.1176310

Gong, Z., Lei, D., Wang, C., Yu, C., Xia, K., Shu, J., Ying, L., Du, J., Wang, J., Huang, X., Ni, L., Wang, C., Lin, J., Li, F., You, Z., & Liang, C. (2020). Bioactive Elastic Scaffolds Loaded with Neural Stem Cells Promote Rapid Spinal Cord Regeneration. *ACS Biomaterials Science & Engineering*, *6*(11), 6331–6343. https://doi.org/10.1021/acsbiomaterials.0c01057

Gossard, J.-P., Brownstone, R. M., Barajon, I., & Hultborn, H. (1994). Transmission in a locomotor-related group Ib pathway from hindlimb extensor muscles in the cat. *Experimental Brain Research*, *98*(2). https://doi.org/10.1007/BF00228410

Granier, C., Schwarting, J., Fourli, E., Laage-Gaupp, F., Hennrich, A. A., Schmalz, A., Jacobi, A., Wesolowski, M., Conzelmann, K. K., & Bareyre, F. M. (2020). Formation of somatosensory detour circuits mediates functional recovery following dorsal column injury. *Scientific Reports*, *10*(1), 10953. https://doi.org/10.1038/s41598-020-67866-x

Grau, J. W., Huang, Y.-J., Turtle, J. D., Strain, M. M., Miranda, R. C., Garraway, S. M., & Hook, M. A. (2017). When Pain Hurts: Nociceptive Stimulation Induces a State of Maladaptive Plasticity and Impairs Recovery after Spinal Cord Injury. *Journal of Neurotrauma*, *34*(10), 1873–1890. https://doi.org/10.1089/neu.2016.4626

Griffin, J. M., & Bradke, F. (2020). Therapeutic repair for spinal cord injury: combinatory approaches to address a multifaceted problem. *EMBO Molecular Medicine*, *12*(3). https://doi.org/10.15252/emmm.201911505

Grillner, S. (1981). Control of Locomotion in Bipeds, Tetrapods, and Fish. In *Comprehensive Physiology* (pp. 1179–1236). Wiley. https://doi.org/10.1002/cphy.cp010226

Grillner, S. (2003). The motor infrastructure: from ion channels to neuronal networks. *Nature Reviews Neuroscience*, *4*(7), 573–586. https://doi.org/10.1038/nrn1137

Grillner, S., & Kozlov, A. (2021). The CPGs for Limbed Locomotion–Facts and Fiction. *International Journal of Molecular Sciences*, *22*(11), 5882. https://doi.org/10.3390/ijms22115882

Gris, D., Marsh, D. R., Oatway, M. A., Chen, Y., Hamilton, E. F., Dekaban, G. A., & Weaver, L. C. (2004). Transient Blockade of the CD11d/CD18 Integrin Reduces Secondary Damage after Spinal Cord Injury, Improving Sensory, Autonomic, and Motor Function. *The Journal of Neuroscience*, *24*(16), 4043–4051. https://doi.org/10.1523/JNEUROSCI.5343-03.2004

Grulova, I., Slovinska, L., Blaško, J., Devaux, S., Wisztorski, M., Salzet, M., Fournier, I., Kryukov, O., Cohen, S., & Cizkova, D. (2015). Delivery of Alginate Scaffold Releasing Two Trophic Factors for Spinal Cord Injury Repair. *Scientific Reports*, *5*(1), 13702. https://doi.org/10.1038/srep13702

Gu, Y., Cheng, X., Huang, X., Yuan, Y., Qin, S., Tan, Z., Wang, D., Hu, X., He, C., & Su, Z. (2019). Conditional ablation of reactive astrocytes to dissect their roles in spinal cord injury and repair. *Brain, Behavior, and Immunity*, *80*, 394–405. https://doi.org/10.1016/j.bbi.2019.04.016

Guijarro-Belmar, A., Varone, A., Baltzer, M. R., Kataria, S., Tanriver-Ayder, E., Watzlawick, R., Sena, E., Cunningham, C. J., Rajnicek, A. M., Macleod, M., Huang, W., Currie, G. L., & McCann, S. K. (2022). Effectiveness of biomaterial-based combination strategies for spinal cord repair – a systematic review and meta-analysis of preclinical literature. *Spinal Cord*, *60*(12), 1041–1049. https://doi.org/10.1038/s41393-022-00811-z

Guo, B., & Ma, P. X. (2014). Synthetic biodegradable functional polymers for tissue engineering: a brief review. *Science China Chemistry*, *57*(4), 490–500. https://doi.org/10.1007/s11426-014-5086-y

Guo, Y.-S., Yuan, M., Han, Y., Shen, X.-Y., Gao, Z.-K., & Bi, X. (2022). Effects of enriched environment on microglia and functional white matter recovery in rats with post stroke cognitive

impairment. *Neurochemistry International*, *154*, 105295. https://doi.org/10.1016/j.neuint.2022.105295
Hachem, L. D., & Fehlings, M. G. (2021). Pathophysiology of Spinal Cord Injury. *Neurosurgery Clinics of North America*, *32*(3), 305–313. https://doi.org/10.1016/j.nec.2021.03.002
Hadjiantoniou, S. V., Sean, D., Ignacio, M., Godin, M., Slater, G. W., & Pelling, A. E. (2016). Physical confinement signals regulate the organization of stem cells in three dimensions. *Journal of The Royal Society Interface*, *13*(123), 20160613. https://doi.org/10.1098/rsif.2016.0613
Hakim, J. S., Rodysill, B. R., Chen, B. K., Schmeichel, A. M., Yaszemski, M. J., Windebank, A. J., & Madigan, N. N. (2019). Combinatorial tissue engineering partially restores function after spinal cord injury. *Journal of Tissue Engineering and Regenerative Medicine*, *13*(5), 857–873. https://doi.org/10.1002/term.2840
HALL, E. D., & BRAUGHLER, J. M. (1986). Role of Lipid Peroxidation in Post-Traumatic Spinal Cord Degeneration: A Review. *Central Nervous System Trauma*, *3*(4), 281–294. https://doi.org/10.1089/cns.1986.3.281
Hama, H., Hara, C., Yamaguchi, K., & Miyawaki, A. (2004). PKC Signaling Mediates Global Enhancement of Excitatory Synaptogenesis in Neurons Triggered by Local Contact with Astrocytes. *Neuron*, *41*(3), 405–415. https://doi.org/10.1016/S0896-6273(04)00007-8
Hara, M., Kobayakawa, K., Ohkawa, Y., Kumamaru, H., Yokota, K., Saito, T., Kijima, K., Yoshizaki, S., Harimaya, K., Nakashima, Y., & Okada, S. (2017). Interaction of reactive astrocytes with type I collagen induces astrocytic scar formation through the integrin–N-cadherin pathway after spinal cord injury. *Nature Medicine*, *23*(7), 818–828. https://doi.org/10.1038/nm.4354
Harkema, S., Gerasimenko, Y., Hodes, J., Burdick, J., Angeli, C., Chen, Y., Ferreira, C., Willhite, A., Rejc, E., Grossman, R. G., & Edgerton, V. R. (2011). Effect of epidural stimulation of the lumbosacral spinal cord on voluntary movement, standing, and assisted stepping after motor complete paraplegia: a case study. *The Lancet*, *377*(9781), 1938–1947. https://doi.org/10.1016/S0140-6736(11)60547-3
Harris, A. F., Lacombe, J., Liyanage, S., Han, M. Y., Wallace, E., Karsunky, S., Abidi, N., & Zenhausern, F. (2021). Supercritical carbon dioxide decellularization of plant material to generate 3D biocompatible scaffolds. *Scientific Reports*, *11*(1), 3643. https://doi.org/10.1038/s41598-021-83250-9
Harris, A. F., Lacombe, J., & Zenhausern, F. (2021). The Emerging Role of Decellularized Plant-Based Scaffolds as a New Biomaterial. *International Journal of Molecular Sciences*, *22*(22), 12347. https://doi.org/10.3390/ijms222212347
Harvey, A. R., Lovett, S. J., Majda, B. T., Yoon, J. H., Wheeler, L. P. G., & Hodgetts, S. I. (2015). Neurotrophic factors for spinal cord repair: Which, where, how and when to apply, and for what period of time? *Brain Research*, *1619*, 36–71. https://doi.org/10.1016/j.brainres.2014.10.049
Hausmann, O. N. (2003). Post-traumatic inflammation following spinal cord injury. *Spinal Cord*, *41*(7), 369–378. https://doi.org/10.1038/sj.sc.3101483
He, B.-L., Ba, Y., Wang, X., Liu, S., Liu, G., Ou, S., Gu, Y., Pan, X., & Wang, T.-H. (2013). BDNF expression with functional improvement in transected spinal cord treated with neural stem cells in adult rats. *Neuropeptides*, *47*(1), 1–7. https://doi.org/10.1016/j.npep.2012.06.001
He, X., Yang, L., Dong, K., Zhang, F., Liu, Y., Ma, B., Chen, Y., Hai, J., Zhu, R., & Cheng, L. (2022). Biocompatible exosome-modified fibrin gel accelerates the recovery of spinal cord injury by VGF-mediated oligodendrogenesis. *Journal of Nanobiotechnology*, *20*(1), 360. https://doi.org/10.1186/s12951-022-01541-3

He, Y., Liu, X., & Chen, Z. (2020). Glial Scar—a Promising Target for Improving Outcomes After CNS Injury. *Journal of Molecular Neuroscience*, *70*(3), 340–352. https://doi.org/10.1007/s12031-019-01417-6

Head, S. I., & Bush, B. M. H. (1991). Proprioceptive reflex interactions with central motor rhythms in the isolated thoracic ganglion of the shore crab. *Journal of Comparative Physiology A*, *168*(4), 445–459. https://doi.org/10.1007/BF00199604

Hellenbrand, D. J., Kaeppler, K. E., Hwang, E., Ehlers, M. E., Toigo, R. D., Giesler, J. D., Vassar-Olsen, E. R., & Hanna, A. (2013). Basic techniques for long distance axon tracing in the spinal cord. *Microscopy Research and Technique*, *76*(12), 1240–1249. https://doi.org/10.1002/jemt.22291

Hellenbrand, D. J., Quinn, C. M., Piper, Z. J., Morehouse, C. N., Fixel, J. A., & Hanna, A. S. (2021). Inflammation after spinal cord injury: a review of the critical timeline of signaling cues and cellular infiltration. *Journal of Neuroinflammation*, *18*(1), 284. https://doi.org/10.1186/s12974-021-02337-2

Hickey, R. J., Leblanc Latour, M., Harden, J. L., & Pelling, A. E. (2023). Designer Scaffolds for Interfacial Bioengineering. *Advanced Engineering Materials*, *25*(10). https://doi.org/10.1002/adem.202201415

Hickey, R. J., Modulevsky, D. J., Cuerrier, C. M., & Pelling, A. E. (2018a). Customizing the Shape and Microenvironment Biochemistry of Biocompatible Macroscopic Plant-Derived Cellulose Scaffolds. *ACS Biomaterials Science & Engineering*, *4*(11), 3726–3736. https://doi.org/10.1021/acsbiomaterials.8b00178

Hickey, R. J., Modulevsky, D. J., Cuerrier, C. M., & Pelling, A. E. (2018b). Customizing the Shape and Microenvironment Biochemistry of Biocompatible Macroscopic Plant-Derived Cellulose Scaffolds. *ACS Biomaterials Science & Engineering*, *4*(11), 3726–3736. https://doi.org/10.1021/acsbiomaterials.8b00178

Hickey, R. J., & Pelling, A. E. (2019). Cellulose Biomaterials for Tissue Engineering. *Frontiers in Bioengineering and Biotechnology*, *7*. https://doi.org/10.3389/fbioe.2019.00045

Hicks, A. L., Martin, K. A., Ditor, D. S., Latimer, A. E., Craven, C., Bugaresti, J., & McCartney, N. (2003). Long-term exercise training in persons with spinal cord injury: effects on strength, arm ergometry performance and psychological well-being. *Spinal Cord*, *41*(1), 34–43. https://doi.org/10.1038/sj.sc.3101389

Hollis, E. R., Ishiko, N., Pessian, M., Tolentino, K., Lee-Kubli, C. A., Calcutt, N. A., & Zou, Y. (2015). Remodelling of spared proprioceptive circuit involving a small number of neurons supports functional recovery. *Nature Communications*, *6*(1), 6079. https://doi.org/10.1038/ncomms7079

Hong, H., Seo, Y. B., Kim, D. Y., Lee, J. S., Lee, Y. J., Lee, H., Ajiteru, O., Sultan, M. T., Lee, O. J., Kim, S. H., & Park, C. H. (2020). Digital light processing 3D printed silk fibroin hydrogel for cartilage tissue engineering. *Biomaterials*, *232*, 119679. https://doi.org/10.1016/j.biomaterials.2019.119679

Honig, F., Vermeulen, S., Zadpoor, A. A., de Boer, J., & Fratila-Apachitei, L. E. (2020). Natural Architectures for Tissue Engineering and Regenerative Medicine. *Journal of Functional Biomaterials*, *11*(3), 47. https://doi.org/10.3390/jfb11030047

Hu, X., Xu, W., Ren, Y., Wang, Z., He, X., Huang, R., Ma, B., Zhao, J., Zhu, R., & Cheng, L. (2023). Spinal cord injury: molecular mechanisms and therapeutic interventions. *Signal Transduction and Targeted Therapy*, *8*(1), 245. https://doi.org/10.1038/s41392-023-01477-6

Hu, Y., Zhang, H., Wei, H., Cheng, H., Cai, J., Chen, X., Xia, L., Wang, H., & Chai, R. (2022). Scaffolds with anisotropic structure for neural tissue engineering. *Engineered Regeneration*, *3*(2), 154–162. https://doi.org/10.1016/j.engreg.2022.04.001

Huang, L., Wang, Y., Zhu, M., Wan, X., Zhang, H., Lei, T., Blesch, A., & Liu, S. (2020). Anisotropic Alginate Hydrogels Promote Axonal Growth across Chronic Spinal Cord Transections after Scar Removal. *ACS Biomaterials Science & Engineering*, *6*(4), 2274–2286. https://doi.org/10.1021/acsbiomaterials.9b01802

Huebner, E. A., & Strittmatter, S. M. (2009). *Axon Regeneration in the Peripheral and Central Nervous Systems* (pp. 305–360). https://doi.org/10.1007/400_2009_19

Hultborn, H., Denton, M. E., Wienecke, J., & Nielsen, J. B. (2003). Variable amplification of synaptic input to cat spinal motoneurones by dendritic persistent inward current. *The Journal of Physiology*, *552*(3), 945–952. https://doi.org/10.1113/jphysiol.2003.050971

Hung, T.-K., Chang, G.-L., Lin, H.-S., Walter, F. R., & Bunegin, L. (1981). Stress-strain relationship of the spinal cord of anesthetized cats. *Journal of Biomechanics*, *14*(4), 269–276. https://doi.org/10.1016/0021-9290(81)90072-5

Hur, E.-M., Saijilafu, & Zhou, F.-Q. (2012). Growing the growth cone: remodeling the cytoskeleton to promote axon regeneration. *Trends in Neurosciences*, *35*(3), 164–174. https://doi.org/10.1016/j.tins.2011.11.002

Husch, A., Van Patten, G. N., Hong, D. N., Scaperotti, M. M., Cramer, N., & Harris-Warrick, R. M. (2012). Spinal Cord Injury Induces Serotonin Supersensitivity without Increasing Intrinsic Excitability of Mouse V2a Interneurons. *The Journal of Neuroscience*, *32*(38), 13145–13154. https://doi.org/10.1523/JNEUROSCI.2995-12.2012

Hutson, T. H., Kathe, C., Palmisano, I., Bartholdi, K., Hervera, A., De Virgiliis, F., McLachlan, E., Zhou, L., Kong, G., Barraud, Q., Danzi, M. C., Medrano-Fernandez, A., Lopez-Atalaya, J. P., Boutillier, A. L., Sinha, S. H., Singh, A. K., Chaturbedy, P., Moon, L. D. F., Kundu, T. K., … Di Giovanni, S. (2019). Cbp-dependent histone acetylation mediates axon regeneration induced by environmental enrichment in rodent spinal cord injury models. *Science Translational Medicine*, *11*(487). https://doi.org/10.1126/scitranslmed.aaw2064

Hwang, D. W., Jin, Y., Lee, D. H., Kim, H. Y., Cho, H. N., Chung, H. J., Park, Y., Youn, H., Lee, S. J., Lee, H. J., Kim, S. U., Wang, K.-C., & Lee, D. S. (2014). In Vivo Bioluminescence Imaging for Prolonged Survival of Transplanted Human Neural Stem Cells Using 3D Biocompatible Scaffold in Corticectomized Rat Model. *PLoS ONE*, *9*(9), e105129. https://doi.org/10.1371/journal.pone.0105129

Hyatt, A. J. T., Wang, D., Kwok, J. C., Fawcett, J. W., & Martin, K. R. (2010). Controlled release of chondroitinase ABC from fibrin gel reduces the level of inhibitory glycosaminoglycan chains in lesioned spinal cord. *Journal of Controlled Release*, *147*(1), 24–29. https://doi.org/10.1016/j.jconrel.2010.06.026

Ichiyama, R. M., Gerasimenko, Yu. P., Zhong, H., Roy, R. R., & Edgerton, V. R. (2005). Hindlimb stepping movements in complete spinal rats induced by epidural spinal cord stimulation. *Neuroscience Letters*, *383*(3), 339–344. https://doi.org/10.1016/j.neulet.2005.04.049

Indurkar, A., Pandit, A., Jain, R., & Dandekar, P. (2021). Plant-based biomaterials in tissue engineering. *Bioprinting*, *21*, e00127. https://doi.org/10.1016/j.bprint.2020.e00127

Jacobi, A., & Bareyre, F. (2015). Regulation of axonal remodeling following spinal cord injury. *Neural Regeneration Research*, *10*(10), 1555. https://doi.org/10.4103/1673-5374.167748

Jarrah, R., Sammak, S. El, Onyedimma, C., Ghaith, A. K., Moinuddin, F. M., Bhandarkar, A. R., Siddiqui, A., Madigan, N., & Bydon, M. (2022). The Role of Alginate Hydrogels as a Potential Treatment Modality for Spinal Cord Injury: A Comprehensive Review of the Literature. *Neurospine*, *19*(2), 272–280. https://doi.org/10.14245/ns.2244186.093

Jiang, Y.-Q., Zaaimi, B., & Martin, J. H. (2016). Competition with Primary Sensory Afferents Drives Remodeling of Corticospinal Axons in Mature Spinal Motor Circuits. *The Journal of Neuroscience : The Official Journal of the Society for Neuroscience*, *36*(1), 193–203. https://doi.org/10.1523/JNEUROSCI.3441-15.2016

Jin, D., Liu, Y., Sun, F., Wang, X., Liu, X., & He, Z. (2015). Restoration of skilled locomotion by sprouting corticospinal axons induced by co-deletion of PTEN and SOCS3. *Nature Communications*, *6*(1), 8074. https://doi.org/10.1038/ncomms9074

Johansson, B. B., & Belichenko, P. V. (2002). Neuronal Plasticity and Dendritic Spines: Effect of Environmental Enrichment on Intact and Postischemic Rat Brain. *Journal of Cerebral Blood Flow & Metabolism*, *22*(1), 89–96. https://doi.org/10.1097/00004647-200201000-00011

Johansson, C. B., Momma, S., Clarke, D. L., Risling, M., Lendahl, U., & Frisén, J. (1999). Identification of a Neural Stem Cell in the Adult Mammalian Central Nervous System. *Cell*, *96*(1), 25–34. https://doi.org/10.1016/S0092-8674(00)80956-3

JOHNSON, J., & WANG, M. Y. (2008). Spinal Cord Injury-induced Immunodepression Syndrome. *Neurosurgery*, *63*(6), N13. https://doi.org/10.1227/01.NEU.0000313631.97644.D7

Johnson, P. J., Parker, S. R., & Sakiyama-Elbert, S. E. (2010). Fibrin-based tissue engineering scaffolds enhance neural fiber sprouting and delay the accumulation of reactive astrocytes at the lesion in a subacute model of spinal cord injury. *Journal of Biomedical Materials Research Part A*, *92A*(1), 152–163. https://doi.org/10.1002/jbm.a.32343

Jones, T. B. (2014). Lymphocytes and autoimmunity after spinal cord injury. *Experimental Neurology*, *258*, 78–90. https://doi.org/10.1016/j.expneurol.2014.03.003

Joseph, G., Orme, R. P., Kyriacou, T., Fricker, R. A., & Roach, P. (2021). Effects of Surface Chemistry Interaction on Primary Neural Stem Cell Neurosphere Responses. *ACS Omega*, *6*(30), 19901–19910. https://doi.org/10.1021/acsomega.1c02796

Karimi-Abdolrezaee, S., Schut, D., Wang, J., & Fehlings, M. G. (2012). Chondroitinase and Growth Factors Enhance Activation and Oligodendrocyte Differentiation of Endogenous Neural Precursor Cells after Spinal Cord Injury. *PLoS ONE*, *7*(5). https://doi.org/10.1371/journal.pone.0037589

Kataoka, K., Suzuki, Y., Kitada, M., Hashimoto, T., Chou, H., Bai, H., Ohta, M., Wu, S., Suzuki, K., & Ide, C. (2004). Alginate Enhances Elongation of Early Regenerating Axons in Spinal Cord of Young Rats. *Tissue Engineering*, *10*(3–4), 493–504. https://doi.org/10.1089/107632704323061852

Kathe, C., Skinnider, M. A., Hutson, T. H., Regazzi, N., Gautier, M., Demesmaeker, R., Komi, S., Ceto, S., James, N. D., Cho, N., Baud, L., Galan, K., Matson, K. J. E., Rowald, A., Kim, K., Wang, R., Minassian, K., Prior, J. O., Asboth, L., … Courtine, G. (2022). The neurons that restore walking after paralysis. *Nature*, *611*(7936), 540–547. https://doi.org/10.1038/s41586-022-05385-7

Kazim, S. F., Bowers, C. A., Cole, C. D., Varela, S., Karimov, Z., Martinez, E., Ogulnick, J. V., & Schmidt, M. H. (2021). Corticospinal Motor Circuit Plasticity After Spinal Cord Injury: Harnessing Neuroplasticity to Improve Functional Outcomes. *Molecular Neurobiology*, *58*(11), 5494–5516. https://doi.org/10.1007/s12035-021-02484-w

Keirstead, H. S., Nistor, G., Bernal, G., Totoiu, M., Cloutier, F., Sharp, K., & Steward, O. (2005). Human Embryonic Stem Cell-Derived Oligodendrocyte Progenitor Cell Transplants Remyelinate and Restore Locomotion after Spinal Cord Injury. *The Journal of Neuroscience*, *25*(19), 4694–4705. https://doi.org/10.1523/JNEUROSCI.0311-05.2005

Kerschensteiner, M., Schwab, M. E., Lichtman, J. W., & Misgeld, T. (2005). In vivo imaging of axonal degeneration and regeneration in the injured spinal cord. *Nature Medicine*, *11*(5), 572–577. https://doi.org/10.1038/nm1229

Khalki, L., Sadlaoud, K., Lerond, J., Coq, J.-O., Brezun, J.-M., Vinay, L., Coulon, P., & Bras, H. (2018). Changes in innervation of lumbar motoneurons and organization of premotor network following training of transected adult rats. *Experimental Neurology*, *299*, 1–14. https://doi.org/10.1016/j.expneurol.2017.09.002

Kim, D., Zai, L., Liang, P., Schaffling, C., Ahlborn, D., & Benowitz, L. I. (2013). Inosine Enhances Axon Sprouting and Motor Recovery after Spinal Cord Injury. *PLoS ONE*, *8*(12), e81948. https://doi.org/10.1371/journal.pone.0081948

Kiss Bimbova, K., Bacova, M., Kisucka, A., Galik, J., Zavacky, P., & Lukacova, N. (2022). Activation of Three Major Signaling Pathways After Endurance Training and Spinal Cord Injury. *Molecular Neurobiology*, *59*(2), 950–967. https://doi.org/10.1007/s12035-021-02628-y

Kjell, J., & Olson, L. (2016a). Rat models of spinal cord injury: from pathology to potential therapies. *Disease Models & Mechanisms*, *9*(10), 1125–1137. https://doi.org/10.1242/dmm.025833

Kjell, J., & Olson, L. (2016b). Rat models of spinal cord injury: from pathology to potential therapies. *Disease Models & Mechanisms*, *9*(10), 1125–1137. https://doi.org/10.1242/dmm.025833

Klarner, T., & Zehr, E. P. (2018). Sherlock Holmes and the curious case of the human locomotor central pattern generator. *Journal of Neurophysiology*, *120*(1), 53–77. https://doi.org/10.1152/jn.00554.2017

Kobravi, H. R., Moghimi, A., & Khodadadi, Z. (2017). Effect of Treadmill Training Protocols on Locomotion Recovery in Spinalized Rats. *Journal of Medical Signals and Sensors*, *7*(1), 53–57.

Koffler, J., Zhu, W., Qu, X., Platoshyn, O., Dulin, J. N., Brock, J., Graham, L., Lu, P., Sakamoto, J., Marsala, M., Chen, S., & Tuszynski, M. H. (2019). Biomimetic 3D-printed scaffolds for spinal cord injury repair. *Nature Medicine*, *25*(2), 263–269. https://doi.org/10.1038/s41591-018-0296-z

Koopmans, G. C., Deumens, R., Honig, W. M. M., Hamers, F. P. T., Mey, J., van Kleef, M., & Joosten, E. A. (2012). Functional Recovery, Serotonergic Sprouting, and Endogenous Progenitor Fates in Response to Delayed Environmental Enrichment after Spinal Cord Injury. *Journal of Neurotrauma*, *29*(3), 514–527. https://doi.org/10.1089/neu.2011.1949

Koseki, H., Donegá, M., Lam, B. Y., Petrova, V., van Erp, S., Yeo, G. S., Kwok, J. C., ffrench-Constant, C., Eva, R., & Fawcett, J. W. (2017). Selective rab11 transport and the intrinsic regenerative ability of CNS axons. *ELife*, *6*. https://doi.org/10.7554/eLife.26956

Kourgiantaki, A., Tzeranis, D. S., Karali, K., Georgelou, K., Bampoula, E., Psilodimitrakopoulos, S., Yannas, I. V., Stratakis, E., Sidiropoulou, K., Charalampopoulos, I., & Gravanis, A. (2020). Neural stem cell delivery via porous collagen scaffolds promotes neuronal differentiation and locomotion recovery in spinal cord injury. *Npj Regenerative Medicine*, *5*(1), 12. https://doi.org/10.1038/s41536-020-0097-0

Kozlov, A., Huss, M., Lansner, A., Kotaleski, J. H., & Grillner, S. (2009). Simple cellular and network control principles govern complex patterns of motor behavior. *Proceedings of the National Academy of Sciences*, *106*(47), 20027–20032. https://doi.org/10.1073/pnas.0906722106

Krenz, N. R., & Weaver, L. C. (1998). Sprouting of primary afferent fibers after spinal cord transection in the rat. *Neuroscience*, *85*(2), 443–458. https://doi.org/10.1016/S0306-4522(97)00622-2

Kubinová, Š., & Syková, E. (2010). Nanotechnologies in regenerative medicine. *Minimally Invasive Therapy & Allied Technologies*, *19*(3), 144–156. https://doi.org/10.3109/13645706.2010.481398

Kulkarni, R., Thakur, A., & Kumar, H. (2022). Microtubule Dynamics Following Central and Peripheral Nervous System Axotomy. *ACS Chemical Neuroscience*, *13*(9), 1358–1369. https://doi.org/10.1021/acschemneuro.2c00189

Kushchayev, S. V., Giers, M. B., Hom Eng, D., Martirosyan, N. L., Eschbacher, J. M., Mortazavi, M. M., Theodore, N., Panitch, A., & Preul, M. C. (2016). Hyaluronic acid scaffold has a

neuroprotective effect in hemisection spinal cord injury. *Journal of Neurosurgery: Spine*, *25*(1), 114–124. https://doi.org/10.3171/2015.9.SPINE15628

Lacroix, S., Hamilton, L. K., Vaugeois, A., Beaudoin, S., Breault-Dugas, C., Pineau, I., Lévesque, S. A., Grégoire, C.-A., & Fernandes, K. J. L. (2014). Central Canal Ependymal Cells Proliferate Extensively in Response to Traumatic Spinal Cord Injury but Not Demyelinating Lesions. *PLoS ONE*, *9*(1), e85916. https://doi.org/10.1371/journal.pone.0085916

Lagerström, M. C., Rogoz, K., Abrahamsen, B., Persson, E., Reinius, B., Nordenankar, K., Ölund, C., Smith, C., Mendez, J. A., Chen, Z.-F., Wood, J. N., Wallén-Mackenzie, Å., & Kullander, K. (2010). VGLUT2-Dependent Sensory Neurons in the TRPV1 Population Regulate Pain and Itch. *Neuron*, *68*(3), 529–542. https://doi.org/10.1016/j.neuron.2010.09.016

Lai, B.-Q., Zeng, X., Han, W.-T., Che, M.-T., Ding, Y., Li, G., & Zeng, Y.-S. (2021). Stem cell-derived neuronal relay strategies and functional electrical stimulation for treatment of spinal cord injury. *Biomaterials*, *279*, 121211. https://doi.org/10.1016/j.biomaterials.2021.121211

Laliberte, A. M., Farah, C., Steiner, K. R., Tariq, O., & Bui, T. V. (2022). Changes in Sensorimotor Connectivity to dI3 Interneurons in Relation to the Postnatal Maturation of Grasping. *Frontiers in Neural Circuits*, *15*. https://doi.org/10.3389/fncir.2021.768235

Laliberte, A. M., Goltash, S., Lalonde, N. R., & Bui, T. V. (2019a). Propriospinal Neurons: Essential Elements of Locomotor Control in the Intact and Possibly the Injured Spinal Cord. *Frontiers in Cellular Neuroscience*, *13*. https://doi.org/10.3389/fncel.2019.00512

Laliberte, A. M., Goltash, S., Lalonde, N. R., & Bui, T. V. (2019b). Propriospinal Neurons: Essential Elements of Locomotor Control in the Intact and Possibly the Injured Spinal Cord. *Frontiers in Cellular Neuroscience*, *13*. https://doi.org/10.3389/fncel.2019.00512

Lavrov, I., Courtine, G., Dy, C. J., van den Brand, R., Fong, A. J., Gerasimenko, Y., Zhong, H., Roy, R. R., & Edgerton, V. R. (2008). Facilitation of Stepping with Epidural Stimulation in Spinal Rats: Role of Sensory Input. *The Journal of Neuroscience*, *28*(31), 7774–7780. https://doi.org/10.1523/JNEUROSCI.1069-08.2008

Leal-Filho, M. (2011). Spinal cord injury: From inflammation to glial scar. *Surgical Neurology International*, *2*(1), 112. https://doi.org/10.4103/2152-7806.83732

Leblond, H., L'Espérance, M., Orsal, D., & Rossignol, S. (2003). Treadmill Locomotion in the Intact and Spinal Mouse. *The Journal of Neuroscience*, *23*(36), 11411–11419. https://doi.org/10.1523/JNEUROSCI.23-36-11411.2003

Leclech, C., & Villard, C. (2020). Cellular and Subcellular Contact Guidance on Microfabricated Substrates. *Frontiers in Bioengineering and Biotechnology*, *8*. https://doi.org/10.3389/fbioe.2020.551505

Lee, H. J., Malone, P. S., Chung, J., White, J. M., Wilson, N., Tidwell, J., & Tansey, K. E. (2019). Central Plasticity of Cutaneous Afferents Is Associated with Nociceptive Hyperreflexia after Spinal Cord Injury in Rats. *Neural Plasticity*, *2019*, 1–15. https://doi.org/10.1155/2019/6147878

Lee, H.-G., & Quintana, F. J. (2024). Astrocytes at the border of repair. *Nature Neuroscience*, *27*(8), 1445–1446. https://doi.org/10.1038/s41593-024-01670-y

Lee, J., Jung, H., Park, N., Park, S.-H., & Ju, J. H. (2019). Induced Osteogenesis in Plants Decellularized Scaffolds. *Scientific Reports*, *9*(1), 20194. https://doi.org/10.1038/s41598-019-56651-0

Lee, J. K., & Zheng, B. (2012). Role of myelin-associated inhibitors in axonal repair after spinal cord injury. *Experimental Neurology*, *235*(1), 33–42. https://doi.org/10.1016/j.expneurol.2011.05.001

Lee, K. Y., & Mooney, D. J. (2012). Alginate: Properties and biomedical applications. *Progress in Polymer Science*, *37*(1), 106–126. https://doi.org/10.1016/j.progpolymsci.2011.06.003

Lee, S., Choi, E., Cha, M.-J., & Hwang, K.-C. (2015). Cell Adhesion and Long-Term Survival of Transplanted Mesenchymal Stem Cells: A Prerequisite for Cell Therapy. *Oxidative Medicine and Cellular Longevity*, *2015*, 1–9. https://doi.org/10.1155/2015/632902

Lemieux, M., Karimi, N., & Bretzner, F. (2024). Functional plasticity of glutamatergic neurons of medullary reticular nuclei after spinal cord injury in mice. *Nature Communications*, *15*(1), 1542. https://doi.org/10.1038/s41467-024-45300-4

Li, J., Luo, W., Xiao, C., Zhao, J., Xiang, C., Liu, W., & Gu, R. (2023). Recent advances in endogenous neural stem/progenitor cell manipulation for spinal cord injury repair. *Theranostics*, *13*(12), 3966–3987. https://doi.org/10.7150/thno.84133

Li, S., & Stys, P. K. (2000a). Mechanisms of Ionotropic Glutamate Receptor-Mediated Excitotoxicity in Isolated Spinal Cord White Matter. *The Journal of Neuroscience*, *20*(3), 1190–1198. https://doi.org/10.1523/JNEUROSCI.20-03-01190.2000

Li, S., & Stys, P. K. (2000b). Mechanisms of Ionotropic Glutamate Receptor-Mediated Excitotoxicity in Isolated Spinal Cord White Matter. *The Journal of Neuroscience*, *20*(3), 1190–1198. https://doi.org/10.1523/JNEUROSCI.20-03-01190.2000

Li, W., Tang, Q. Y., Jadhav, A. D., Narang, A., Qian, W. X., Shi, P., & Pang, S. W. (2015). Large-scale Topographical Screen for Investigation of Physical Neural-Guidance Cues. *Scientific Reports*, *5*(1), 8644. https://doi.org/10.1038/srep08644

Li, X., Fan, C., Xiao, Z., Zhao, Y., Zhang, H., Sun, J., Zhuang, Y., Wu, X., Shi, J., Chen, Y., & Dai, J. (2018). A collagen microchannel scaffold carrying paclitaxel-liposomes induces neuronal differentiation of neural stem cells through Wnt/β-catenin signaling for spinal cord injury repair. *Biomaterials*, *183*, 114–127. https://doi.org/10.1016/j.biomaterials.2018.08.037

Li, X., Li, M., Tian, L., Chen, J., Liu, R., & Ning, B. (2020). Reactive Astrogliosis: Implications in Spinal Cord Injury Progression and Therapy. *Oxidative Medicine and Cellular Longevity*, *2020*, 1–14. https://doi.org/10.1155/2020/9494352

Li, X., Liu, D., Xiao, Z., Zhao, Y., Han, S., Chen, B., & Dai, J. (2019). Scaffold-facilitated locomotor improvement post complete spinal cord injury: Motor axon regeneration versus endogenous neuronal relay formation. *Biomaterials*, *197*, 20–31. https://doi.org/10.1016/j.biomaterials.2019.01.012

Li, X., Zhao, Y., Cheng, S., Han, S., Shu, M., Chen, B., Chen, X., Tang, F., Wang, N., Tu, Y., Wang, B., Xiao, Z., Zhang, S., & Dai, J. (2017). Cetuximab modified collagen scaffold directs neurogenesis of injury-activated endogenous neural stem cells for acute spinal cord injury repair. *Biomaterials*, *137*, 73–86. https://doi.org/10.1016/j.biomaterials.2017.05.027

Li, X.-Y., Wan, Y., Tang, S.-J., Guan, Y., Wei, F., & Ma, D. (2016). Maladaptive Plasticity and Neuropathic Pain. *Neural Plasticity*, *2016*, 1–2. https://doi.org/10.1155/2016/4842159

Lim, S. H., Liu, X. Y., Song, H., Yarema, K. J., & Mao, H.-Q. (2010). The effect of nanofiber-guided cell alignment on the preferential differentiation of neural stem cells. *Biomaterials*, *31*(34), 9031–9039. https://doi.org/10.1016/j.biomaterials.2010.08.021

Lin, S., Li, Y., Lucas-Osma, A. M., Hari, K., Stephens, M. J., Singla, R., Heckman, C. J., Zhang, Y., Fouad, K., Fenrich, K. K., & Bennett, D. J. (2019). Locomotor-related V3 interneurons initiate and coordinate muscles spasms after spinal cord injury. *Journal of Neurophysiology*, *121*(4), 1352–1367. https://doi.org/10.1152/jn.00776.2018

Liu, F., Xu, J., Wu, L., Zheng, T., Han, Q., Liang, Y., Zhang, L., Li, G., & Yang, Y. (2021). The Influence of the Surface Topographical Cues of Biomaterials on Nerve Cells in Peripheral Nerve Regeneration: A Review. *Stem Cells International*, *2021*, 1–13. https://doi.org/10.1155/2021/8124444

Liu, Q., Telezhkin, V., Jiang, W., Gu, Y., Wang, Y., Hong, W., Tian, W., Yarova, P., Zhang, G., Lee, S. M., Zhang, P., Zhao, M., Allen, N. D., Hirsch, E., Penninger, J., & Song, B. (2023). Electric field stimulation boosts neuronal differentiation of neural stem cells for spinal cord injury treatment via PI3K/Akt/GSK-3β/β-catenin activation. *Cell & Bioscience*, *13*(1), 4. https://doi.org/10.1186/s13578-023-00954-3

Liu, Q., Zhang, B., Liu, C., & Zhao, D. (2017). Molecular mechanisms underlying the positive role of treadmill training in locomotor recovery after spinal cord injury. *Spinal Cord*, *55*(5), 441–446. https://doi.org/10.1038/sc.2016.134

Liu, S., Xie, Y.-Y., & Wang, B. (2019). Role and prospects of regenerative biomaterials in the repair of spinal cord injury. *Neural Regeneration Research*, *14*(8), 1352. https://doi.org/10.4103/1673-5374.253512

Llorente, V., Velarde, P., Desco, M., & Gómez-Gaviro, M. V. (2022). Current Understanding of the Neural Stem Cell Niches. *Cells*, *11*(19), 3002. https://doi.org/10.3390/cells11193002

Loh, Q. L., & Choong, C. (2013). Three-Dimensional Scaffolds for Tissue Engineering Applications: Role of Porosity and Pore Size. *Tissue Engineering Part B: Reviews*, *19*(6), 485–502. https://doi.org/10.1089/ten.teb.2012.0437

Lorach, H., Galvez, A., Spagnolo, V., Martel, F., Karakas, S., Intering, N., Vat, M., Faivre, O., Harte, C., Komi, S., Ravier, J., Collin, T., Coquoz, L., Sakr, I., Baaklini, E., Hernandez-Charpak, S. D., Dumont, G., Buschman, R., Buse, N., … Courtine, G. (2023). Walking naturally after spinal cord injury using a brain–spine interface. *Nature*, *618*(7963), 126–133. https://doi.org/10.1038/s41586-023-06094-5

Lu, H. F., Lim, S.-X., Leong, M. F., Narayanan, K., Toh, R. P. K., Gao, S., & Wan, A. C. A. (2012). Efficient neuronal differentiation and maturation of human pluripotent stem cells encapsulated in 3D microfibrous scaffolds. *Biomaterials*, *33*(36), 9179–9187. https://doi.org/10.1016/j.biomaterials.2012.09.006

Lu, X., Perera, T. H., Aria, A. B., & Smith Callahan, L. A. (2018). Polyethylene glycol in spinal cord injury repair: a critical review. *Journal of Experimental Pharmacology*, *Volume 10*, 37–49. https://doi.org/10.2147/JEP.S148944

Luca, A. C., Mersch, S., Deenen, R., Schmidt, S., Messner, I., Schäfer, K.-L., Baldus, S. E., Huckenbeck, W., Piekorz, R. P., Knoefel, W. T., Krieg, A., & Stoecklein, N. H. (2013). Impact of the 3D Microenvironment on Phenotype, Gene Expression, and EGFR Inhibition of Colorectal Cancer Cell Lines. *PLoS ONE*, *8*(3), e59689. https://doi.org/10.1371/journal.pone.0059689

Luo, Y., Xue, F., Liu, K., Li, B., Fu, C., & Ding, J. (2021). Physical and biological engineering of polymer scaffolds to potentiate repair of spinal cord injury. *Materials & Design*, *201*, 109484. https://doi.org/10.1016/j.matdes.2021.109484

Ma, M., Basso, D. M., Walters, P., Stokes, B. T., & Jakeman, L. B. (2001). Behavioral and Histological Outcomes Following Graded Spinal Cord Contusion Injury in the C57Bl/6 Mouse. *Experimental Neurology*, *169*(2), 239–254. https://doi.org/10.1006/exnr.2001.7679

Macgregor, M., Williams, R., Downes, J., Bachhuka, A., & Vasilev, K. (2017). The Role of Controlled Surface Topography and Chemistry on Mouse Embryonic Stem Cell Attachment, Growth and Self-Renewal. *Materials (Basel, Switzerland)*, *10*(9). https://doi.org/10.3390/ma10091081

MacKay-Lyons, M. (2002). Central Pattern Generation of Locomotion: A Review of the Evidence. *Physical Therapy*, *82*(1), 69–83. https://doi.org/10.1093/ptj/82.1.69

Maegele, M., Lippert-Gruener, M., Ester-Bode, T., Garbe, J., Bouillon, B., Neugebauer, E., Klug, N., Lefering, R., Neiss, W. F., & Angelov, D. N. (2005). Multimodal early onset stimulation combined with enriched environment is associated with reduced CNS lesion volume and enhanced reversal of

neuromotor dysfunction after traumatic brain injury in rats. *European Journal of Neuroscience*, *21*(9), 2406–2418. https://doi.org/10.1111/j.1460-9568.2005.04070.x

Manira, A. El. (2009). Excitatory CPG Interneurons. In *Encyclopedia of Neuroscience* (pp. 1483–1486). Springer Berlin Heidelberg. https://doi.org/10.1007/978-3-540-29678-2_3194

Manouze, H., Ghestem, A., Poillerat, V., Bennis, M., Ba-M'hamed, S., Benoliel, J. J., Becker, C., & Bernard, C. (2019). Effects of Single Cage Housing on Stress, Cognitive, and Seizure Parameters in the Rat and Mouse Pilocarpine Models of Epilepsy. *Eneuro*, *6*(4), ENEURO.0179-18.2019. https://doi.org/10.1523/ENEURO.0179-18.2019

Marei, I., Abu Samaan, T., Al-Quradaghi, M. A., Farah, A. A., Mahmud, S. H., Ding, H., & Triggle, C. R. (2022). 3D Tissue-Engineered Vascular Drug Screening Platforms: Promise and Considerations. *Frontiers in Cardiovascular Medicine*, *9*. https://doi.org/10.3389/fcvm.2022.847554

Maxime Leblanc Latour. (2020). Plant-derived Cellulose Scaffolds for Bone Tissue Engineering. *BioRxiv*.

Mayer, W. P., & Akay, T. (2018). Stumbling corrective reaction elicited by mechanical and electrical stimulation of the saphenous nerve in walking mice. *Journal of Experimental Biology*. https://doi.org/10.1242/jeb.178095

Mazzaro, N., Grey, M. J., & Sinkjær, T. (2005). Contribution of Afferent Feedback to the Soleus Muscle Activity During Human Locomotion. *Journal of Neurophysiology*, *93*(1), 167–177. https://doi.org/10.1152/jn.00283.2004

McDonald, M. W., Hayward, K. S., Rosbergen, I. C. M., Jeffers, M. S., & Corbett, D. (2018). Is Environmental Enrichment Ready for Clinical Application in Human Post-stroke Rehabilitation? *Frontiers in Behavioral Neuroscience*, *12*. https://doi.org/10.3389/fnbeh.2018.00135

McKerracher, L., & Rosen, K. M. (2015). MAG, myelin and overcoming growth inhibition in the CNS. *Frontiers in Molecular Neuroscience*, *8*. https://doi.org/10.3389/fnmol.2015.00051

Meletis, K., Barnabé-Heider, F., Carlén, M., Evergren, E., Tomilin, N., Shupliakov, O., & Frisén, J. (2008). Spinal Cord Injury Reveals Multilineage Differentiation of Ependymal Cells. *PLoS Biology*, *6*(7), e182. https://doi.org/10.1371/journal.pbio.0060182

Merlet, A. N., Harnie, J., & Frigon, A. (2021). Inhibition and Facilitation of the Spinal Locomotor Central Pattern Generator and Reflex Circuits by Somatosensory Feedback From the Lumbar and Perineal Regions After Spinal Cord Injury. *Frontiers in Neuroscience*, *15*. https://doi.org/10.3389/fnins.2021.720542

Merlet, A. N., Harnie, J., Macovei, M., Doelman, A., Gaudreault, N., & Frigon, A. (2020). Mechanically stimulating the lumbar region inhibits locomotor-like activity and increases the gain of cutaneous reflexes from the paws in spinal cats. *Journal of Neurophysiology*, *123*(3), 1026–1041. https://doi.org/10.1152/jn.00747.2019

Meshkini, A., Ohadi, M. A. D., Mirghaderi, P., Mirzaei, F., Rafiei, E., Allahyari, N., Namvar, M., & Iranmehr, A. (2024). Combined treatment with Minocycline and methylprednisolone in acute traumatic spinal cord Injury: A pilot study. *Interdisciplinary Neurosurgery*, *36*, 101883. https://doi.org/10.1016/j.inat.2023.101883

Metavarayuth, K., Sitasuwan, P., Zhao, X., Lin, Y., & Wang, Q. (2016). Influence of Surface Topographical Cues on the Differentiation of Mesenchymal Stem Cells in Vitro. *ACS Biomaterials Science & Engineering*, *2*(2), 142–151. https://doi.org/10.1021/acsbiomaterials.5b00377

METZ, G. A. S., CURT, A., van de MEENT, H., KLUSMAN, I., SCHWAB, M. E., & DIETZ, V. (2000). Validation of the Weight-Drop Contusion Model in Rats: A Comparative Study of Human Spinal Cord Injury. *Journal of Neurotrauma*, *17*(1), 1–17. https://doi.org/10.1089/neu.2000.17.1

Modulevsky, D. J., Cuerrier, C. M., & Pelling, A. E. (2016). Biocompatibility of Subcutaneously Implanted Plant-Derived Cellulose Biomaterials. *PLOS ONE*, *11*(6), e0157894. https://doi.org/10.1371/journal.pone.0157894

Modulevsky, D. J., Lefebvre, C., Haase, K., Al-Rekabi, Z., & Pelling, A. E. (2014). Apple Derived Cellulose Scaffolds for 3D Mammalian Cell Culture. *PLoS ONE*, *9*(5), e97835. https://doi.org/10.1371/journal.pone.0097835

Mohammed, H., & Hollis, E. R. (2018). Cortical Reorganization of Sensorimotor Systems and the Role of Intracortical Circuits After Spinal Cord Injury. *Neurotherapeutics*, *15*(3), 588–603. https://doi.org/10.1007/s13311-018-0638-z

Moritz, C., Field-Fote, E. C., Tefertiller, C., van Nes, I., Trumbower, R., Kalsi-Ryan, S., Purcell, M., Janssen, T. W. J., Krassioukov, A., Morse, L. R., Zhao, K. D., Guest, J., Marino, R. J., Murray, L. M., Wecht, J. M., Rieger, M., Pradarelli, J., Turner, A., D'Amico, J., … Courtine, G. (2024). Non-invasive spinal cord electrical stimulation for arm and hand function in chronic tetraplegia: a safety and efficacy trial. *Nature Medicine*, *30*(5), 1276–1283. https://doi.org/10.1038/s41591-024-02940-9

Mothe, A. J., Tam, R. Y., Zahir, T., Tator, C. H., & Shoichet, M. S. (2013). Repair of the injured spinal cord by transplantation of neural stem cells in a hyaluronan-based hydrogel. *Biomaterials*, *34*(15), 3775–3783. https://doi.org/10.1016/j.biomaterials.2013.02.002

Muir, G. D., & Steeves, J. D. (1995). Phasic cutaneous input facilitates locomotor recovery after incomplete spinal injury in the chick. *Journal of Neurophysiology*, *74*(1), 358–368. https://doi.org/10.1152/jn.1995.74.1.358

Murray, Katherine C., et al. "Motoneuron Excitability and Muscle Spasms Are Regulated by 5-HT_{2B} and 5-HT_{2C} Receptor Activity." *Journal of Neurophysiology*, vol. 105, no. 2, Feb. 2011, pp. 731–48. *DOI.org (Crossref)*, https://doi.org/10.1152/jn.00774.2010.

Musienko, P. E., Bogacheva, I. N., & Gerasimenko, Yu. P. (2007). Significance of peripheral feedback in the generation of stepping movements during epidural stimulation of the spinal cord. *Neuroscience and Behavioral Physiology*, *37*(2), 181–190. https://doi.org/10.1007/s11055-007-0166-5

Nakagawa, H., Ninomiya, T., Yamashita, T., & Takada, M. (2015). Reorganization of corticospinal tract fibers after spinal cord injury in adult macaques. *Scientific Reports*, *5*(1), 11986. https://doi.org/10.1038/srep11986

Nandoe Tewarie, R. S., Hurtado, A., Bartels, R. H., Grotenhuis, A., & Oudega, M. (2009). Stem Cell-Based Therapies for Spinal Cord Injury. *The Journal of Spinal Cord Medicine*, *32*(2), 105–114. https://doi.org/10.1080/10790268.2009.11760761

Neves, L. T., Paz, L. V., Wieck, A., Mestriner, R. G., de Miranda Monteiro, V. A. C., & Xavier, L. L. (2023). Environmental Enrichment in Stroke Research: an Update. *Translational Stroke Research*. https://doi.org/10.1007/s12975-023-01132-w

Nguyen, L. H., Gao, M., Lin, J., Wu, W., Wang, J., & Chew, S. Y. (2017). Three-dimensional aligned nanofibers-hydrogel scaffold for controlled non-viral drug/gene delivery to direct axon regeneration in spinal cord injury treatment. *Scientific Reports*, *7*(1), 42212. https://doi.org/10.1038/srep42212

O'Bryant, A. J., Allred, R. P., Maldonado, M. A., Cormack, L. K., & Jones, T. A. (2011). Breeder and batch-dependent variability in the acquisition and performance of a motor skill in adult Long–Evans rats. *Behavioural Brain Research*, *224*(1), 112–120. https://doi.org/10.1016/j.bbr.2011.05.028

Okada, S., Hara, M., Kobayakawa, K., Matsumoto, Y., & Nakashima, Y. (2018). Astrocyte reactivity and astrogliosis after spinal cord injury. *Neuroscience Research*, *126*, 39–43. https://doi.org/10.1016/j.neures.2017.10.004

Oliver, K. M., Florez-Paz, D. M., Badea, T. C., Mentis, G. Z., Menon, V., & de Nooij, J. C. (2021). Molecular correlates of muscle spindle and Golgi tendon organ afferents. *Nature Communications*, *12*(1), 1451. https://doi.org/10.1038/s41467-021-21880-3

Onifer, S. M., Smith, G. M., & Fouad, K. (2011). Plasticity After Spinal Cord Injury: Relevance to Recovery and Approaches to Facilitate It. *Neurotherapeutics*, *8*(2), 283–293. https://doi.org/10.1007/s13311-011-0034-4

Oral, I., Guzel, H., & Ahmetli, G. (2011). Measuring the Young's modulus of polystyrene-based composites by tensile test and pulse-echo method. *Polymer Bulletin*, *67*(9), 1893–1906. https://doi.org/10.1007/s00289-011-0530-z

Orlovsky, G., Deliagina, T. G., & Grillner, S. (1999). *Neuronal Control of LocomotionFrom Mollusc to Man*. Oxford University Press. https://doi.org/10.1093/acprof:oso/9780198524052.001.0001

Ortiz-Álvarez, G., Daclin, M., Shihavuddin, A., Lansade, P., Fortoul, A., Faucourt, M., Clavreul, S., Lalioti, M.-E., Taraviras, S., Hippenmeyer, S., Livet, J., Meunier, A., Genovesio, A., & Spassky, N. (2019). Adult Neural Stem Cells and Multiciliated Ependymal Cells Share a Common Lineage Regulated by the Geminin Family Members. *Neuron*, *102*(1), 159-172.e7. https://doi.org/10.1016/j.neuron.2019.01.051

Pakulska, M. M., Tator, C. H., & Shoichet, M. S. (2017). Local delivery of chondroitinase ABC with or without stromal cell-derived factor 1α promotes functional repair in the injured rat spinal cord. *Biomaterials*, *134*. https://doi.org/10.1016/j.biomaterials.2017.04.016

Panter, S. S., Yum, S. W., & Faden, A. I. (1990). Alteration in extracellular amino acids after traumatic spinal cord injury. *Annals of Neurology*, *27*(1), 96–99. https://doi.org/10.1002/ana.410270115

Park, E., Velumian, A. A., & Fehlings, M. G. (2004). The Role of Excitotoxicity in Secondary Mechanisms of Spinal Cord Injury: A Review with an Emphasis on the Implications for White Matter Degeneration. *Journal of Neurotrauma*, *21*(6), 754–774. https://doi.org/10.1089/0897715041269641

Park, H., Latash, E. M., Molkov, Y. I., Klishko, A. N., Frigon, A., DeWeerth, S. P., & Prilutsky, B. I. (2019). Cutaneous sensory feedback from paw pads affects lateral balance control during split-belt locomotion in the cat. *Journal of Experimental Biology*. https://doi.org/10.1242/jeb.198648

Pawar, K., Cummings, B. J., Thomas, A., Shea, L. D., Levine, A., Pfaff, S., & Anderson, A. J. (2015). Biomaterial bridges enable regeneration and re-entry of corticospinal tract axons into the caudal spinal cord after SCI: Association with recovery of forelimb function. *Biomaterials*, *65*, 1–12. https://doi.org/10.1016/j.biomaterials.2015.05.032

Pearson, K. G. (2004). *Generating the walking gait: role of sensory feedback* (pp. 123–129). https://doi.org/10.1016/S0079-6123(03)43012-4

Pearson, K. G., & Collins, D. F. (1993). Reversal of the influence of group Ib afferents from plantaris on activity in medial gastrocnemius muscle during locomotor activity. *Journal of Neurophysiology*, *70*(3), 1009–1017. https://doi.org/10.1152/jn.1993.70.3.1009

Peng, W., Li, D., Dai, K., Wang, Y., Song, P., Li, H., Tang, P., Zhang, Z., Li, Z., Zhou, Y., & Zhou, C. (2022). Recent progress of collagen, chitosan, alginate and other hydrogels in skin repair and wound dressing applications. *International Journal of Biological Macromolecules*, *208*, 400–408. https://doi.org/10.1016/j.ijbiomac.2022.03.002

Perez-Gianmarco, L., & Kukley, M. (2023). Understanding the Role of the Glial Scar through the Depletion of Glial Cells after Spinal Cord Injury. *Cells*, *12*(14), 1842. https://doi.org/10.3390/cells12141842

Pestana, F., Edwards-Faret, G., Belgard, T. G., Martirosyan, A., & Holt, M. G. (2020). No Longer Underappreciated: The Emerging Concept of Astrocyte Heterogeneity in Neuroscience. *Brain Sciences*, *10*(3), 168. https://doi.org/10.3390/brainsci10030168

Phan, N. V., Wright, T., Rahman, M. M., Xu, J., & Coburn, J. M. (2020). In Vitro Biocompatibility of Decellularized Cultured Plant Cell-Derived Matrices. *ACS Biomaterials Science & Engineering*, *6*(2), 822–832. https://doi.org/10.1021/acsbiomaterials.9b00870

Popovich, P. G., Guan, Z., Wei, P., Huitinga, I., van Rooijen, N., & Stokes, B. T. (1999). Depletion of Hematogenous Macrophages Promotes Partial Hindlimb Recovery and Neuroanatomical Repair after Experimental Spinal Cord Injury. *Experimental Neurology*, *158*(2), 351–365. https://doi.org/10.1006/exnr.1999.7118

Proske, U., & Gandevia, S. C. (2012). The Proprioceptive Senses: Their Roles in Signaling Body Shape, Body Position and Movement, and Muscle Force. *Physiological Reviews*, *92*(4), 1651–1697. https://doi.org/10.1152/physrev.00048.2011

Prüss, H., Tedeschi, A., Thiriot, A., Lynch, L., Loughhead, S. M., Stutte, S., Mazo, I. B., Kopp, M. A., Brommer, B., Blex, C., Geurtz, L.-C., Liebscher, T., Niedeggen, A., Dirnagl, U., Bradke, F., Volz, M. S., DeVivo, M. J., Chen, Y., von Andrian, U. H., & Schwab, J. M. (2017). Spinal cord injury-induced immunodeficiency is mediated by a sympathetic-neuroendocrine adrenal reflex. *Nature Neuroscience*, *20*(11), 1549–1559. https://doi.org/10.1038/nn.4643

Qian, C., & Zhou, F.-Q. (2020). Updates and challenges of axon regeneration in the mammalian central nervous system. *Journal of Molecular Cell Biology*, *12*(10), 798–806. https://doi.org/10.1093/jmcb/mjaa026

Quadri, S. A., Farooqui, M., Ikram, A., Zafar, A., Khan, M. A., Suriya, S. S., Claus, C. F., Fiani, B., Rahman, M., Ramachandran, A., Armstrong, I. I. T., Taqi, M. A., & Mortazavi, M. M. (2020). Recent update on basic mechanisms of spinal cord injury. *Neurosurgical Review*, *43*(2), 425–441. https://doi.org/10.1007/s10143-018-1008-3

Quraishe, S., Forbes, L. H., & Andrews, M. R. (2018). The Extracellular Environment of the CNS: Influence on Plasticity, Sprouting, and Axonal Regeneration after Spinal Cord Injury. *Neural Plasticity*, *2018*, 1–18. https://doi.org/10.1155/2018/2952386

Rammensee, S., Kang, M. S., Georgiou, K., Kumar, S., & Schaffer, D. V. (2017). Dynamics of Mechanosensitive Neural Stem Cell Differentiation. *Stem Cells*, *35*(2), 497–506. https://doi.org/10.1002/stem.2489

Rank, M. M., Murray, K. C., Stephens, M. J., D'Amico, J., Gorassini, M. A., & Bennett, D. J. (2011). Adrenergic Receptors Modulate Motoneuron Excitability, Sensory Synaptic Transmission and Muscle Spasms After Chronic Spinal Cord Injury. *Journal of Neurophysiology*, *105*(1), 410–422. https://doi.org/10.1152/jn.00775.2010

Rasoulianboroujeni, M., Kiaie, N., Tabatabaei, F. S., Yadegari, A., Fahimipour, F., Khoshroo, K., & Tayebi, L. (2018). Dual Porosity Protein-based Scaffolds with Enhanced Cell Infiltration and Proliferation. *Scientific Reports*, *8*(1), 14889. https://doi.org/10.1038/s41598-018-33245-w

Ratuski, A. S., Améndola, L., Makowska, I. J., & Weary, D. M. (2024). Effects of temporary access to environmental enrichment on measures of laboratory mouse welfare. *Scientific Reports*, *14*(1), 15143. https://doi.org/10.1038/s41598-024-65480-9

Reiner, A., Veenman, C. L., Medina, L., Jiao, Y., Del Mar, N., & Honig, M. G. (2000). Pathway tracing using biotinylated dextran amines. *Journal of Neuroscience Methods*, *103*(1), 23–37. https://doi.org/10.1016/S0165-0270(00)00293-4

Rekling, J. C., Funk, G. D., Bayliss, D. A., Dong, X.-W., & Feldman, J. L. (2000). Synaptic Control of Motoneuronal Excitability. *Physiological Reviews*, *80*(2), 767–852. https://doi.org/10.1152/physrev.2000.80.2.767

Ren, Y.-J., Zhang, H., Huang, H., Wang, X.-M., Zhou, Z.-Y., Cui, F.-Z., & An, Y.-H. (2009). In vitro behavior of neural stem cells in response to different chemical functional groups. *Biomaterials*, *30*(6), 1036–1044. https://doi.org/10.1016/j.biomaterials.2008.10.028

Rivlin, A. S., & Tator, C. H. (1977). Objective clinical assessment of motor function after experimental spinal cord injury in the rat. *Journal of Neurosurgery*, *47*(4), 577–581. https://doi.org/10.3171/jns.1977.47.4.0577

Robbins, E. R., Pins, G. D., Laflamme, M. A., & Gaudette, G. R. (2020). Creation of a contractile biomaterial from a decellularized spinach leaf without <scp>ECM</scp> protein coating: An in vitro study. *Journal of Biomedical Materials Research Part A*, *108*(10), 2123–2132. https://doi.org/10.1002/jbm.a.36971

Roberts, I. V., Bukhary, D., Valdivieso, C. Y. L., & Tirelli, N. (2020). Fibrin Matrices as (Injectable) Biomaterials: Formation, Clinical Use, and Molecular Engineering. *Macromolecular Bioscience*, *20*(1). https://doi.org/10.1002/mabi.201900283

Rodríguez-Barrera, R., Rivas-González, M., García-Sánchez, J., Mojica-Torres, D., & Ibarra, A. (2021). Neurogenesis after Spinal Cord Injury: State of the Art. *Cells*, *10*(6), 1499. https://doi.org/10.3390/cells10061499

Rodriguez-Jimenez, F. J., Jendelova, P., & Erceg, S. (2023). The activation of dormant ependymal cells following spinal cord injury. *Stem Cell Research & Therapy*, *14*(1), 175. https://doi.org/10.1186/s13287-023-03395-4

Rosenzweig, E. S., Brock, J. H., Culbertson, M. D., Lu, P., Moseanko, R., Edgerton, V. R., Havton, L. A., & Tuszynski, M. H. (2009). Extensive spinal decussation and bilateral termination of cervical corticospinal projections in rhesus monkeys. *Journal of Comparative Neurology*, *513*(2), 151–163. https://doi.org/10.1002/cne.21940

Rosenzweig, E. S., Courtine, G., Jindrich, D. L., Brock, J. H., Ferguson, A. R., Strand, S. C., Nout, Y. S., Roy, R. R., Miller, D. M., Beattie, M. S., Havton, L. A., Bresnahan, J. C., Edgerton, V. R., & Tuszynski, M. H. (2010). Extensive spontaneous plasticity of corticospinal projections after primate spinal cord injury. *Nature Neuroscience*, *13*(12), 1505–1510. https://doi.org/10.1038/nn.2691

Rossi, C., Angelucci, A., Costantin, L., Braschi, C., Mazzantini, M., Babbini, F., Fabbri, M. E., Tessarollo, L., Maffei, L., Berardi, N., & Caleo, M. (2006). Brain-derived neurotrophic factor (BDNF) is required for the enhancement of hippocampal neurogenesis following environmental enrichment. *European Journal of Neuroscience*, *24*(7), 1850–1856. https://doi.org/10.1111/j.1460-9568.2006.05059.x

Rossignol, S., Dubuc, R., & Gossard, J.-P. (2006). Dynamic Sensorimotor Interactions in Locomotion. *Physiological Reviews*, *86*(1), 89–154. https://doi.org/10.1152/physrev.00028.2005

Rossignol, S., & Frigon, A. (2011). Recovery of Locomotion After Spinal Cord Injury: Some Facts and Mechanisms. *Annual Review of Neuroscience*, *34*(1), 413–440. https://doi.org/10.1146/annurev-neuro-061010-113746

Rossignol, S., Martinez, M., Escalona, M., Kundu, A., Delivet-Mongrain, H., Alluin, O., & Gossard, J.-P. (2015). *The "beneficial" effects of locomotor training after various types of spinal lesions in cats and rats* (pp. 173–198). https://doi.org/10.1016/bs.pbr.2014.12.009

Rowald, A., Komi, S., Demesmaeker, R., Baaklini, E., Hernandez-Charpak, S. D., Paoles, E., Montanaro, H., Cassara, A., Becce, F., Lloyd, B., Newton, T., Ravier, J., Kinany, N., D'Ercole, M., Paley, A., Hankov, N., Varescon, C., McCracken, L., Vat, M., … Courtine, G. (2022). Activity-dependent spinal cord neuromodulation rapidly restores trunk and leg motor functions after complete paralysis. *Nature Medicine*, *28*(2), 260–271. https://doi.org/10.1038/s41591-021-01663-5

Rudge, J., & Silver, J. (1990). Inhibition of neurite outgrowth on astroglial scars in vitro. *The Journal of Neuroscience*, *10*(11), 3594–3603. https://doi.org/10.1523/JNEUROSCI.10-11-03594.1990

Rust, R., & Kaiser, J. (2017). Insights into the Dual Role of Inflammation after Spinal Cord Injury. *The Journal of Neuroscience*, *37*(18), 4658–4660. https://doi.org/10.1523/JNEUROSCI.0498-17.2017

Rybak, I. A., Stecina, K., Shevtsova, N. A., & McCrea, D. A. (2006). Modelling spinal circuitry involved in locomotor pattern generation: insights from the effects of afferent stimulation. *The Journal of Physiology*, *577*(2), 641–658. https://doi.org/10.1113/jphysiol.2006.118711

Saha, K., Keung, A. J., Irwin, E. F., Li, Y., Little, L., Schaffer, D. V., & Healy, K. E. (2008). Substrate Modulus Directs Neural Stem Cell Behavior. *Biophysical Journal*, *95*(9), 4426–4438. https://doi.org/10.1529/biophysj.108.132217

Saleeba, C., Dempsey, B., Le, S., Goodchild, A., & McMullan, S. (2019). A Student's Guide to Neural Circuit Tracing. *Frontiers in Neuroscience*, *13*. https://doi.org/10.3389/fnins.2019.00897

Salehi, A., Mobarhan, M. A., Mohammadi, J., Shahsavarani, H., Shokrgozar, M. A., & Alipour, A. (2020). Efficient mineralization and osteogenic gene overexpression of mesenchymal stem cells on decellularized spinach leaf scaffold. *Gene*, *757*, 144852. https://doi.org/10.1016/j.gene.2020.144852

Santuz, A., Laflamme, O. D., & Akay, T. (2022). The brain integrates proprioceptive information to ensure robust locomotion. *The Journal of Physiology*, *600*(24), 5267–5294. https://doi.org/10.1113/JP283181

Sarker, M. D., Naghieh, S., McInnes, A. D., Schreyer, D. J., & Chen, X. (2018). Regeneration of peripheral nerves by nerve guidance conduits: Influence of design, biopolymers, cells, growth factors, and physical stimuli. *Progress in Neurobiology*, *171*, 125–150. https://doi.org/10.1016/j.pneurobio.2018.07.002

Sartori, A. M., Hofer, A.-S., & Schwab, M. E. (2020). Recovery after spinal cord injury is enhanced by anti-Nogo-A antibody therapy — from animal models to clinical trials. *Current Opinion in Physiology*, *14*, 1–6. https://doi.org/10.1016/j.cophys.2019.11.001

Sasaki, M., Lankford, K. L., Zemedkun, M., & Kocsis, J. D. (2004). Identified Olfactory Ensheathing Cells Transplanted into the Transected Dorsal Funiculus Bridge the Lesion and Form Myelin. *The Journal of Neuroscience*, *24*(39), 8485–8493. https://doi.org/10.1523/JNEUROSCI.1998-04.2004

Saur, L., Baptista, P. P. A., de Senna, P. N., Paim, M. F., Nascimento, P. do, Ilha, J., Bagatini, P. B., Achaval, M., & Xavier, L. L. (2014). Physical exercise increases GFAP expression and induces morphological changes in hippocampal astrocytes. *Brain Structure and Function*, *219*(1), 293–302. https://doi.org/10.1007/s00429-012-0500-8

Schachtrup, C., Ryu, J. K., Helmrick, M. J., Vagena, E., Galanakis, D. K., Degen, J. L., Margolis, R. U., & Akassoglou, K. (2010). Fibrinogen Triggers Astrocyte Scar Formation by Promoting the Availability of Active TGF-β after Vascular Damage. *The Journal of Neuroscience*, *30*(17), 5843–5854. https://doi.org/10.1523/JNEUROSCI.0137-10.2010

Schackel, T., Kumar, P., Günther, M., Liu, S., Brunner, M., Sandner, B., Puttagunta, R., Müller, R., Weidner, N., & Blesch, A. (2019). Peptides and Astroglia Improve the Regenerative Capacity of Alginate Gels in the Injured Spinal Cord. *Tissue Engineering Part A*, *25*(7–8), 522–537. https://doi.org/10.1089/ten.tea.2018.0082

Schanne, F. A. X., Kane, A. B., Young, E. E., & Farber, J. L. (1979). Calcium Dependence of Toxic Cell Death: A Final Common Pathway. *Science*, *206*(4419), 700–702. https://doi.org/10.1126/science.386513

Schieber, M. H. (2007). *Chapter 2 Comparative anatomy and physiology of the corticospinal system* (pp. 15–37). https://doi.org/10.1016/S0072-9752(07)80005-4

Schober, A. L., Wicki-Stordeur, L. E., Murai, K. K., & Swayne, L. A. (2022). Foundations and implications of astrocyte heterogeneity during brain development and disease. *Trends in Neurosciences*, *45*(9), 692–703. https://doi.org/10.1016/j.tins.2022.06.009

Schwab, J. M., Haider, C., Kopp, M. A., Zrzavy, T., Endmayr, V., Ricken, G., Kubista, H., Haider, T., Liebscher, T., Lübstorf, T., Blex, C., Serdani-Neuhaus, L., Curt, A., Cinelli, P., Scivoletto, G., Fehlings, M. G., May, C., Guntermann, A., Marcus, K., … Höftberger, R. (2023). Lesional Antibody Synthesis and Complement Deposition Associate With De Novo Antineuronal Antibody Synthesis After Spinal Cord Injury. *Neurology Neuroimmunology & Neuroinflammation*, *10*(3). https://doi.org/10.1212/NXI.0000000000200099

Sekhon, L. H. S., & Fehlings, M. G. (2001). Epidemiology, Demographics, and Pathophysiology of Acute Spinal Cord Injury. *Spine*, *26*(Supplement), S2–S12. https://doi.org/10.1097/00007632-200112151-00002

Serradj, N., Agger, S. F., & Hollis, E. R. (2017). Corticospinal circuit plasticity in motor rehabilitation from spinal cord injury. *Neuroscience Letters*, *652*, 94–104. https://doi.org/10.1016/j.neulet.2016.12.003

Setien, M. B., Smith, K. R., Howard, K., Williams, K., Suhr, S. T., & Purcell, E. K. (2020). Differentiation and characterization of neurons derived from rat iPSCs. *Journal of Neuroscience Methods*, *338*, 108693. https://doi.org/10.1016/j.jneumeth.2020.108693

Shah, P. K., Garcia-Alias, G., Choe, J., Gad, P., Gerasimenko, Y., Tillakaratne, N., Zhong, H., Roy, R. R., & Edgerton, V. R. (2013). Use of quadrupedal step training to re-engage spinal interneuronal networks and improve locomotor function after spinal cord injury. *Brain : A Journal of Neurology*, *136*(Pt 11), 3362–3377. https://doi.org/10.1093/brain/awt265

Shahriari, D., Koffler, J. Y., Tuszynski, M. H., Campana, W. M., & Sakamoto, J. S. (2017). Hierarchically Ordered Porous and High-Volume Polycaprolactone Microchannel Scaffolds Enhanced Axon Growth in Transected Spinal Cords. *Tissue Engineering Part A*, *23*(9–10), 415–425. https://doi.org/10.1089/ten.tea.2016.0378

Sharif-Alhoseini, M., Khormali, M., Rezaei, M., Safdarian, M., Hajighadery, A., Khalatbari, M. M., Safdarian, M., Meknatkhah, S., Rezvan, M., Chalangari, M., Derakhshan, P., & Rahimi-Movaghar, V. (2017). Animal models of spinal cord injury: a systematic review. *Spinal Cord*, *55*(8), 714–721. https://doi.org/10.1038/sc.2016.187

Sharifi, A., Zandieh, A., Behroozi, Z., Hamblin, M. R., Mayahi, S., Yousefifard, M., & Ramezani, F. (2022). Sustained delivery of chABC improves functional recovery after a spine injury. *BMC Neuroscience*, *23*(1), 60. https://doi.org/10.1186/s12868-022-00734-8

Sharma, K., Selzer, M. E., & Li, S. (2012). Scar-mediated inhibition and CSPG receptors in the CNS. *Experimental Neurology*, *237*(2), 370–378. https://doi.org/10.1016/j.expneurol.2012.07.009

Sheets, K. T., Ewend, M. G., Mohiti-Asli, M., Tuin, S. A., Loboa, E. G., Aboody, K. S., & Hingtgen, S. D. (2020). Developing Implantable Scaffolds to Enhance Neural Stem Cell Therapy for Post-

Operative Glioblastoma. *Molecular Therapy*, *28*(4), 1056–1067. https://doi.org/10.1016/j.ymthe.2020.02.008
Shen, H., Fan, C., You, Z., Xiao, Z., Zhao, Y., & Dai, J. (2022). Advances in Biomaterial-Based Spinal Cord Injury Repair. *Advanced Functional Materials*, *32*(13). https://doi.org/10.1002/adfm.202110628
Shibata, T., Tashiro, S., Shinozaki, M., Hashimoto, S., Matsumoto, M., Nakamura, M., Okano, H., & Nagoshi, N. (2021). Treadmill training based on the overload principle promotes locomotor recovery in a mouse model of chronic spinal cord injury. *Experimental Neurology*, *345*, 113834. https://doi.org/10.1016/j.expneurol.2021.113834
Siegel, C. S., Fink, K. L., Strittmatter, S. M., & Cafferty, W. B. J. (2015). Plasticity of Intact Rubral Projections Mediates Spontaneous Recovery of Function after Corticospinal Tract Injury. *The Journal of Neuroscience*, *35*(4), 1443–1457. https://doi.org/10.1523/JNEUROSCI.3713-14.2015
Singh, A. V., Raymond, M., Pace, F., Certo, A., Zuidema, J. M., McKay, C. A., Gilbert, R. J., Lu, X. L., & Wan, L. Q. (2015). Astrocytes Increase ATP Exocytosis Mediated Calcium Signaling in Response to Microgroove Structures. *Scientific Reports*, *5*(1), 7847. https://doi.org/10.1038/srep07847
Sitoci-Ficici, K. H., Matyash, M., Uckermann, O., Galli, R., Leipnitz, E., Later, R., Ikonomidou, C., Gelinsky, M., Schackert, G., & Kirsch, M. (2018). Non-functionalized soft alginate hydrogel promotes locomotor recovery after spinal cord injury in a rat hemimyelonectomy model. *Acta Neurochirurgica*, *160*(3), 449–457. https://doi.org/10.1007/s00701-017-3389-4
Sławińska, U., Majczyński, H., Dai, Y., & Jordan, L. M. (2012). The upright posture improves plantar stepping and alters responses to serotonergic drugs in spinal rats. *The Journal of Physiology*, *590*(7), 1721–1736. https://doi.org/10.1113/jphysiol.2011.224931
Slotkin, J. R., Pritchard, C. D., Luque, B., Ye, J., Layer, R. T., Lawrence, M. S., O'Shea, T. M., Roy, R. R., Zhong, H., Vollenweider, I., Edgerton, V. R., Courtine, G., Woodard, E. J., & Langer, R. (2017). Biodegradable scaffolds promote tissue remodeling and functional improvement in non-human primates with acute spinal cord injury. *Biomaterials*, *123*, 63–76. https://doi.org/10.1016/j.biomaterials.2017.01.024
Smith, R. R., Burke, D. A., Baldini, A. D., Shum-Siu, A., Baltzley, R., Bunger, M., & Magnuson, D. S. K. (2006). The Louisville Swim Scale: A Novel Assessment of Hindlimb Function following Spinal Cord Injury in Adult Rats. *Journal of Neurotrauma*, *23*(11), 1654–1670. https://doi.org/10.1089/neu.2006.23.1654
Smith, R. R., Shum-Siu, A., Baltzley, R., Bunger, M., Baldini, A., Burke, D. A., & Magnuson, D. S. K. (2006a). Effects of Swimming on Functional Recovery after Incomplete Spinal Cord Injury in Rats. *Journal of Neurotrauma*, *23*(6), 908–919. https://doi.org/10.1089/neu.2006.23.908
Smith, R. R., Shum-Siu, A., Baltzley, R., Bunger, M., Baldini, A., Burke, D. A., & Magnuson, D. S. K. (2006b). Effects of swimming on functional recovery after incomplete spinal cord injury in rats. *Journal of Neurotrauma*, *23*(6), 908–919. https://doi.org/10.1089/neu.2006.23.908
Sofroniew, M. V. (2009). Molecular dissection of reactive astrogliosis and glial scar formation. *Trends in Neurosciences*, *32*(12), 638–647. https://doi.org/10.1016/j.tins.2009.08.002
Sofroniew, M. V. (2015). Astrocyte barriers to neurotoxic inflammation. *Nature Reviews Neuroscience*, *16*(5), 249–263. https://doi.org/10.1038/nrn3898
Squair, J. W., Milano, M., de Coucy, A., Gautier, M., Skinnider, M. A., James, N. D., Cho, N., Lasne, A., Kathe, C., Hutson, T. H., Ceto, S., Baud, L., Galan, K., Aureli, V., Laskaratos, A., Barraud, Q., Deming, T. J., Kohman, R. E., Schneider, B. L., … Anderson, M. A. (2023). Recovery of walking

after paralysis by regenerating characterized neurons to their natural target region. *Science*, *381*(6664), 1338–1345. https://doi.org/10.1126/science.adi6412

Starkey, M. L., Bleul, C., Kasper, H., Mosberger, A. C., Zörner, B., Giger, S., Gullo, M., Buschmann, F., & Schwab, M. E. (2014). High-Impact, Self-Motivated Training Within an Enriched Environment With Single Animal Tracking Dose-Dependently Promotes Motor Skill Acquisition and Functional Recovery. *Neurorehabilitation and Neural Repair*, *28*(6), 594–605. https://doi.org/10.1177/1545968314520721

Sterner, R. C., & Sterner, R. M. (2023). Immune response following traumatic spinal cord injury: Pathophysiology and therapies. *Frontiers in Immunology*, *13*. https://doi.org/10.3389/fimmu.2022.1084101

Straley, K. S., Foo, C. W. P., & Heilshorn, S. C. (2010). Biomaterial Design Strategies for the Treatment of Spinal Cord Injuries. *Journal of Neurotrauma*, *27*(1), 1–19. https://doi.org/10.1089/neu.2009.0948

Subramony, S. D., Dargis, B. R., Castillo, M., Azeloglu, E. U., Tracey, M. S., Su, A., & Lu, H. H. (2013). The guidance of stem cell differentiation by substrate alignment and mechanical stimulation. *Biomaterials*, *34*(8), 1942–1953. https://doi.org/10.1016/j.biomaterials.2012.11.012

Sugai, K., Nishimura, S., Kato-Negishi, M., Onoe, H., Iwanaga, S., Toyama, Y., Matsumoto, M., Takeuchi, S., Okano, H., & Nakamura, M. (2015). Neural stem/progenitor cell-laden microfibers promote transplant survival in a mouse transected spinal cord injury model. *Journal of Neuroscience Research*, *93*(12), 1826–1838. https://doi.org/10.1002/jnr.23636

Sun, Y., Yang, C., Zhu, X., Wang, J., Liu, X., Yang, X., An, X., Liang, J., Dong, H., Jiang, W., Chen, C., Wang, Z., Sun, H., Tu, Y., Zhang, S., Chen, F., & Li, X. (2019). 3D printing collagen/chitosan scaffold ameliorated axon regeneration and neurological recovery after spinal cord injury. *Journal of Biomedical Materials Research Part A*, *107*(9), 1898–1908. https://doi.org/10.1002/jbm.a.36675

Tai, W. L., Sun, L., Li, H., Gu, P., Joosten, E. A., & Cheung, C. W. (2021). Additive Effects of Environmental Enrichment and Ketamine on Neuropathic Pain Relief by Reducing Glutamatergic Activation in Spinal Cord Injury in Rats. *Frontiers in Neuroscience*, *15*. https://doi.org/10.3389/fnins.2021.635187

Takeoka, A. (2020). Proprioception: Bottom-up directive for motor recovery after spinal cord injury. *Neuroscience Research*, *154*, 1–8. https://doi.org/10.1016/j.neures.2019.07.005

Takeoka, A., & Arber, S. (2019). Functional Local Proprioceptive Feedback Circuits Initiate and Maintain Locomotor Recovery after Spinal Cord Injury. *Cell Reports*, *27*(1), 71-85.e3. https://doi.org/10.1016/j.celrep.2019.03.010

Takeoka, A., Vollenweider, I., Courtine, G., & Arber, S. (2014). Muscle Spindle Feedback Directs Locomotor Recovery and Circuit Reorganization after Spinal Cord Injury. *Cell*, *159*(7), 1626–1639. https://doi.org/10.1016/j.cell.2014.11.019

Tamura, A., Lee, D. H., Arisaka, Y., Kang, T. W., & Yui, N. (2022). Post-Cross-Linking of Collagen Hydrogels by Carboxymethylated Polyrotaxanes for Simultaneously Improving Mechanical Strength and Cell Proliferation. *ACS Biomaterials Science & Engineering*, *8*(2), 588–597. https://doi.org/10.1021/acsbiomaterials.1c01521

Tang, Q., Xue, H., Zhang, Q., Guo, Y., Xu, H., Liu, Y., & Liu, J. (2021). *Evaluation of the clinical efficacy of stem cell transplantation in the treatment of spinal cord injury: systematic review and meta-analysis*. https://doi.org/10.37766/inplasy2021.4.0034

Tang, Y., Yu, P., & Cheng, L. (2017). Current progress in the derivation and therapeutic application of neural stem cells. *Cell Death & Disease*, *8*(10), e3108–e3108. https://doi.org/10.1038/cddis.2017.504

Tazerart, S., Viemari, J.-C., Darbon, P., Vinay, L., & Brocard, F. (2007). Contribution of Persistent Sodium Current to Locomotor Pattern Generation in Neonatal Rats. *Journal of Neurophysiology*, *98*(2), 613–628. https://doi.org/10.1152/jn.00316.2007

Tejeda, G., Ciciriello, A. J., & Dumont, C. M. (2022). Biomaterial Strategies to Bolster Neural Stem Cell-Mediated Repair of the Central Nervous System. *Cells Tissues Organs*, *211*(6), 655–669. https://doi.org/10.1159/000515351

Temple, J., Velliou, E., Shehata, M., Lévy, R., & Gupta, P. (2022). Current strategies with implementation of three-dimensional cell culture: the challenge of quantification. *Interface Focus*, *12*(5). https://doi.org/10.1098/rsfs.2022.0019

Thompson, R. E., Pardieck, J., Smith, L., Kenny, P., Crawford, L., Shoichet, M., & Sakiyama-Elbert, S. (2018). Effect of hyaluronic acid hydrogels containing astrocyte-derived extracellular matrix and/or V2a interneurons on histologic outcomes following spinal cord injury. *Biomaterials*, *162*, 208–223. https://doi.org/10.1016/j.biomaterials.2018.02.013

Toker, M., Rostami, S., Kesici, M., Gul, O., Kocaturk, O., Odabas, S., & Garipcan, B. (2020a). Decellularization and characterization of leek: a potential cellulose-based biomaterial. *Cellulose*, *27*(13), 7331–7348. https://doi.org/10.1007/s10570-020-03278-4

Toker, M., Rostami, S., Kesici, M., Gul, O., Kocaturk, O., Odabas, S., & Garipcan, B. (2020b). Decellularization and characterization of leek: a potential cellulose-based biomaterial. *Cellulose*, *27*(13), 7331–7348. https://doi.org/10.1007/s10570-020-03278-4

Toker-Bayraktar, M., Erenay, B., Altun, B., Odabaş, S., & Garipcan, B. (2023). Plant-derived biomaterials and scaffolds. *Cellulose*, *30*(5), 2731–2751. https://doi.org/10.1007/s10570-023-05078-y

Tsai, E. C., Dalton, P. D., Shoichet, M. S., & Tator, C. H. (2004). Synthetic Hydrogel Guidance Channels Facilitate Regeneration of Adult Rat Brainstem Motor Axons after Complete Spinal Cord Transection. *Journal of Neurotrauma*, *21*(6), 789–804. https://doi.org/10.1089/0897715041269687

Tsintou, M., Dalamagkas, K., & Seifalian, A. (2015). Advances in regenerative therapies for spinal cord injury: a biomaterials approach. *Neural Regeneration Research*, *10*(5), 726. https://doi.org/10.4103/1673-5374.156966

Tysseling-Mattiace, V. M., Sahni, V., Niece, K. L., Birch, D., Czeisler, C., Fehlings, M. G., Stupp, S. I., & Kessler, J. A. (2008). Self-Assembling Nanofibers Inhibit Glial Scar Formation and Promote Axon Elongation after Spinal Cord Injury. *The Journal of Neuroscience*, *28*(14), 3814–3823. https://doi.org/10.1523/JNEUROSCI.0143-08.2008

Ueno, M., Nakamura, Y., Li, J., Gu, Z., Niehaus, J., Maezawa, M., Crone, S. A., Goulding, M., Baccei, M. L., & Yoshida, Y. (2018). Corticospinal Circuits from the Sensory and Motor Cortices Differentially Regulate Skilled Movements through Distinct Spinal Interneurons. *Cell Reports*, *23*(5), 1286-1300.e7. https://doi.org/10.1016/j.celrep.2018.03.137

Urdzíková, L., Růžička, J., LaBagnara, M., Kárová, K., Kubinová, Š., Jiráková, K., Murali, R., Syková, E., Jhanwar-Uniyal, M., & Jendelová, P. (2014). Human Mesenchymal Stem Cells Modulate Inflammatory Cytokines after Spinal Cord Injury in Rat. *International Journal of Molecular Sciences*, *15*(7), 11275–11293. https://doi.org/10.3390/ijms150711275

Vagaska, B., Gillham, O., & Ferretti, P. (2020). Modelling human CNS injury with human neural stem cells in 2- and 3-Dimensional cultures. *Scientific Reports*, *10*(1), 6785. https://doi.org/10.1038/s41598-020-62906-y

Valbuena Valecillos, A. D., Gater, D. R., & Alvarez, G. (2022). Concomitant Brain Injury and Spinal Cord Injury Management Strategies: A Narrative Review. *Journal of Personalized Medicine*, *12*(7), 1108. https://doi.org/10.3390/jpm12071108

van Niekerk, E. A., Tuszynski, M. H., Lu, P., & Dulin, J. N. (2016). Molecular and Cellular Mechanisms of Axonal Regeneration After Spinal Cord Injury. *Molecular & Cellular Proteomics*, *15*(2), 394–408. https://doi.org/10.1074/mcp.R115.053751

Varhama, K., Oda, H., Shima, A., & Takeuchi, S. (2019). Decellularized Plant Leaves for 3D Cell Culturing. *2019 IEEE 32nd International Conference on Micro Electro Mechanical Systems (MEMS)*, 226–228. https://doi.org/10.1109/MEMSYS.2019.8870620

Venkatesan, J., & Kim, S.-K. (2010). Chitosan Composites for Bone Tissue Engineering—An Overview. *Marine Drugs*, *8*(8), 2252–2266. https://doi.org/10.3390/md8082252

Verkhratsky, A., Parpura, V., Li, B., & Scuderi, C. (2021). *Astrocytes: The Housekeepers and Guardians of the CNS* (pp. 21–53). https://doi.org/10.1007/978-3-030-77375-5_2

Visavadiya, N. P., Patel, S. P., VanRooyen, J. L., Sullivan, P. G., & Rabchevsky, A. G. (2016). Cellular and subcellular oxidative stress parameters following severe spinal cord injury. *Redox Biology*, *8*, 59–67. https://doi.org/10.1016/j.redox.2015.12.011

Wang, A., Zhang, G., Xiaochen Wang, Zhang, C., Tao Song, & Huo, X. (2016). Combination of applied electric field and polyethylene glycol effectively enhance functional recovery in acute spinal cord injury of rats. *2016 Asia-Pacific International Symposium on Electromagnetic Compatibility (APEMC)*, 1075–1077. https://doi.org/10.1109/APEMC.2016.7522949

Wang, H., Liu, N.-K., Zhang, Y. P., Deng, L., Lu, Q.-B., Shields, C. B., Walker, M. J., Li, J., & Xu, X.-M. (2015). Treadmill training induced lumbar motoneuron dendritic plasticity and behavior recovery in adult rats after a thoracic contusive spinal cord injury. *Experimental Neurology*, *271*, 368–378. https://doi.org/10.1016/j.expneurol.2015.07.004

Wang, J., Chu, R., Ni, N., & Nan, G. (2020). The effect of Matrigel as scaffold material for neural stem cell transplantation for treating spinal cord injury. *Scientific Reports*, *10*(1), 2576. https://doi.org/10.1038/s41598-020-59148-3

Wang, J., Yang, J., Ma, Y., Hua, Z., Guo, Y., Gu, X., & Zhang, Y. (2015). Nogo-A expression dynamically varies after spinal cord injury. *Neural Regeneration Research*, *10*(2), 225. https://doi.org/10.4103/1673-5374.152375

Wang, J.-H., Hung, C.-H., & Young, T.-H. (2006). Proliferation and differentiation of neural stem cells on lysine–alanine sequential polymer substrates. *Biomaterials*, *27*(18), 3441–3450. https://doi.org/10.1016/j.biomaterials.2006.02.002

Wang, X., He, J., Wang, Y., & Cui, F.-Z. (2012). Hyaluronic acid-based scaffold for central neural tissue engineering. *Interface Focus*, *2*(3), 278–291. https://doi.org/10.1098/rsfs.2012.0016

Wang, Y., Dominko, T., & Weathers, P. J. (2020a). Using decellularized grafted leaves as tissue engineering scaffolds for mammalian cells. *In Vitro Cellular & Developmental Biology - Plant*, *56*(6), 765–774. https://doi.org/10.1007/s11627-020-10077-w

Wang, Y., Dominko, T., & Weathers, P. J. (2020b). Using decellularized grafted leaves as tissue engineering scaffolds for mammalian cells. *In Vitro Cellular & Developmental Biology - Plant*, *56*(6), 765–774. https://doi.org/10.1007/s11627-020-10077-w

Wang, Y., Wu, W., Wu, X., Sun, Y., Zhang, Y. P., Deng, L.-X., Walker, M. J., Qu, W., Chen, C., Liu, N.-K., Han, Q., Dai, H., Shields, L. B., Shields, C. B., Sengelaub, D. R., Jones, K. J., Smith, G. M., & Xu, X.-M. (2018). Remodeling of lumbar motor circuitry remote to a thoracic spinal cord injury promotes locomotor recovery. *ELife*, *7*. https://doi.org/10.7554/eLife.39016

Weaver, L. C., Cassam, A. K., Krassioukov, A. V., & Llewellyn-Smith, I. J. (1997). Changes in immunoreactivity for growth associated protein-43 suggest reorganization of synapses on spinal sympathetic neurons after cord transection. *Neuroscience*, *81*(2), 535–551. https://doi.org/10.1016/S0306-4522(97)00151-6

Wei, Y., Marshall, A. G., McGlone, F. P., Makdani, A., Zhu, Y., Yan, L., Ren, L., & Wei, G. (2024). Human tactile sensing and sensorimotor mechanism: from afferent tactile signals to efferent motor control. *Nature Communications*, *15*(1), 6857. https://doi.org/10.1038/s41467-024-50616-2

Weishaupt, N., Hurd, C., Wei, D. Z., & Fouad, K. (2013). Reticulospinal plasticity after cervical spinal cord injury in the rat involves withdrawal of projections below the injury. *Experimental Neurology*, *247*, 241–249. https://doi.org/10.1016/j.expneurol.2013.05.003

Weiss, S., Dunne, C., Hewson, J., Wohl, C., Wheatley, M., Peterson, A. C., & Reynolds, B. A. (1996). Multipotent CNS Stem Cells Are Present in the Adult Mammalian Spinal Cord and Ventricular Neuroaxis. *The Journal of Neuroscience*, *16*(23), 7599–7609. https://doi.org/10.1523/JNEUROSCI.16-23-07599.1996

West, S. J., Bannister, K., Dickenson, A. H., & Bennett, D. L. (2015). Circuitry and plasticity of the dorsal horn – Toward a better understanding of neuropathic pain. *Neuroscience*, *300*, 254–275. https://doi.org/10.1016/j.neuroscience.2015.05.020

Whetstone, W. D., Hsu, J. C., Eisenberg, M., Werb, Z., & Noble-Haeusslein, L. J. (2003). Blood-spinal cord barrier after spinal cord injury: Relation to revascularization and wound healing. *Journal of Neuroscience Research*, *74*(2), 227–239. https://doi.org/10.1002/jnr.10759

Windhorst, U. (2007). Muscle proprioceptive feedback and spinal networks. *Brain Research Bulletin*, *73*(4–6), 155–202. https://doi.org/10.1016/j.brainresbull.2007.03.010

Xiao, Z., Tang, F., Zhao, Y., Han, G., Yin, N., Li, X., Chen, B., Han, S., Jiang, X., Yun, C., Zhao, C., Cheng, S., Zhang, S., & Dai, J. (2018). Significant Improvement of Acute Complete Spinal Cord Injury Patients Diagnosed by a Combined Criteria Implanted with NeuroRegen Scaffolds and Mesenchymal Stem Cells. *Cell Transplantation*, *27*(6), 907–915. https://doi.org/10.1177/0963689718766279

Xiong, Y.-J., Soomro, S., Huang, Z.-H., Yu, P.-P., Ping, J., & Fu, H. (2023). Poly-L-ornithine blocks the inhibitory effects of fibronectin on oligodendrocyte differentiation and promotes myelin repair. *Neural Regeneration Research*, *18*(4), 832. https://doi.org/10.4103/1673-5374.353493

Xu, N., Åkesson, E., Holmberg, L., & Sundström, E. (2015). A sensitive and reliable test instrument to assess swimming in rats with spinal cord injury. *Behavioural Brain Research*, *291*, 172–183. https://doi.org/10.1016/j.bbr.2015.05.004

Xue, W., Shi, W., Kong, Y., Kuss, M., & Duan, B. (2021). Anisotropic scaffolds for peripheral nerve and spinal cord regeneration. *Bioactive Materials*, *6*(11), 4141–4160. https://doi.org/10.1016/j.bioactmat.2021.04.019

Yang, T., Dai, Y., Chen, G., & Cui, S. (2020). Dissecting the Dual Role of the Glial Scar and Scar-Forming Astrocytes in Spinal Cord Injury. *Frontiers in Cellular Neuroscience*, *14*. https://doi.org/10.3389/fncel.2020.00078

Yang, Y., Fan, Y., Zhang, H., Zhang, Q., Zhao, Y., Xiao, Z., Liu, W., Chen, B., Gao, L., Sun, Z., Xue, X., Shu, M., & Dai, J. (2021). Small molecules combined with collagen hydrogel direct neurogenesis and migration of neural stem cells after spinal cord injury. *Biomaterials*, *269*, 120479. https://doi.org/10.1016/j.biomaterials.2020.120479

Yao, S., Yu, S., Cao, Z., Yang, Y., Yu, X., Mao, H.-Q., Wang, L.-N., Sun, X., Zhao, L., & Wang, X. (2018). Hierarchically aligned fibrin nanofiber hydrogel accelerated axonal regrowth and locomotor function recovery in rat spinal cord injury. *International Journal of Nanomedicine*, *Volume 13*, 2883–2895. https://doi.org/10.2147/IJN.S159356

Yen, S.-C., Landry, J. M., & Wu, M. (2014). Augmented multisensory feedback enhances locomotor adaptation in humans with incomplete spinal cord injury. *Human Movement Science*, *35*, 80–93. https://doi.org/10.1016/j.humov.2014.03.006

Yoon, H., Walters, G., Paulsen, A. R., & Scarisbrick, I. A. (2017). Astrocyte heterogeneity across the brain and spinal cord occurs developmentally, in adulthood and in response to demyelination. *PLOS ONE*, *12*(7), e0180697. https://doi.org/10.1371/journal.pone.0180697

Yoshii, Y., Furukawa, T., Waki, A., Okuyama, H., Inoue, M., Itoh, M., Zhang, M.-R., Wakizaka, H., Sogawa, C., Kiyono, Y., Yoshii, H., Fujibayashi, Y., & Saga, T. (2015). High-throughput screening with nanoimprinting 3D culture for efficient drug development by mimicking the tumor environment. *Biomaterials*, *51*, 278–289. https://doi.org/10.1016/j.biomaterials.2015.02.008

Yousefifard, M., Rahimi-Movaghar, V., Nasirinezhad, F., Baikpour, M., Safari, S., Saadat, S., Moghadas Jafari, A., Asady, H., Razavi Tousi, S. M. T., & Hosseini, M. (2016). Neural stem/progenitor cell transplantation for spinal cord injury treatment; A systematic review and meta-analysis. *Neuroscience*, *322*, 377–397. https://doi.org/10.1016/j.neuroscience.2016.02.034

Yu, P., Zhang, W., Liu, Y., Sheng, C., So, K.-F., Zhou, L., & Zhu, H. (2019). *The effects and potential mechanisms of locomotor training on improvements of functional recovery after spinal cord injury* (pp. 199–217). https://doi.org/10.1016/bs.irn.2019.08.003

Yu, Z., Li, H., Xia, P., Kong, W., Chang, Y., Fu, C., Wang, K., Yang, X., & Qi, Z. (2020). Application of fibrin-based hydrogels for nerve protection and regeneration after spinal cord injury. *Journal of Biological Engineering*, *14*(1), 22. https://doi.org/10.1186/s13036-020-00244-3

Zehr, E. P., & Stein, R. B. (1999). What functions do reflexes serve during human locomotion? *Progress in Neurobiology*, *58*(2), 185–205. https://doi.org/10.1016/S0301-0082(98)00081-1

Zhang, S., Wang, X.-J., Li, W.-S., Xu, X.-L., Hu, J.-B., Kang, X.-Q., Qi, J., Ying, X.-Y., You, J., & Du, Y.-Z. (2018). Polycaprolactone/polysialic acid hybrid, multifunctional nanofiber scaffolds for treatment of spinal cord injury. *Acta Biomaterialia*, *77*, 15–27. https://doi.org/10.1016/j.actbio.2018.06.038

Zhang, Z., Wang, F., & Song, M. (2019). The cell repair research of spinal cord injury: a review of cell transplantation to treat spinal cord injury. *Journal of Neurorestoratology*, *7*(2), 55–62. https://doi.org/10.26599/JNR.2019.9040011

Zhao, X.-M., He, X.-Y., Liu, J., Xu, Y., Xu, F.-F., Tan, Y.-X., Zhang, Z.-B., & Wang, T.-H. (2019). Neural Stem Cell Transplantation Improves Locomotor Function in Spinal Cord Transection Rats Associated with Nerve Regeneration and IGF-1 R Expression. *Cell Transplantation*, *28*(9–10), 1197–1211. https://doi.org/10.1177/0963689719860128

Zheng, B., & Tuszynski, M. H. (2023). Regulation of axonal regeneration after mammalian spinal cord injury. *Nature Reviews Molecular Cell Biology*. https://doi.org/10.1038/s41580-022-00562-y

Zheng, Y., Mao, Y.-R., Yuan, T.-F., Xu, D.-S., & Cheng, L.-M. (2020). Multimodal treatment for spinal cord injury: a sword of neuroregeneration upon neuromodulation. *Neural Regeneration Research*, *15*(8), 1437. https://doi.org/10.4103/1673-5374.274332

Zhou, P., Xu, P., Guan, J., Zhang, C., Chang, J., Yang, F., Xiao, H., Sun, H., Zhang, Z., Wang, M., Hu, J., & Mao, Y. (2020). Promoting 3D neuronal differentiation in hydrogel for spinal cord regeneration. *Colloids and Surfaces B: Biointerfaces*, *194*, 111214. https://doi.org/10.1016/j.colsurfb.2020.111214

Zhou, X., Shi, G., Fan, B., Cheng, X., Zhang, X., Wang, X., Liu, S., Hao, Y., Wei, Z., Wang, L., & Feng, S. (2018). Polycaprolactone electrospun fiber scaffold loaded with iPSCs-NSCs and ASCs as a novel tissue engineering scaffold for the treatment of spinal cord injury. *International Journal of Nanomedicine*, *Volume 13*, 6265–6277. https://doi.org/10.2147/IJN.S175914

Zhu, J., Wu, X., & Zhang, H. (2005). Adult Neural Stem Cell Therapy: Expansion In Vitro, Tracking In Vivo and Clinical Transplantation. *Current Drug Targets*, *6*(1), 97–110. https://doi.org/10.2174/1389450053345055

Zhu, T., Jiang, J., Zhao, J., Chen, S., & Yan, X. (2019). Regulating Preparation Of Functional Alginate-Chitosan Three-Dimensional Scaffold For Skin Tissue Engineering. *International Journal of Nanomedicine*, *Volume 14*, 8891–8903. https://doi.org/10.2147/IJN.S210329

Zill, S. N. (1985). Proprioceptive Feedback and the Control of Cockroach Walking. In *Feedback and Motor Control in Invertebrates and Vertebrates* (pp. 187–208). Springer Netherlands. https://doi.org/10.1007/978-94-011-7084-0_12

Zou, Y., Ma, D., Shen, H., Zhao, Y., Xu, B., Fan, Y., Sun, Z., Chen, B., Xue, W., Shi, Y., Xiao, Z., Gu, R., & Dai, J. (2020). Aligned collagen scaffold combination with human spinal cord-derived neural stem cells to improve spinal cord injury repair. *Biomaterials Science*, *8*(18), 5145–5156. https://doi.org/10.1039/D0BM00431F

Zou, Y., Yin, Y., Xiao, Z., Zhao, Y., Han, J., Chen, B., Xu, B., Cui, Y., Ma, X., & Dai, J. (2022). Transplantation of collagen sponge-based three-dimensional neural stem cells cultured in a RCCS facilitates locomotor functional recovery in spinal cord injury animals. *Biomaterials Science*, *10*(4), 915–924. https://doi.org/10.1039/D1BM01744F